RUSSIAN GEOGRAPHICAL SOCIETY

FACULTY OF GEOGRAPHY,
LOMONOSOV MOSCOW STATE UNIVERSITY

INSTITUTE OF GEOGRAPHY,
RUSSIAN ACADEMY OF SCIENCES

No. 01 [v. 07]
2014

GEOGRAPHY
ENVIRONMENT
SUSTAINABILITY

EDITORIAL BOARD

CONTENTS

EDITORIAL

The main goal of "GEOGRAPHY, ENVIRONMENT, SUSTAINABILITY" journal (GES Journal) is to provide in depth discussion of theoretical, methodological, and practical aspects of interdisciplinary areas reflected in the title of the journal, as well as of a wide range of their diverse applications.

Modern age is the time of deep transformation of nature and society, which makes an impact on the fundamental principles of geographical science. It is the epoch of emergence of new ideas, methods, and approaches to explore the changing world from the new positions. Population growth, food and resource security, natural resource management, and environmental protection stand out among the urgent global geographic problems. Sustainable development becomes the issue of paramount importance.

Achieving sustainable development is possible only through reconciling conflicts and finding compromises in the "nature-society" system. Such conflicts are associated with impacts on the environment and the need for its protection, use of resources and preservation of their stocks, biological and social aspects of humans, scientific-technical progress and humanity, increase in consumption and moral aspects of self-limitation, traditional and innovation aspects in development, etc.

Mankind is facing environmental changes caused by various natural-anthropogenic processes. Society is on the threshold of a period of economic and ecological adaptation to a rapidly changing environment. Therefore, the task of the GES journal is to provide a forum for discussion on spatial features of future changes and opportunities to overcome the difficulties encountered on the path of sustainable development of nature and society.

For centuries, maps have been the main tool of modeling and analysis in the Earth sciences and society. Only recently, remote sensing methods and geoinformation systems have emerged and geoinformatics began to advance to the leading position. Specifically creation of digital spatial models and their implementation in different areas of everyday life have created the foundation of the information revolution, though it does not undermine the achievements of traditional cartography and other established sciences. Mobility, agility, relevancy, and involvement in a wide range of social aspects are the iconic moments of the modern process of social development.

Readers of GES journal will not only find current information on the aforementioned issues, but will have an opportunity to take advantage of its integration capabilities, complexity, a variety of problems covered, and the focus on innovation. The main sections of the journal cover theory of geography, ecology, and sustainable development; natural resource management; natural resources; global and regional changes of the environment and climate; sustainable regional development; applied aspects of geography and ecology; geoinformatics and environmental mapping; environmental problems of the oil-gas sector; preservation of biodiversity; health and the environment; and education for sustainable development.

Among the authors of the journal are well-known experts in different fields of geographic science and related scientific disciplines, as well as young scientists who have just begun to publish their research results. The journal provides all its authors with a wide range of opportunities for an open scientific discussion and fruitful exchange of views.

The main criteria for selection of papers for publication is their relevance to the development of theory and practice, i.e., global or regional levels of research and quality of information and statistics background, methodology, and information and illustration supporting material. All papers submitted by authors undergo independent double-review; the papers with positive reviews are accepted for publication upon the decision of the Editorial Board of the journal. The languages of the journal are English and French, i.e., working languages of the majority of international organizations.

The journal targets Russian and international geographers, ecologists, and experts in the fields of environmental protection, management of natural resources, GIS-technologies, geographic mapping, and education for sustainable development, and environmental practitioners.

Pavel G. Talalay
Polar Research Center, Jilin University, No. 938 Ximinzhu str., Changchun City, Jilin Province, China, 130021, Tel/Fax +86 431 88502797, e-mail: ptalalay@yahoo.com

EXPLORATION OF GAMBURTSEV SUBGLACIAL MOUNTAINS (EAST ANTARCTICA): BACKGROUND AND PLANS FOR THE NEAR FUTURE

ABSTRACT. The Gamburtsev Subglacial Mountains (GSM), located in the central East Antarctica, were discovered by the Soviet team of the 3rd Complex Antarctic Expedition in 1958–1959. The GSM has highly dissected Alpine topography reaching maximum elevations of 3000 m. The mechanism driving uplift of the young-shaped GSM in the middle of the old East Antarctic Shield is unknown. With only limited constraints available on the topography, geology, and lithospheric structure, the origin of the GSM has been a matter of considerable speculation. The latest interpretation suggested that the GSM were formed during Permian and Cretaceous (roughly 250–100 Ma ago) due to the combination of rift-flank uplift, root buoyancy and the isostatic response. Later on the Antarctic Ice Sheet covered the range and protected it from erosion. However, this theory cannot explain lack of erosion process during many millions years in between uplifting and beginning of glaciation. The next step of the GSM exploration focuses on the direct observation of ice sheet bed by drilling. In order to penetrate into subglacial bedrock in the GSM region the development activity already has been started in China. It is proposed to use cable-suspended drilling technology and movable drilling shelter that can be transported to the chosen site with crawler-tractor. The first field tests of the drilling equipment are planned to carry out near Antarctic coast in season 2015–2016, and drilling to the bedrock would be finished during next two seasons.

KEY WORDS: subglacial environment, Antarctic tectonics, bedrock drilling

INTRODUCTION

Covering nearly 14 million km^2, Antarctica is the coldest, driest, highest, and windiest continent on the Earth. While it is challenging to live and work in this extreme environment, this region offers many opportunities for scientific research. One of the most important frontiers of Antarctic exploration is study of subglacial topography and geology, which is less well known than the topography of Moon and Mars, obviously because of the thick ice sheet covered about 98% of the continent and extremely severe conditions.

The rocks of the Antarctic crust are exposed primarily on the Antarctic Peninsula, in the Transantarctic Mountains of East Antarctica, a major mountain belt some 3000 km in length that rises to over 4500 m in height, in the Ellsworth Mountains of West Antarctica, and in the extinct volcanoes of Marie Byrd Land (Fig. 1). In addition, small mountain ranges project through the East Antarctic ice sheet in Dronning Maud Land, in Enderby Land, in Mac. Robertson Land, and in a few places in Wilkes Land. The Sentinel Range of the Ellsworth Mountains in West Antarctica includes the Vinson Massif, which contains the highest peak in Antarctica at 4901 m a.s.l. [Stonehouse, 2002].

The present elevation of the bedrock surface of some parts of East and West Antarctica is actually below sea level (Fig. 2). For example, two large subglacial basins in Wilkes Land of East Antarctica lie below sea level. The bedrock surface of most of West Antarctica is also below sea level partly because

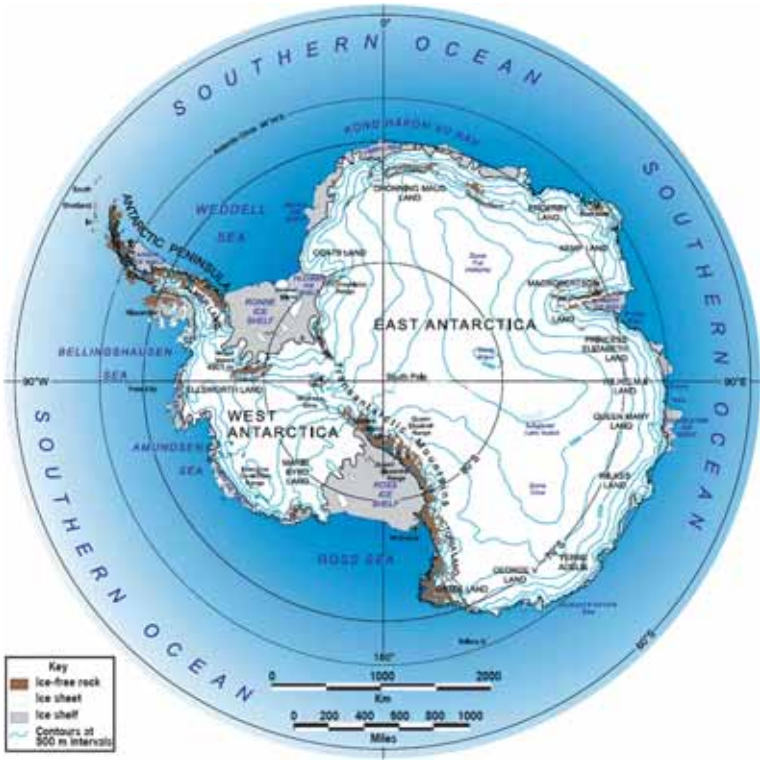

Fig. 1. Antarctic surface topography. Transantarctic Mountains divide Antarctica in two parts: West Antarctica and East Antarctica correspond roughly to the eastern and western hemispheres relative to the Greenwich meridian [http://geology.com/world/antarctica-satellite-image.shtml]

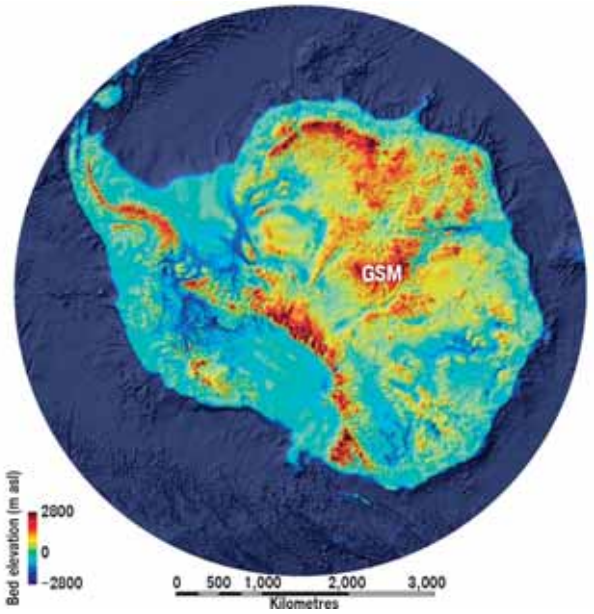

Fig. 2. Antarctic bedrock topography. Bedmap2 bed elevation grid is based on data from a variety of sources, including many substantial surveys undertaken over the past 50 years [Fretwell et al., 2013]

of the mass of the overlying ice sheet. The Gamburtsev Subglacial Mountains (GSM), located in central East Antarctica, has highly dissected Alpine topography reaching maximum elevations of 3000 m and a median elevation of about 1400 m in the north–south-trending [Ferraccioli et al., 2011].

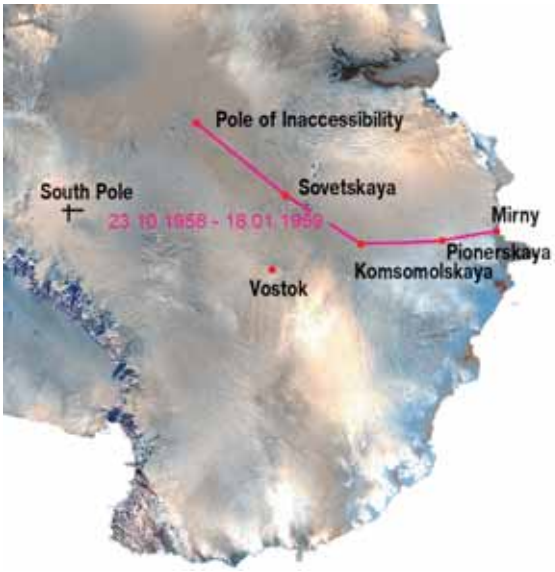

Fig. 3. Traverse route of the 3rd Complex Antarctic Expedition (23.10.1958–18.01.1959)

Among other subglacial objects the GSM are one of the most enigmatic features on the Earth. The range has become the subject of great scientific interest because the mechanism driving uplift of the young-shaped GSM in the middle of the old East Antarctic Shield is unknown [Talalay and Markov, 2012]. The GSM may have served as a nucleation point for the first large-scale ice sheet that formed in Antarctica as the Earth's climate cooled roughly 34 Ma ago [DeConto and Pollard, 2003]. The tectonic and glacial histories of Antarctica are tightly linked [Zapol, 2011]. Without its high topography, the history of the Antarctic ice sheet would have been quite different. Without the continental glaciation the subglacial mountains of Antarctica would have been quite different. Understanding the mechanisms and timing of the formation of the GSM is linked to the understanding of the changing climate of Antarctica and of the planet in the past.

DISCOVERY

The GSM were discovered by the Soviet team of the 3rd Complex Antarctic Expedition[1] in 1958–1959. The unique traverse from Mirny station to the Pole of Inaccessibility was underway during 88 days and overcome about 4300 km (Fig. 3). As a result of seismic and gravimetric surveys the first profile of the East Antarctic Ice Sheet has been built (Fig. 4), and in the region of the highest point of the ice sheet a huge subglacial mountain range was discovered [Sorokhtin et al., 1960]. It was named as 'Gory Podlyednye Gamburtseva', for Soviet geophysicist Grigory Gamburtsev (1903–1955), one of the creators of modern seismology. The Advisory Committee on Antarctic Names (ACAN) accepted the English interpretation of this geographical feature 'Gamburtsev Subglacial Mountains' in 1975.

After the GSM discovery first geophysics appeared here only in 1974. The joint project of the airborne radio-echo sounding carried out by the Scott Polar Research Institute (Cambridge, UK), U.S. National Science Foundation and the Technical University of Denmark yielded multiple bedrock profiles in this region [Turchetti et al., 2008]. The presence of the GSM was confirmed, and the map of Antarctic bed topography issued in 1983 contained a quite detailed description of the GSM [Drewry, 1983].

Exploring the history of the East Antarctic ice sheet and lithospheric structure of the GSM were the primary goals of the Fourth International Polar Year (2007–2009). At that time multi-national and multi-disciplinary Antarctica's Gamburtsev Province (AGAP)

[1] Complex Antarctic Expedition, USSR (the 1st CAE was formed in 1956); later, the expeditions were referred to as Soviet Antarctic Expeditions (SAE) and Russian Antarctic Expeditions (RAE).

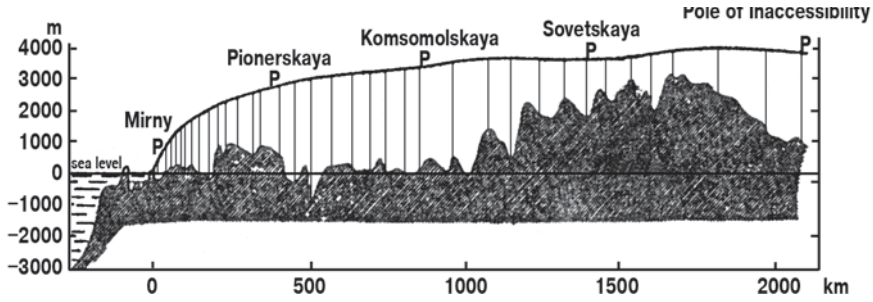

Fig. 4. First profile of East Antarctica: vertical lines indicate the points of joint seismic and gravimetric observations, between which the profile was built according to the gravity survey [Sorokhtin et al., 1960]

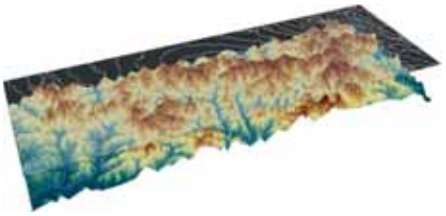

Fig. 5. 3D-modell of the GSM built up according with results of AGAP geophysical survey (Credit: T. Creyts, Lamont-Doherty Earth Observatory of Columbia University, USA)

project was founded by 7 countries: Australia, Canada, China, Germany, Japan, the United Kingdom, and the United States [Bell, 2008]. Unfortunately, Russian scientists, discoverers of the GSM, did not attend this project. The AGAP partnership included aerogeophysics, traverse programs, passive seismic experiments and shallow ice core drilling. The surveys were targeted at understanding the tectonic origin of these enigmatic mountains to provide crucial new inputs into ice sheet and climate models. The modern-day remote-sensing technology and 3D-modelling revealed a very jagged landscape of the GSM (Fig. 5).

It was found that the GSM have about the same size as the European Alps, and very sharp peaks and valleys are remarkably similar to the Alps themselves. It should be noted that Alps were formed as a result of the collision of the European and African tectonic plates and uplifted during the Paleogene and Neogene periods (i.e., about 65 to 2,6 Ma ago). It all adds to the mystery from the tectonic perspective of how the GSM were created in the central part of East Antarctic Shield, where such processes do not occur, at least in the last 100 million years.

In this connection one of the scientists joked: "It is like opening the door of an Egyptian pyramid and finding an astronaut inside". There is no good reason for an astronaut to be inside an Egyptian pyramid just as there is no good reason for a major mountain range in the middle of the East Antarctica.

ORIGIN

Even the intensive research of the GSM was carried out within AGAP project, only limited constraints on the topography, geology, and lithospheric structure are still available, and the origin of the GSM has been a matter of considerable speculation [Hansen et al., 2010]. Some studies have suggested that the GSM were uplifted by a mantle plume, forming a volcano-capped dome, similar to the Hoggar massif in Africa [Sleep, 2006]. Other studies have suggested that the GSM developed through multiple Proterozoic or early Paleozoic orogenic events associated with the assembly of Gondwana [Fitzsimons, 2000, 2003]. Alternatively, the GSM may have resulted from far-field compression associated with the formation of Pangaea during the late Carboniferous–early Permian [Veevers, 1994].

The latest conception [Ferraccioli et al., 2011] proposed that the root formed during the Proterozoic assembly of interior East

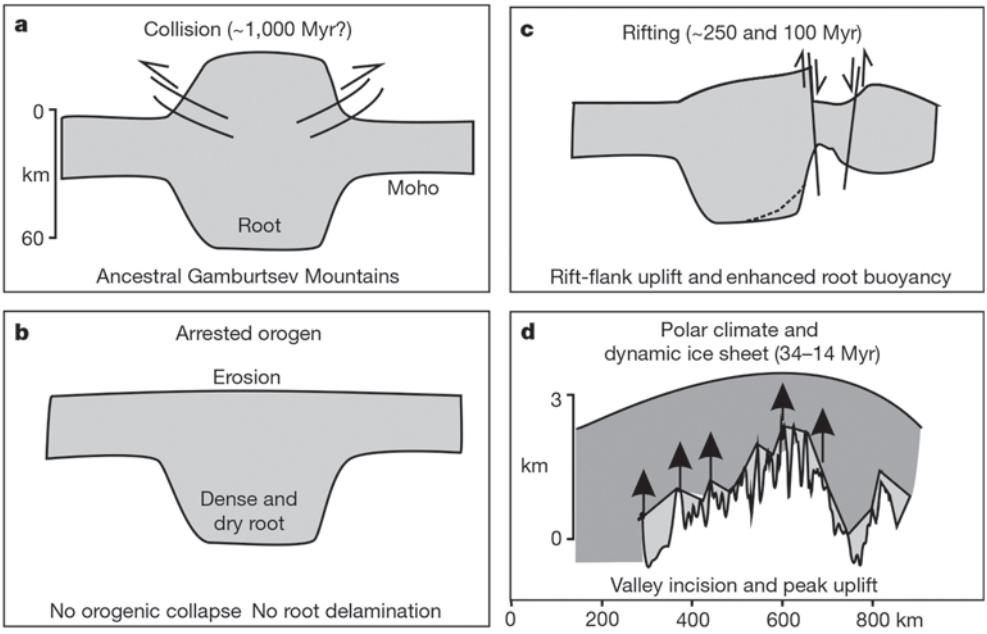

Fig. 6. Schematic of the elements contributing to the GSM uplift – explanations are given in the text [Ferraccioli et al., 2011]

Antarctica (about 1 Ga ago) was preserved as in some old orogens (Fig. 6, a), and post-collisional orogenic collapse and major Moho re-equilibration did not occur, preserving a dry and dense root like that in the Trans-Hudson orogen and the Urals (Fig. 6, b). Permian and Cretaceous (roughly 250–100 Ma ago) rifting drove flexural uplift and, through possible heating and/or depressurization, reduced the density of the root and released its latent buoyancy, to help produce the broad GSM rift-flank (Fig. 6, c). Fluvial and glacial erosion in the valleys uplifted the peaks, creating the modern high-relief Alpine topography of the GSM. The East Antarctic Ice Sheet has preserved the rugged topography of the GSM for at least 14 million years (Fig. 6, d).

So, according to the most of the interpretations while the mountains may look young, the evidence would suggest they must be quite old. The main problem of such standpoint is that it cannot explain lack of erosion process during many millions years in between the GSM uplift and beginning of glaciation that protected mountains from weathering. With no rock samples available, geochronologic constraints on the age of the GSM have not been acquired. The only one way to clear up the GSM age and origin is direct observation of ice sheet bed by drilling.

PLANS FOR THE NEAR FUTURE

Drilling operations in Antarctica are complicated by extremely low temperature at the surface and within ice sheet, by ice flow, the absence of roads and infrastructures, storms, winds, snowfalls, etc. All those are the reasons that up to the present moment bedrock cores were never obtained at inland of Antarctica. To recover subglacial bedrock samples, two types of subglacial drilling technologies might be considered [Talalay, 2013]: (1) commercial drill rigs with conventional core barrel, or wire-line core barrel, or coiled tubing, and (2) electromechanical cable-suspended drilling with near-bottom fluid circulation. These drilling technologies have different concepts, limits, performance, and applicable scopes.

To use commercial drill rigs in these heavy conditions, many components such as

hydraulic system, fluid processing system and some others should be principally re-designed as they are not able to work at low-temperatures. Commercial drill rigs operate as outdoor machines, use tents, or primitive shelters that are not enough at extremely low temperatures and storm winds in Antarctica. In addition, commercial drill rigs are still very heavy and power consuming. They require a large logistical load to move and support, so that using in Antarctica not only disadvantageously but also in some cases impossible.

In our opinion, the most effective method to penetrate subglacial bedrocks is electromechanical cable-suspended drilling technology. This was confirmed by five successful projects carried out by U.S. and Russian specialists in the past (Table 1). The main feature of the electromechanical cable-suspended drills is that an armored cable with a winch is used instead of a pipe-string to provide power to the down-hole motor system and to retrieve the down-hole unit. The use of armored cable allows a significant reduction in power and material consumption, a decrease in the time of round-trip operations, and a simplification in the cleaning of the hole from the cuttings.

In order to penetrate through the Antarctic Ice Sheet in the GSM region the development activity already has been started in Jilin University, China. It is assumed to choose the drill site with the ice thickness at most of 1000 m (ideally 600–800 m) and to pierce into the mountain slope to a depth of few meters (Fig. 7). The expected average daily production of ice drilling would be not less than 25 m/day.

All drilling equipment (two 50-kW diesel generators, winch, control desk, etc.) will be installed inside a movable sledge-mounted

Table 1. Subglacial drilling experience with electromechanical cable-suspended drills

Years	Till & bedrock interval (core length)	Location	References
1966	1387.5–1391 m (3.5 m)	Camp Century, Greenland	Ueda and Garfield, 1968
1988	457–461.6 m (4.6 m)	Vavilov Glacier, Severnaya Zemlya	Vasiliev and Talalay, 2010
1994	3051.5–3053 m (1.5 m)	Summit (GISP2), Greenland	Gow and Meese, 1996
1994	554 m (0,1 m)	Taylor Dome, Antarctica	Steig et al., 2000
2001	722–724 m (2.0 m)	Akademiya Nauk Glacier, Severnaya Zemlya	Vasiliev and Talalay, 2010

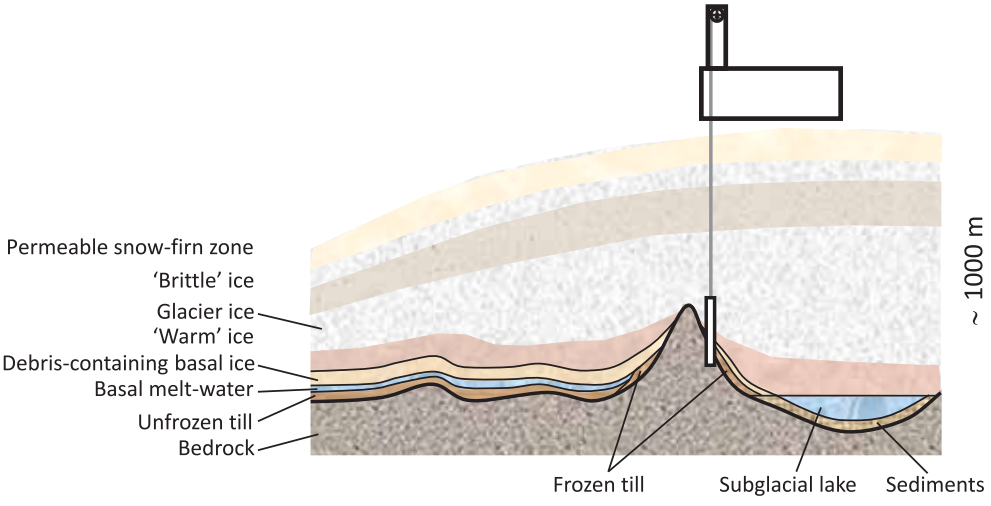

Fig. 7. Schematic layering inside and beneath ice sheet: due to modelling, water on the base of the ice sheet is observed if thickness of ice sheet is more than 2000 m, and over the mountain ridge the bed should be frozen

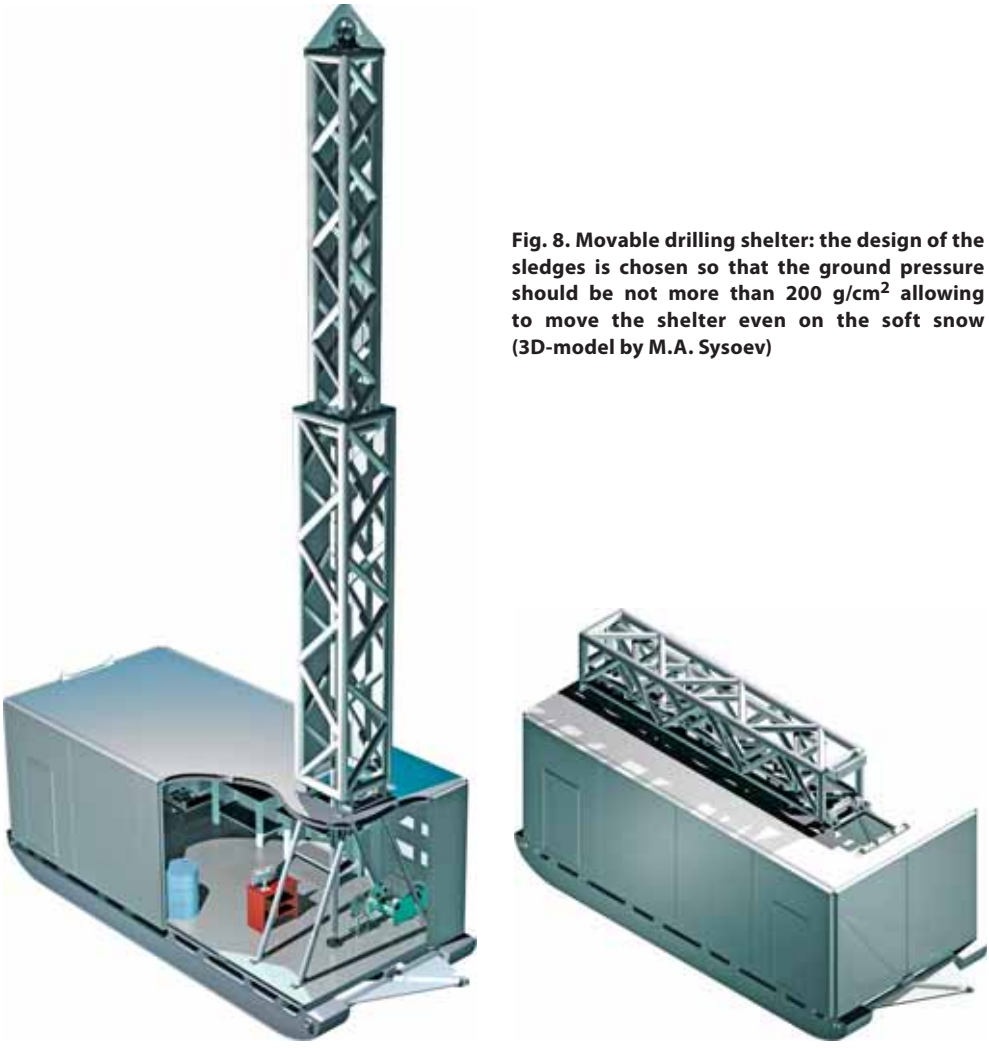

Fig. 8. Movable drilling shelter: the design of the sledges is chosen so that the ground pressure should be not more than 200 g/cm^2 allowing to move the shelter even on the soft snow (3D-model by M.A. Sysoev)

warm-keeping and wind-protecting drilling shelter that has dimensions of 7,5×4,0×3,0 m. Mast has two positions: horizontal for transportation and vertical working position (Fig. 8). Mast height is 12 m from the floor of the shelter. Total weight of drilling equipment (without drilling fluid) is near 20 tons. Drilling shelter is transported to the chosen site with crawler-tractor, and all equipment is ready to start drilling immediately upon arrival to the site.

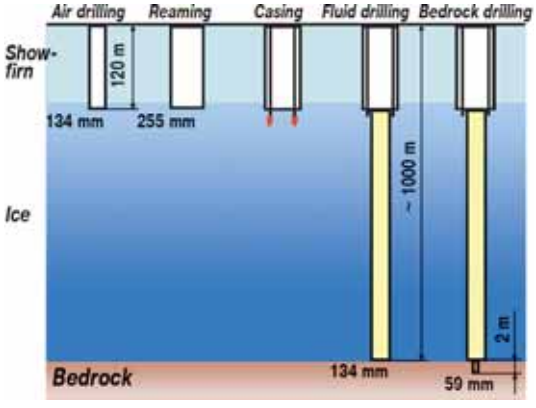

Fig. 9. Proposed borehole construction and drilling technology

Proposed borehole construction includes five following steps (Fig. 9):

(1) dry core drilling of upper permeable snow-firn layer with bottom-air reverse circulation; (2) reaming; (3) casing installation with thermal casing shoe; (4) fluid core drilling of glacial ice with bottom-fluid reverse circulation; (5) bedrock core drilling.

To drill through ice and bedrock a new multipurpose cable-suspended Ice and Bedrock Electromechanical Drill 'IBED' is designed with modulus structure in order to solve three different tasks (Fig. 10): (1) modulus A + B + E for dry core drilling with

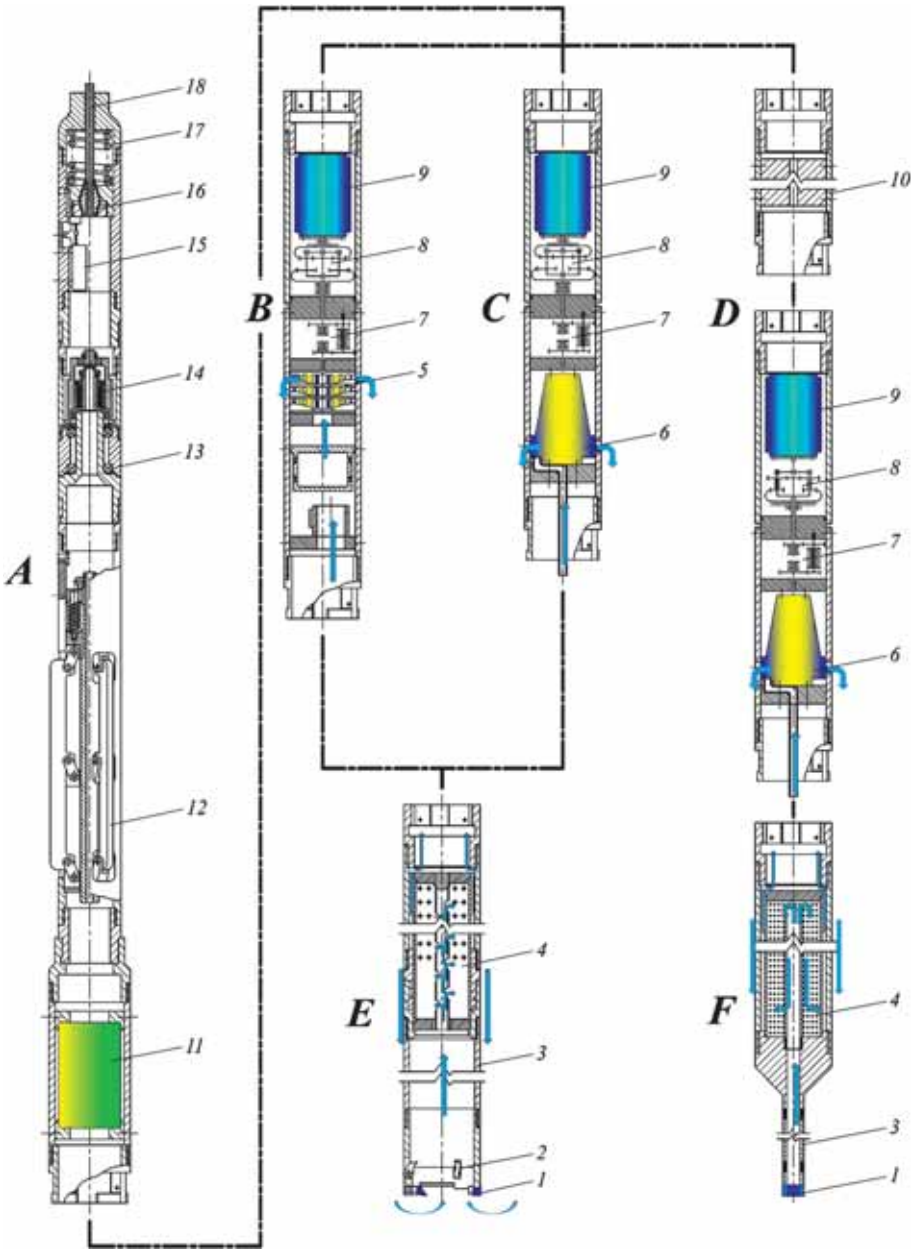

Fig. 10. General schematic of electromechanical IBED drill:

1 – drill bit; 2 – core catcher; 3 – core barrel; 4 – chips chamber; 5 – air pump; 6 – fluid pump; 7, 8 – gear reducer; 9 – electric motor; 10 – dead weight; 11 – pressure chamber; 12 – antitorque section; 13 – bearing assembly; 14 – slip rings; 15 – load sensor; 16 – cable termination; 17 – spring; 18 – armored cable

bottom-air reverse circulation; (2) modulus A + C + E for fluid ice core drilling; (3) modulus A + D + F for bedrock core drilling. Different sections of the drill are easily replaced as all of them have the same bayonet joint.

The upper part is the same for all variants; it includes four sections: cable termination, slip rings section, antitorque system, electronic pressure chamber. The motor-gear sections are differed by rotation speed of the output shaft of the gear-reducer. All modulus contain 3 kW AC3×380 V submersible motor of Grundfos MS4000 type. The motor is pre-lubricated and can keep outer pressure up to 15 MPa. Gear-reducer for drilling in ice lowers the drill bit rotation speed to 100 rpm; gear reducer for subglacial drilling lowers the drill bit rotation speed to 500 rpm. In addition, module for dry core drilling contains vacuum pump for near bottom air reverse circulation instead of liquid-driven pump that is installed into other two variants. The rotation speed of air-driven pump is increased by the gear to 6000 rpm.

In modules for drilling with liquid the shaft from the motor connects with two gear-reduces: one for rotation of the core barrel and drill bit, and another one for driving of the pump. The pump is the Rotan CD33EM-3U332 pump with an internal idler gear. The capacity of the pump is 38–41 L/min with maximal pumping pressure of 0,2 MPa.

IBED lower part for drilling in ice consists from two parts: chip chamber for filtration of drilling fluid and collecting chips, and core barrel with the drill bit. The outer/inner diameter of the ice core drill bit is 134/110 mm. Length of the core barrel is 2,5 m. Lower part of the bedrock variant is adapted for coring bedrock using special teeth diamond bit and contains standard 2-m length core barrel borrowed from conventional diamond drill string, chip chamber for gravity separation of rock cuttings and dead weights (appr. 200 kg) for increasing of the load on the diamond drill bit. The outer/inner diameters of the diamond bit are

Fig. 11. Stand for testing electromechanical IBED drill (Chungchun-city, China, 2013)

57/41 mm. To test shortened version of IBED drill the special stand has been built that can simulate borehole conditions (Fig. 11). The preliminary tests showed that teeth diamond drill bit could penetrate into the granite with average rate of 3,18 m/h at low load (3 kN) and torque (28,8 N m).

The new approaches of subglacial bedrock drilling technology are connected with utilization of environmental friendly, low-toxic drilling fluids, e.g. low-molecular dimethyl siloxane oils or ester type. They have suitable density-viscosity properties, and can be consider as a viable alternative for drilling in glacial ice and subglacial bedrock.

According to approved schedule, the first field tests are planned to carry out just outside Zhongshan Station near Antarctic coast in season 2015–2016. Next season 2016–2017 the movable drilling shelter is planned to be transported to the chosen drilling site in the GSM region, and drilling to the bedrock would be finished during two seasons.

ACKNOWLEDGMENT

Subglacial drilling project in the region of GSM is funded by National Science Foundation of China (project No. 41327804) and Geological Survey of China (project No. 3R212W324424). Author thanks all team members of Polar Research Center, Jilin University for hard working on the designing and testing of new drilling equipment for subglacial exploration. ■

REFERENCES

1. Bell, R.E. (2008). Antarctic Earth System Science in the International Polar Year 2007–2008. Antarctica: A Keystone in a Changing World. Proceedings of the 10th International Symposium on Antarctic Earth Science. Eds.: A.K. Cooper, P.J. Barrett, H. Stagg, B. Storey, E. Stump, W. Wise, and the 10th ISAES editorial team. Washington, DC: The National Academies Press, pp. 7–18.

2. DeConto, R.M., Pollard, D. (2003). Rapid Cenozoic glaciation of Antarctica induced by declining atmospheric CO_2. Nature, Vol. 421, pp. 245–249.

3. Drewry, D.J. (ed.) (1983). Antarctica: Glaciological and Geophysical Folio, Scott Polar Research Institute, University of Cambridge.

4. Ferraccioli, F., Finn, C.A., Jordan, T.A., Bell, R.A., Anderson, L.M., and Damaske, D. (2011). East Antarctic rifting triggers uplift of the Gamburtsev Mountains. Nature, Vol. 479, pp. 388–392.

5. Fitzsimons, I.C.W. (2000). Grenville-age basement provinces in East Antarctica: evidence for three separate collisional orogens. Geology, Vol. 28, pp. 879–882.

6. Fitzsimons, I.C.W. (2003). Proterozoic basement provinces of southern and southwestern Australia, and their correlation with Antarctica. Geol. Soc. Spec. Pub. 206, pp. 93–130.

7. Fretwell, P. and 59 others. (2013). Bedmap 2: improved ice bed, surface and thickness datasets for Antarctica. The Cryosphere, Vol. 7, pp. 375–393.

8. Gow, A.J., Meese, D.A. (1996). Nature of basal debris in the GISP2 and Byrd ice cores and its relevance to bed processes. Annals of Glaciology, Vol. 22, pp. 134–140.

9. Hansen, S.E., Nyblade, A.A., Heeszel, D.S., Wiens, D.A., Shore, P., and Kanao, M. (2010). Crustal structure of the Gamburtsev Mountains, East Antarctica, from S-wave receiver functions and Rayleigh wave phase velocities. Earth and Planetary Science Letters. Vol. 300, pp. 395–401.

10. Sleep, N.H. (2006). Mantle plumes from top to bottom. Earth Sci. Rev., Vol. 77, pp. 231–271.

11. Sorokhtin, O.G., Avsyuk, Yu.N., Kondratyev, O.K. (1960). The methodology and the main results of seismic and gravity studies of the structure of East Antarctica. Proceedings of the Academy of Sciences of the USSR, Geophysical Series, Vol. 3, pp. 396–401. [In Russian].

12. Steig, E.J., Morse, D.L., Waddington, E.D., Stuiver, M., Grootes, P.M., Mayewski, P.M., Whitlow, S.I., and Twickler, M.S. (2000). Wisconsinan and Holocene climate history from an ice core at Taylor Dome, western Ross Embayment, Antarctica. Geografiska Annaler, Vol. 82A, pp. 213–235.

13. Stonehouse B. (ed.) (2002). Encyclopedia of Antarctica and the Southern Ocean. Wiley, Chichester, England. 391 p.

14. Talalay, P.G., Markov A.N. (2012). Gamburtsev Mountains – the range, which nobody seen. Nature, Vol. 2, pp. 29–38. [In Russian].

15. Talalay, P.G. (2013). Subglacial till and bedrock drilling. Cold Regions Science and Technology, Vol. 86, pp. 142–166.

16. Turchetti, S., Dean, K., Naylor, S., and Siegert, M. (2008). Accidents and opportunities: a history of the radio echo-sounding of Antarctica, 1958–79. British Journal for the History of Science, Vol. 41 (3), pp. 417–444.

17. Ueda, H.T., Garfield, D.E. (1968). Drilling through the Greenland Ice Sheet. Hanover, USA. CRREL Spec. Rep. 126, 7 p.

18. Vasiliev, N.I., Talalay, P.G. (2010). Subglacial drilling on Severnaya Zemlya archipelago. Transactions of the 8th International Research-to-Practice Conference "Mineral resources development of Polar Regions: Problems and Solving". 7–9 Apr., 2010, Vorkuta, Russia, pp. 27–31. [In Russian].

19. Veevers, J.J. (1994). Case for the Gamburtsev Subglacial Mountains of East Antarctica originating by mid-Carboniferous shortening of an intracratonic basin. Geology, Vol. 22, pp. 593–596.

20. Zapol, W.M. (chair) (2011). Future Science Opportunities in Antarctica and the Southern Ocean. The National Academies Press, Washington D.C., USA, 195 p.

Pavel G. Talalay graduated with honor from the Leningrad Mining Institute and obtained Diploma of Mining Engineer in 1984. During the period from 1984 to 2010 he worked as engineer, senior engineer, researcher, associate professor, professor, head of the department at the Leningrad Mining Institute (since 1991 St. Petersburg State Mining Institute). He received degrees of Candidate of Technical Sciences in 1994, and Doctor of Technical Sciences in 2007. In 2010 he has got a grant from "The Thousand Talents Program" organized by the Central Coordination Committee on the Recruitment of Talents, China, and since September 2010 he has been engaged in research at the Jilin University as Professor of the College of Construction Engineering. Since December 2010 he became a director of the just-established Polar Research Center at Jilin University. His research interests are associated with different aspects of drilling technology in Polar Regions, especially on glaciers and ice sheets. He is the author of about 150 publications. Main publications: Fifty years of Soviet and Russian drilling activity in Polar and Non-Polar ice. A chronological history (2007, with co-author); Twenty years of drilling the deepest hole in ice (2011, with co-authors); Subglacial till and bedrock drilling (2013).

Vladimir Klimenko[1], Vladimir Matskovsky[2*], Dittmar Dahlmann[3]
[1] Moscow Power Engineering Institute, Moscow, Russia; e-mail: nilgpe@mpei.ru
[2] Institute of Geography, Russian Academy of Sciences, Moscow, Russia;
e-mail: matskovsky@igras.ru
[*] **Corresponding author**
[3] Rhenish Friedrich-Wilhelm University, Bonn, Germany; e-mail: d.dahlmann@uni-bonn.de

MULTI-ARCHIVE TEMPERATURE RECONSTRUCTION OF THE RUSSIAN ARCTIC FOR THE PAST TWO MILLENNIA

ABSTRACT. We present a multi-archival mean annual quantitative temperature reconstruction for Northeastern Europe covering the period of the past two millennia based on tree-ring, pollen, and historical data. This reconstruction was developed primarily to build up a comparative chronology of climatic and historical events in the study region. Five different calibration and verification approaches were used. A comparison of mean decadal temperature reconstruction for Northeastern Europe with those for larger regions and the Hemisphere shows that larger climatic events were visible both in the whole Northern Hemisphere and its separate regions. Less significant climatic events on a regional level may differ considerably from the overall climate signature on the hemispheric level. Highest pre-industrial mean annual temperatures in AD 981–990 were 1,0°C warmer and lowest in AD 1811–1820 were 1,3°C colder than average in AD 1951–1980. The new reconstruction shows much higher degree of variability as compared to Panarctic and hemispheric reconstructions.

KEY WORDS: climate change, Arctic, palaeogeography, temperature reconstruction, multi-proxy, historical climatology

INTRODUCTION

A link between climatic and cultural changes is particularly strong in marginal areas of human inhabitance, such as arid areas (steppes, deserts, and semideserts) and high-latitude regions like Northeastern Europe. There is a vast body of literature on this subject, ascending to Antiquity, in particular, to the works of Aristotle, Theophrastus, and Hipparchus. During the recent decades, studies of this subject have gained in scope in connection with a massive breakthrough in the field of earth sciences and, in particular, knowledge of the past climates. This has resulted in numerous papers concerning the role of climate in the fate of the various states [see, e.g. Klimenko, 2009; Aimers, Hodell, 2011; Вьntgen et al., 2011]. A study of a possible impact of climate change on the historical process in the Northeastern Europe makes its first steps. However, before one can come to the well-grounded conclusions it is necessary to obtain a high-resolution climatic evidence for a given region for the whole historical period. The main goal of this study is reconstruction of the regional decadal annual temperature variability for the last 2000 years.

STUDY AREA

The study area comprises a region limited by the Kola Peninsula in the west (40°E), Chelyuskin Cape (Taimyr Peninsula) to the east (104°E), and the 60°N latitudinal line in the south (Fig. 1).

The western boundary of the study area is determined by the territory, which Novgorodians started to master in the early twelfth century – it was the time when they

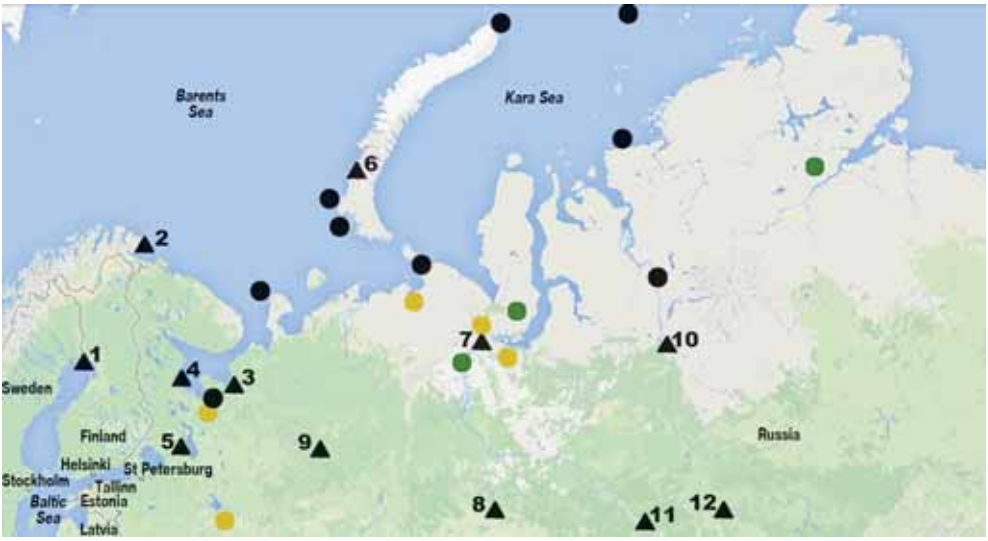

Fig. 1. The map of the study area showing locations of proxy climatic chronologies. Lake-sediment (yellow), tree-ring (green), and major historical (black) evidence. The locations of the long-term meteorological stations within and around the study area (triangles): (1) Haparanda; (2) Vardш; (3) Arkhangelsk; (4) Kem; (5) Petrozavodsk; (6) Malye Karmakuly; (7) Salekhard; (8) Tobolsk; (9) Syktyvkar; (10) Turukhansk; (11) Tomsk; (12) Yeniseysk

first settled on the right bank of the Severnaya Dvina which meant, in fact, the onset of the northeastern territories colonization. An eastern boundary is determined by the main historical scene in a period spanning from the mid-eleventh through the late seventeenth century. On this scene, specifically Taimyr was that natural boundary which could not be crossed through all this time. In this study, we also used some proxy climate data for the adjacent area just beyond the study region. On the one hand, it is connected with a sufficient correlation of remote temperature fields and, on the other hand, with the uniqueness of these data that contain important information.

The principal purpose of this study was the development of a climate reconstruction spanning the past two millennia based on all available proxy data. As the most of exploited proxy data (pollen and historical) represent mean annual air temperature, it is the *mean annual* temperature that was eventually reconstructed.

Moreover, because of the paucity of the high-resolution paleoclimatic evidence in the study region we focus on the *mean decadal* temperature reconstruction that, in fact, corresponds quite well to the principal purpose of building-up a comparative chronology of climatic and historical events. The matter is that human society responds, as a rule, not to a separate albeit significant interannual climate variations, but to more stable excursions with characteristic times comparable to the life expectancy of a human generation (20–22 yr). However, one should take into account that the employed tree-ring data represent only the warm season temperatures. Nevertheless, it doesn't decrease their value because of the well-established correlation between mean annual and summer temperatures, at least, in the study area. Thus, in this paper, we have used tree-ring data, as well as pollen and historical evidence, as proxy climatic data.

MATERIALS, METHODS, AND RESULTS

Proxy data

Various proxy data may have different time resolution. For instance, pollen data rarely achieve resolution better, than

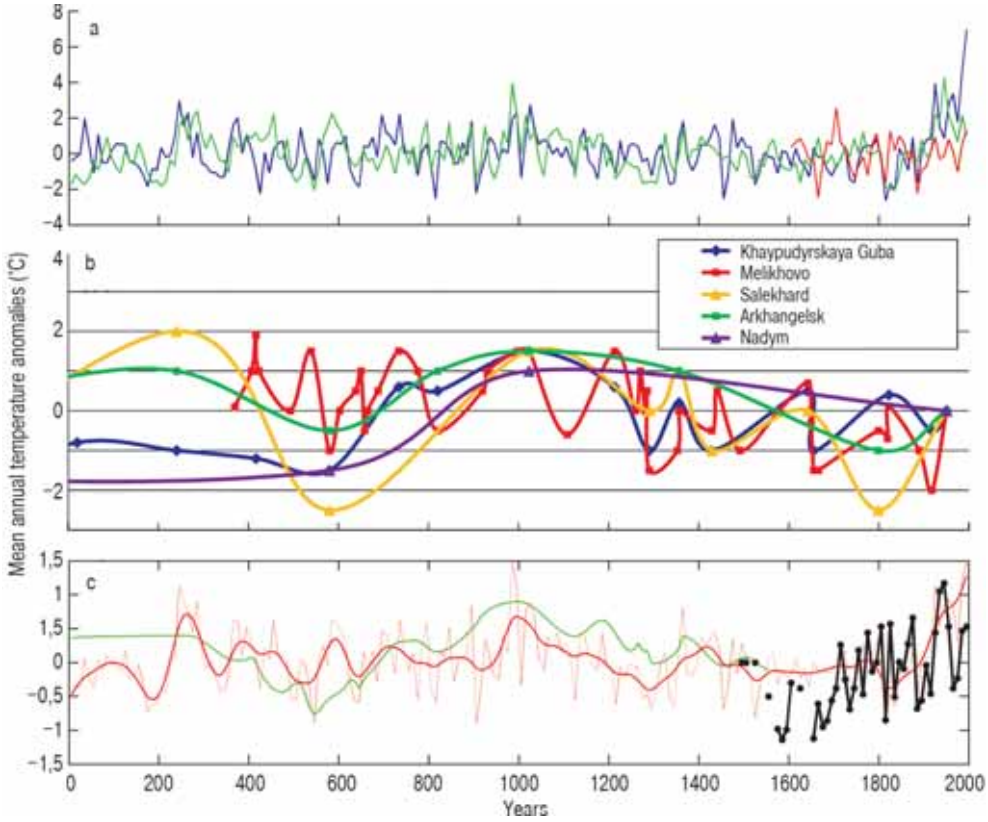

Fig. 2.

a) Variations of tree-ring width for Yamal (blue) [Hantemirov, Shiyatov, 2002], Taymyr (green) [Naurzbaev et al, 2002] and Polar Urals (red) [Gurskaya et al., 2012].
b) Estimated mean annual temperature anomalies based on pollen data [Klimanov et al., 1995; Velichko et al., 1997; Andreev, Klimanov, 2000].
c) Averaged proxy climatic data: pollen (green), tree-ring (red), historical (black) [Klimenko, 2010]. Here and elsewhere, temperature departures are expressed with reference to the period 1951–1980

Table 1. Proxy data used to reconstruct climate of northeastern Europe

Type of data	Location	Reconstructed value	Longitude	Latitude	Start year	End year	Source
Pollen	Nadym	Tr	72	64	545	1555	Velichko et al., 1997
Pollen	Melikhovo	Tr	38	57	370	1555	Klimanov et al., 1995
Pollen	Salekhard	Tr	66	67	0	1555	Velichko et al., 1997
Pollen	Arkhangelsk	Tr	43	64	0	1555	Velichko et al., 1997
Pollen	Khaypudyrskaya Guba	Tr	60	68	0	1555	Andreev, Klimanov, 2000; Velichko et al., 1997
Tree-ring width	Yamal	Тл	70	67	0	1995	Hantemirov, Shiyatov, 2002
Tree-ring width	Taymyr	Тл	102	72	0	1995	Naurzbaev et al., 2002
Tree-ring width	Taymyr	Тл	64	65	1605	1995	Gurskaya et al., 2012
Historical	Northeastern Europe	Tr	50–80	65–80	1495	1995	Klimenko, 2010

50 years, whereas tree-ring data allow a reconstruction with a resolution down to a year and even a season. Eventually, historical data may have a resolution within a day and even a few hours. However, with rising resolution an ability of proxy data to reconstruct long-term climatic variations decreases. This problem is well known for tree-ring data [Jones et al, 2009] and many methods to solve it were proposed. Today, scientific community shares an opinion that in order to develop a high-quality reconstruction, one must employ both high- and low-resolution data. The former allow for a reconstruction of such short-lived events as temperature drops following strong volcanic eruptions and the latter allow for a correct reconstruction of the substantial climatic events amplitude [Klimenko, Sleptsov, 2003; Moberg et al, 2005; Jones et al, 2009].

With that said, in this work, we employed the following proxy data (Fig. 2):

1. Tree-ring data on annual ring width – for a detailed reconstruction of short-term climatic events.

2. Pollen (lake sediment) data – to reconstruct a long-term climatic signal and refine its amplitude.

3. Historical data – potentially the most accurate and detailed source of climatic information but spanning just over 500 years. See Table 1 for the description of all proxy time series used in this study.

Instrumental data

To calibrate the reconstruction and verify its contemporary part we have employed averaged data from twelve long-term meteorological stations located within and around the study area (see Fig. 1). Observations at these stations started in the following years (in chronological order): Arkhangelsk–1813, Petrozavodsk – 1817, Syktyvkar – 1817, Vardш – 1829, Tobolsk – 1829, Tomsk – 1837, Haparanda – 1860, Kem – 1862, Yeniseysk –1871, Turukhansk – 1881, Salekhard and Malye Karmakuly – 1886 (after Global Historical Climatology Network; [Peterson, Vose, 1997]). It should be noted that observations at the central for the study area stations – Salekhard and Malye Karmakuly – commenced later, than on the others, only in AD1886. That is why, although we used all available observational data, but for calibration purposes only a portion of them, after AD 1886, was used (therefore, the first value in the decadal time series refers to AD 1895).

Proxy data assimilation in order to develop a generalized reconstruction

Before composing various proxy data, we had conducted averaging of each type of data. Decadally averaged tree-ring data are presented at Fig. 2c. The lake-sediment data before averaging were slightly chronologically corrected making use of the averaged dendroclimatic data. A need to correct the original radiocarbon datings arises from a relatively low accuracy of the radiocarbon method, which in the time span of this study (0–2000 AD) may exceed a century [Reimer et al, 2009]. Therefore, the major peaks of pollen data were brought into accord with the dendroclimatic extremes after smoothing with a 30-yr running mean. This procedure allowed us to correct the radiocarbon datings that have one to two orders of magnitude larger variance, than the dendrochronological, and also to take into account a possible peaks deviation due to a basically different resolution of various data. See Table 2 for data corrections.

A portion of the pollen data was rejected because of their low reliability. They include, in particular, the data covering the last 450 years because radiocarbon datings within this time frame are very inaccurate and may correspond even to different centuries [Reimer et al, 2009]. We have also rejected the Nadym data prior to AD 545, because the previous dated sample from this site is over 1,000 years older, and the interpolated values show reduced temperatures through 0–545 AD, whereas the data from other sites (non-interpolated) demonstrate centennial-scale variations of a

Table 2. The lake-sediment radiocarbon dating correction using the tree-ring data

C^{14} dating	Tree-ring dating correction	Event	Anomaly sign
241	265	Roman optimum peak	+
580	545	1st millennium A.D. maximum cooling	–
734	735	Early Middle Ages warming peak	+
820	815	Early Viking Age cooling	–
1023	1000	First peak of the Medieval climatic optimum	+
1108	1125	Cool interval of the Medieval optimum	–
1213	1185	Second peak of the Medieval optimum	+
1290	1295	Grand solar activity minimum (Wolf minimum)	–
1356	1365	Grand solar activity maximum	+
1429	1455	Kuwae volcano eruption	–
1441	1505	The Little Arctic optimum	+
1491	1555	Onset of the Arctic cooling	

different sign. After this screening, all pollen data were weighted and averaged.

The datasets from the Arkhangelsk, Salekhard, and Nadym sites were assigned lower weights (0.5) because they are represented in lesser detail compared to the Melikhovo and Khaypudyrskaya Guba and, therefore, contain more interpolated, and not measured values.

The averaged pollen data are presented at Fig. 2c. During the data compiling process, we also considered variants of pollen data assimilation with *no datings correction* and *no data weighting* (i.e. all data averaging with equal weights). The reconstructions developed making use of different variants of pollen data assimilation are presented at Fig. 3 and discussed below.

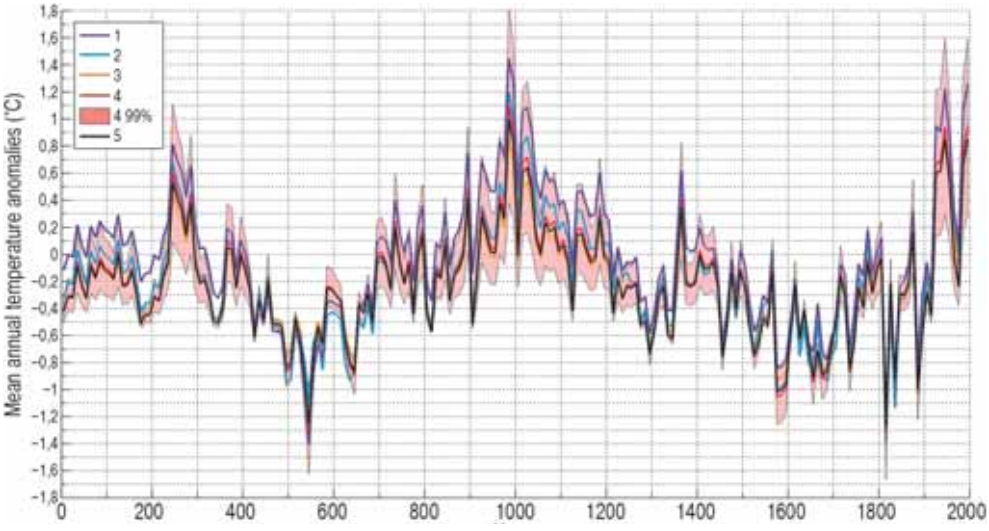

Fig. 3. Different versions of the reconstruction with various modifications of pollen data:

1) no dating correction and no weighting; 2) with dating correction and weighting. Versions of the reconstruction with different calibration: 3) calibration on the instrumental period with the same mean and variation; 4) calibration on the instrumental period, linear regression, with 99% confidence level; 5) calibration based on the arctic amplification effect and minimum values deduced from early instrumental data. Reference period: 1951–1980

Description of averaging and calibration

For the final reconstruction, we used the Composite Plus Scaling (CPS) approach [Jones et al, 2009]. All selected proxy records from our network were assimilated in the following manner: the tree-ring data spanning the whole study period (1–1995 AD) were averaged with pollen (1–1555 AD) and historical (1495–1995 AD) data. The weights were taken equal.

Then we scaled the time series variance according to the known climate characteristics of the study area. Results of the past decade research show that Arctic amplification (larger temperature variability in the Arctic as compared to the variability for the Northern Hemisphere or the globe as a whole) varies within the range from 1,72 (relative to the instrumental data of the past one and a half centuries [Bekryaev et al, 2010]) to 3,4 (relative to the palaeodata through the past 3 million years [Miller et al, 2010]). Winton [2006] found the mean annual Arctic warming, on the average, 1,9 times greater than the global mean based on a set of coupled climatic models. Our reconstructed value of the maximum temperature rise during the Medieval Warm Epoch is 1,1°C; in comparison with a set of recent hemispheric temperature reconstructions [Klimenko, 2009; Moberg et al, 2005], it gives a value of Arctic amplification of 3,8, which is quite close to the upper bound of the indicated range. Nevertheless, we found it useful to bring our reconstructed data to a full correspondence with the available palaeoclimatic evidence and adjust the peak temperature anomaly in the Medieval Warm Epoch to 1,0°C. Because the temperatures at the maximum warmings (in the 980s and the 1940s) were by about 1°C above the reference 1951–1980 baselines, we have preserved variance at the expense of lowering the minimum values. Finally, the minimum values in the 1810s were set at –1,3°C according to the early instrumental data from three meteorological stations: Haparanda, Arkhangelsk, and Petrozavodsk [Peterson, Vose, 1997]. Thus, we calibrated our reconstruction against both the palaeoclimatic and early instrumental data. Besides, we used a standard calibration against the target contemporary instrumental time series. This procedure comprises a calculation of the linear regression coefficients of the reconstructed against the instrumental data with the subsequent correction of the former. We have also employed an alternative calibration approach when variation and mean of reconstructed values are set equal to those of the instrumental data. This calibration approach seems to be preferable to an ordinary linear regression as was demonstrated in [Lee et al, 2007]. See Fig. 3 for all three reconstruction versions with various calibrations and Table 3 for the

Table 3. Statistics of various reconstruction versions (departures in °C)

	R^2 on the instrumental period	Lowest value	Highest value	Mean over the recon-struction	Standard deviation
Calibration based on the effect of Arctic amplification and minimal values from the instrumental data *	0.6311	–1.2800	1.1484	–0.1611	0.4192
Calibration on the instrumental period, linear regression*	0.5410	–1.0858	0.8778	–0.1770	0.3270
Calibration on the instrumental period, mean and variance *	0.5851	–1.4584	1.1623	–0.2509	0.4524
Pollen data with dating correction and without weighting **	0.6543	–1.2800	1.1230	–0.1681	0.4003
Pollen data without dating correction and without weighting **	0.6461	–1.2800	1.0426	–0.2031	0.4085

* Pollen data with dating correction and with weighting.
** Calibration based on the effect of Arctic amplification and the minimal values of the instrumental data.

coefficient of determination (R^2) for these reconstruction models.

Fig. 3 shows that employing different variants of reconstruction calibration as well as different variants of pollen data preprocessing does not have a very strong impact on the scale of temperature variations and does not at all change a sequence of warm and cold episodes during the whole time span of the study. However, based on the whole body of knowledge concerning the Arctic climate change including the data presented in this paper, we are inclined to recommend for comparative climatic/historical studies a reconstruction variant based on the Arctic amplification effect and minimum values deduced from the early instrumental data (black line in Fig. 3).

Temperature reconstruction and its characteristics

A comparison of the final reconstruction with the instrumental record reveals their good correspondence (Fig. 4). The correlation coefficient equals 0,81 for the whole instrumental record since AD 1815, but it reaches 0,91 if we use the instrumental record since AD 1895, when the observations from all the long-term meteorological stations of the region are available (see Fig. 1). The final version of climate history of Northeastern Europe is shown at Fig. 4.

The developed reconstruction shows a high degree of the variability on the multidecadal and centennial timescales. The spectral analysis of the reconstruction was performed by the maximum entropy method (MEM). It revealed statistically significant oscillation modes of the regional temperature with periods of 499, 195, 73, 48, and 24 years (Fig. 5). We argue that the source of the oscillations with the periods around 500 and 200 years, which are apparently global, is the solar activity variation [Klimenko, 1997]. Cycles with these periods are persistently found in time-series of different solar indicators [Fyodorov et al., 1996].

As was shown in our recent study [Klimenko, 2011], a 70-yr periodicity is likely to be attributed to quasiperiodic changes of atmospheric and oceanic circulation to be known as the North-Atlantic Oscillation (NAO) and pulsation of warm water inflow into the Norway and Barents Seas connected to the

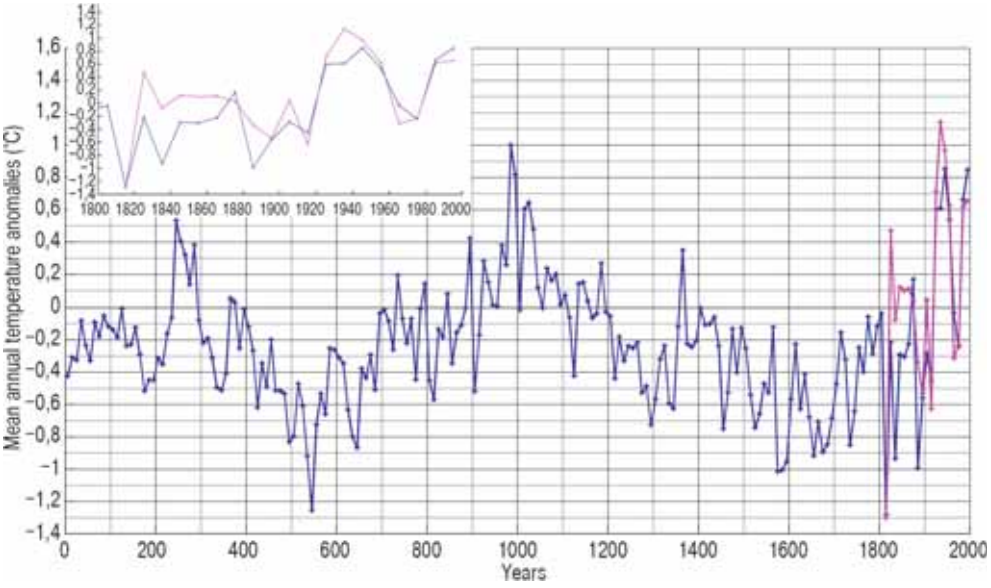

Fig. 4. The final reconstruction of the mean decadal temperature departures for northeastern Europe (blue) and instrumental data (red). The inset denotes the instrumental period. Reference period: 1951–1980

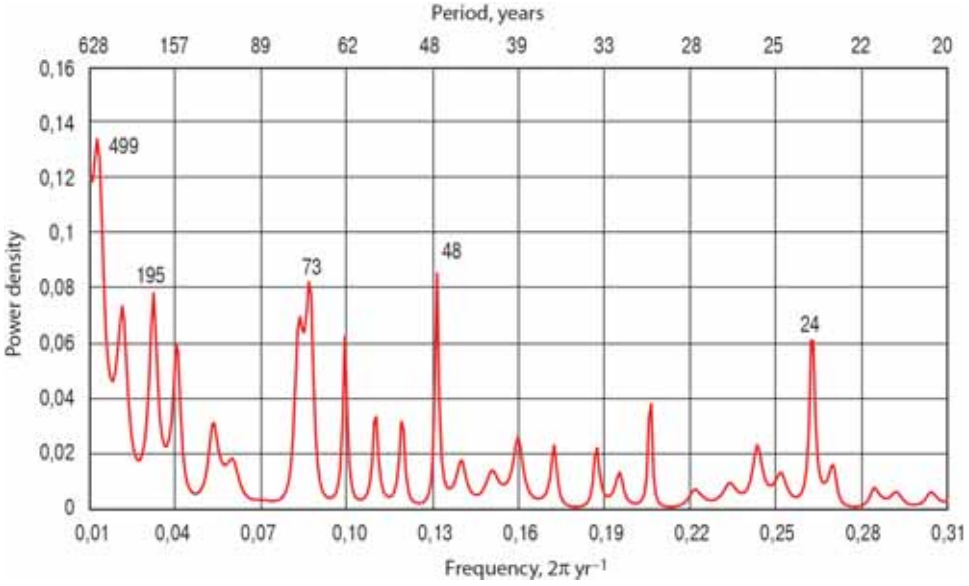

Fig. 5. The power spectral analysis of the final temperature reconstruction. Periods (yr) corresponding to the spectral peaks are shown

NAO (the Atlantic Multidecadal Oscillation, AMO). The same source is likely to explain a 50-yr periodicity – it follows from the results of simulations and reconstructions of the NAO for the last 600 years [Cook et al., 2002].

A bidecadal cycle is usually attributed to the solar forcing, but this explanation can run against some difficulties, because this cycle is well pronounced only in the oceans of the Southern Hemisphere [Klimenko, 2011]. This circumstance urges us to search its origin rather in the dynamics of the Southern Oscillation (SO), whose index has a weak spectral peak of 22 yrs. This assumption is supported by the fact that in the study region, the correlation of meteorological parameters with ENSO events is the strongest for all the extratropical zone of the Northern Hemisphere [Trenberth, 1976].

DISCUSSION

It is interesting to compare the new mean annual temperature chronology with some other reconstructions. To do this, we used a recent regional reconstruction for the Arctic [Kaufman et al., 2009], as well as reconstructions for the Northern Hemisphere [Moberg et al., 2005, Klimenko, 2009; Esper et al., 2002], and for the Northern Hemisphere extratropical regions (30°–90° N) [Ljungqvist, 2010] (Table 4, Fig. 6).

Table 4. Cross-correlations between various reconstructions

	This work	Moberg et al., 2005	Klimenko, 2009	Esper et al., 2002	Ljunqvist, 2010	Kaufman et al., 2009	Klimenko, Sleptsov, 2003
This work	1.000	0.648	0.437	0.593	0.627	0.545	0.306
Moberg et al., 2005		1.000	0.222	0.457	0.509	0.270	0.115
Klimenko, 2009			1.000	0.288	0.492	0.354	0.701
Esper et al., 2002				1.000	0.407	0.535	0.307
Ljunqvist, 2010					1.000	0.612	0.299
Kaufman et al., 2009						1.000	0.298
Klimenko, Sleptsov, 2003							1.000

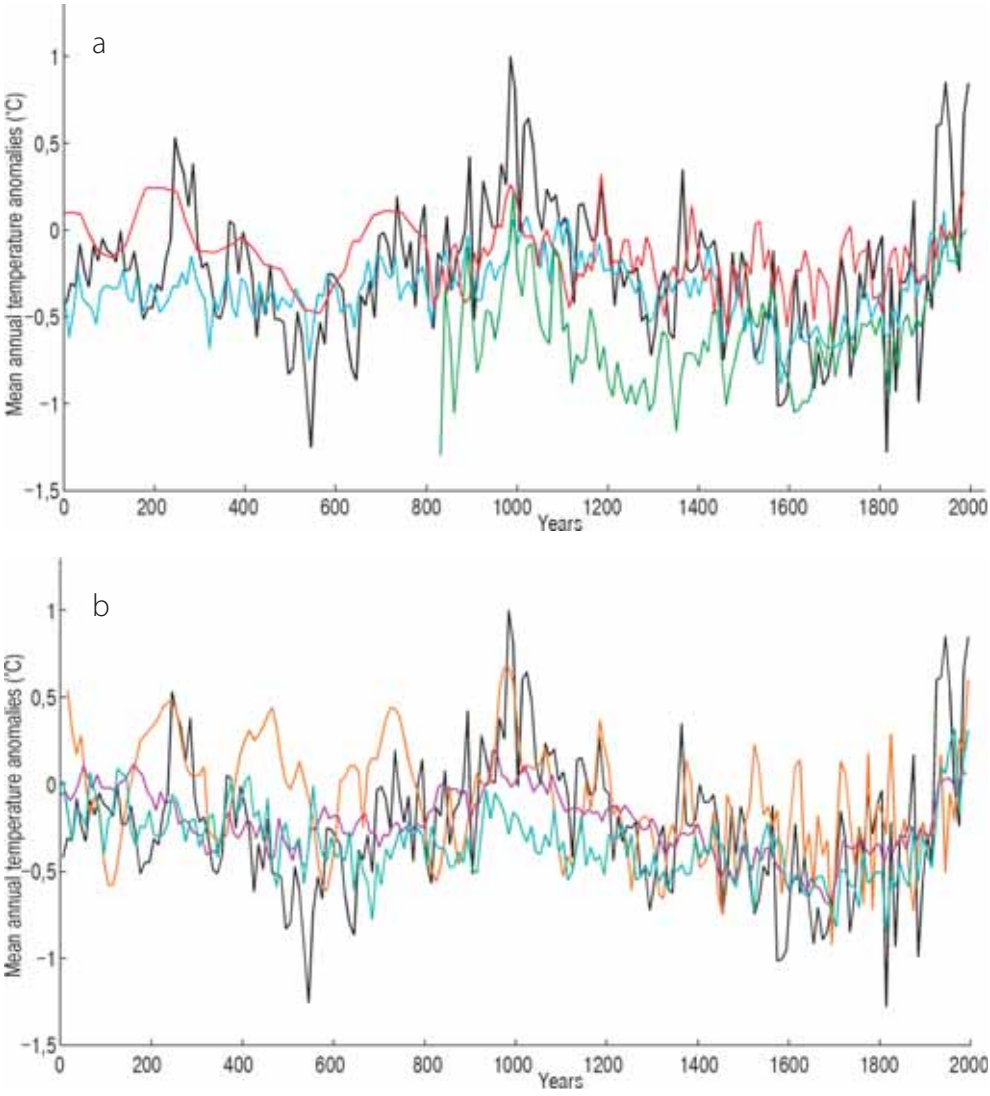

Fig. 6.

a) A comparison of the new chronology for Northeastern Europe (black) with the hemispheric reconstructions of Moberg et al. [2005] (blue), Klimenko [2009] (red) and Esper et al. [2002] (green).
b) A comparison of the new chronology for Northeastern Europe (black) with regional reconstructions: for the extratropical latitudes 30–90°N [Liungqvist, 2010] (purple), Pan-Arctic [Kaufman et al., 2009] (cyan), and the centre of the Russian Plain [Klimenko, Sleptsov, 2003] (orange). Reference period: 1951–1980

It is obvious that temperature variability in our reconstructions is much higher than in others. This fact agrees with the known effect of Arctic amplification (an increase of temperature variations in high latitude regions as compared to the whole Northern Hemisphere). According to the recent research, the effect of Arctic amplification is in the range from 1,7 to 3,4 [Bekryaev et al., 2010; Miller et al., 2010]. Speaking of the Panarctic reconstruction of Kaufman et al. [2009] (Fig. 6b), one can see that temperature variations are rather moderate. This is due to the difference of temperature variations in the Western and Eastern Arctic, which can be even in antiphase. As our reconstruction corresponds to a relatively small region, all the climatic variations should

be more pronounced. This is represented by relatively large temperature variations in our reconstruction.

All the reconstructions represent the following major climatic events of the last two millennia: the Roman Optimum (2nd and 3rd centuries), the cold epoch of the Migration Period (5th and 6th centuries), the Medieval Warm Period (the 10th to 12th centuries), notable cooling of the Little Ice Age (the 13th through the 19th centuries), and, finally, the modern warm stage (20th century). Often, the reconstructions coincide in details: all of them display pronounced warming at the end of 10th century, notable warmth at the end of the 14th and 18th centuries, sharp cold events of the 1450s and 1810s, etc. The latter events are attributed to large eruptions of Kuwae (1453) and Tambora (1815) volcanoes.

Unlike all the other reconstructions, our chronology displays quick alternations of warm and cold episodes, which are common for high latitudes. A large amplitude of temperature variations (as compared to mid latitudes) leads to an occurrence of rather short warm events (of two to four decades long) even during prolonged cold stages like the Little Ice Age (for example in 1350–1370, 1400–1440, 1470–1510, 1770–1810 AD). During these periods, temperature has reached and sometimes even exceeded the modern values. These short episodes are of special interest because they are connected with the main impetuses of pioneering and colonization of the Northeastern European margins [Klimenko et al., 2012]. Interestingly, the existence of the last three warm episodes is supported by recent studies based on different proxy data, early instrumental measurements, and numerical simulation [Crespin et al, 2009].

A comparison of our reconstruction with the reconstruction for extratropical latitudes (Fig. 6b) shows a good correspondence of long-period variations. Nevertheless, the absolute minima of the two reconstructions are different: the reconstruction of Ljungqvist [2010] has its minimum at the boundary between the 17th and 18th centuries, whereas our reconstruction – in the middle of the 6th and in the early 19th century. It can be attributed to different proxy data sets used, as well as to the different geography of the studied regions. For example, a climatic effect of volcanic eruptions is very pronounced in high latitudes while in mid latitudes, an opposite effect (warming) can be observed [Shindell et al., 2004]. This observation can explain the fact that the absolute minimum in our reconstruction occurred in the 1810s during the most powerful volcanic eruption of the last millennium (Tambora, 1815). Other significant cold events also matched the most powerful eruptions (Taupo, AD 177; Rabaul, AD 540; unindentified tropical eruption, AD 639; Ksudach, AD 900; Kuwae, AD 1453; Billy Mitchell, AD 1580; Huaynaputina, AD 1600; Awu, AD 1641; Tarumai, AD 1739; Coseguina, AD 1835; Krakatau, AD 1883; Katmay, AD 1912].

Less pronounced climatic events can differ significantly on a regional scale as is confirmed by the present day climatology [Wanner et al., 2008]. On the global scale, decadal and centennial climate change is probably dominated by radiation factors, while for the Arctic region, circulation factors are often of greater importance [Yamanouchi, 2011].

A comparison of our new reconstruction for Northeastern Europe with the reconstruction for Central Russia [Klimenko, Sleptsov, 2003] also reveals a similar interpretation of large climatic events, such as the Medieval Warm Period, Little Ice Age, and modern warm stage (Fig. 6b). But the Northeastern European chronology displays larger variability and sometimes rather big differences at decadal timescales – for example, warm periods in the late 9th and at the boundary between the 14th and 15th centuries during clearly cool episodes in Central Russia. We believe that these differences are not the shortcomings of any of the two reconstructions but reflect the real variety of climate change episodes in neighboring

regions. This statement is supported by the instrumental meteorological data of the last two centuries, when such effects were really observed – for example, abrupt warmings of the Arctic region in the 1860–70s and 1920–40s took place during stable and even cool climate stages in Central Russia.

CONCLUSIONS

In this study, we presented a multi-archive climatic chronology for Northeastern Europe based on various proxy data: tree-ring, pollen/lake sediment, and historical. We think it correctly represents the climatic history of this region for the last two millennia and can be used to elaborate a comparative chronology of climatic and historical events which has been conducted in our recent work [Klimenko et al, 2012]. Five different versions of temperature reconstruction were developed and one of them may be considered the base-case, because it, to a maximum possible extent, accumulates knowledge concerning the Northeastern European climate change in the contemporary epoch, historical period, as well as on the geological time scale. The comparison of our new reconstruction of decadal mean annual temperature with some other regional and hemispheric reconstructions shows that such large-scale climatic events as the Roman Optimum (2nd–3rd centuries AD), subsequent cooling of the Great Migration Period (5–6th centuries AD), the Medieval Warm Epoch (10–12th centuries AD), the Little Ice Age (13–19th centuries AD), and the present warm stage (20th century) are evident both on the hemispheric and regional scales. But less significant decadal and multidecadal climatic variations on a regional scale can substantially differ from the whole climatic picture on the hemispheric scale. Our reconstruction reveals a larger variance amplitude compared to the other reconstructions. We attribute this feature on one hand, to the Arctic amplification effect and, on the other hand, to a relatively small size of the study area, where climatic variations are nearly synchronous and do not cancel each other when averaged over the region.

ACKNOWLEDGEMENTS

We would like to thank the Alexander von Humboldt Foundation (Germany) for continuing support. The study was partly funded by the Grant of President of the Russian Federation MK-7354.2013.5. ■

REFERENCES

1. Aimers J., Hodell D. (2011) Societal collapse: Drought and the Maya. // Nature. Vol. 479. No. 7371. P. 44–45.

2. Andreev A.A., Klimanov V.A. (2000) Quantitative Holocene climatic reconstruction from Arctic Russia. // J. Paleolimnol., Vol. 24. No. 1. P. 81–91.

3. Bekryaev R.V., Polyakov I.V., Alexeev V.A. (2010) Role of polar amplification in long-term surface air temperature variations and modern Arctic warming. // J. Climate. Vol. 23. No. 14. P. 3888–3906.

4. Bьntgen U., Tegel W., Nicolussi K., McCormick M., Frank D., Trouet V., Kaplan J.O., Herzig F., Heussner K.-U., Wanner H., Luterbacher J., Esper J. (2011) 2500 years of European climate variability and human susceptibility. // Science. Vol. 331. No. 6017. P. 578–582.

5. Cook E.R., D'Arrigo R.D., Mann M.E. (2002) A well- verified, multiproxy reconstruction of the winter North Atlantic Oscillation Index since A.D. 1400 // J. of Climate. Vol. 15. No. 13. P. 1754–1764.

6. Crespin E., Goosse H., Fichefet T. and Mann M.E. (2009) The 15th century Arctic warming in coupled model simulations with data assimilation // Climates of the Past. Vol. 5. No. 3. P. 389–401.

7. Esper J., Cook E.R., Schweingruber F.H. (2002) Low-frequency signals in long tree-ring chronologies for reconstructing past temperature variability. // Science. Vol. 295. No. 5563. P. 2250–2253.

8. Fyodorov M.V., Klimenko V.V. and Dovgalyuk V.V. (1996) Sunspot minima dates: A secular forecast // Solar Physics. Vol. 165. No. 1. P. 193–199.

9. Gurskaya M., Hallinger M., Singh J., Agafonov L., Wilmking M. (2012) Temperature reconstruction in the Ob River valley based on ring widths of three coniferous tree species // Dendrochronologia. Vol. 30. No. 4. P. 302–309.

10. Hantemirov R.M., Shiyatov S.G. (2002) A continuous multimillennial ring-width chronology in Yamal, northwestern Siberia. // The Holocene. Vol. 12. No. 6. P. 717–726.

11. Jones P.D., Briffa K.R., Osborn T.J., Lough J.M., van Ommen T.D., Vinther B.M., Luterbacher J., Wahl E.R., Zwiers F.W., Mann M.E., Schmidt G.A., Ammann C.M., Buckley B.M., Cobb K.M., Esper J., Goosse H., Graham N., Jansen E., Kiefer T., Kull C., Кьttel M., Mosley-Thompson E., Overpeck J.T., Riedwyl N., Schulz M., Tudhope A.W., Villalba R., Wanner H., Wolff E., Xoplaki E. (2009) High-resolution palaeoclimatology of the last millennium: a review of current status and future prospects. // The Holocene. Vol. 19. No. 1. P. 3–49.

12. Kaufman D.S., Schneider D.P., McKay N.P., Ammann C.M., Bradley R.S., Briffa K.R., Miller G.H., Otto-Bliesner B.L., Overpeck J.T., Vinther B.M., Arctic Lakes 2k Project Members (2009) Recent Warming Reverses Long-Term Arctic Cooling. // Science. Vol. 325. No. 5945. P. 1236–1239.

13. Klimanov V.A., Khotinsky N.A., Blagoveschenskaya N.V. (1995) Variations of climate of the Russian Plain during the historical period // Izvestia RAN. Ser. geogr. No. 1. P. 89–96 (in Russian).

14. Klimenko V.V. (1997) On major climatic cycles of Holocene. // Transactions of the Russian Academy of Sciences / Earth Science Sections. 1997. Vol. 357A, No. 9. P. 1339–1342 (in Russian).

15. Klimenko V.V. (2009) Climate: Lost Chapter of the World History. Moscow: MEI Publ (in Russian).

16. Klimenko V.V. (2010) A Composite Reconstruction of the Russian Arctic Climate Back to A.D. 1435. // In: The Polish Climate in the European Context: An Historical Overview. Eds. Przybylak, R., Majorowicz, J., Brбzdil R., Kejna M., Berlin: Springer. Chapter 3. P. 295–326.

17. Klimenko V.V. (2011) Why Is Global Warming Slowing Down? // Doklady Earth Sciences. 2011. Vol. 440. Part 2. P. 1419–1422 (in Russian).

18. Klimenko V.V., Matskovsky V.V., Pakhomova L.Yu. (2012) High latitudes climate variations and pioneering of Northeastern Europe in the Middle Ages // History and Modernity. No. 2. P. 130–163 (in Russian).

19. Klimenko V.V., Sleptsov A.M. (2003) Complex reconstruction of climate of East Europe over the last 2,000 years. // Izvestia RGO. No. 6. P. 45–53 (in Russian).

20. Lee T.C.K., Zwiers F.C. and Tsao M. (2008) Evaluation of proxy-based millennial reconstruction methods // Clim. Dyn. Vol. 31. No. 2–3. P. 263–281.

21. Ljungqvist F.C. (2010) A new reconstruction of temperature variability in the extra-tropical Northern Hemisphere during the last two millennia. // Geogr. Ann. Vol. 92A. No. 3. P. 339–351.

22. Miller G.H., Alley R.B., Brigham-Grette J., Fitzpatrick J.J., Polyak L., Serreze M.C., White J.W.C. (2010) Arctic amplification: can the past constrain the future? // Quaternary Science Reviews. Vol. 29. No. 15–16. P. 1779–1790.

23. Moberg A., Sonechkin D.M., Holmgren K., Datsenko N.M., Karlen W. (2005) Highly variable Northern Hemisphere temperatures reconstructed from low- and high-resolution proxy data. // Nature. Vol. 433. No. 7026. P. 613–617.

24. Naurzbaev M.M., Vaganov E.A., Sidorova O.V., Schweingruber F.H. (2002) Summer temperatures in eastern Taimyr inferred from a 2427-year late-Holocene tree-ring chronology and earlier floating series. // The Holocene. Vol. 12. No. 6. P. 727–736.

25. Peterson T.C., Vose R.S. (1997) An overview of the Global Historical Climatology Network temperature database // Bulletin of the American Meteorological Society, Vol. 78. No. 12. P. 2837–2849.

26. Reimer P.J., Baillie M.G.L., Bard E., Bayliss A., Beck J.W., Blackwell P.G., Bronk Ramsey C., Buck C.E., Burr G.S., Edwards R.L., Friedrich M., Grootes P.M., Guilderson T.P., Hajdas I., Heaton T.J., Hogg A.G., Hughen K.A., Kaiser K.F., Kromer B., McCormac F.G., Manning S.W., Reimer R.W., Richards D.A., Southon J.R., Talamo S., Turney C.S.M., van der Plicht J., Weyhenmeyer C.E. (2009) IntCal09 and Marine09 Radiocarbon Age Calibration Curves, 0-50,000 Years cal BP. // Radiocarbon. Vol. 51. No. 4. P. 1111–1150.

27. Shindell D.T., Schmidt G.A., Mann M.E., Faluvegi G. (2004) Dynamic winter climate response to large tropical volcanic eruptions since 1600 // J. Geophys. Res. Vol. 109. No. D05104. doi:10.1029/2003JD004151.

28. Trenberth K.E. (1976) Spatial and temporal variations of the Southern Oscillation // Quart. J. Royal Met. Soc. Vol. 102. No. 433. P. 639–653.

29. Velichko, A.A., Andreev A.A., Klimanov V.A. (1997) Climate and vegetation dynamics in the tundra and forest zone during the Late Glacial and Holocene. // Quaternary Int. Vol. 41/42. P. 71–96.

30. Wanner H., Beer J., Butikofer J., Crowley T.J., Cubasch U., Fluckiger J., Goosse H., Grosjean M., Joos F., Kaplan J.O., Kuttel M., Muller S.A., Prentice I.C., Solomina O., Stocker T.F., Tarasov P., Wagner M., Widmann M. (2008) Mid- to Late Holocene climate change: an overview. // Quaternary Science Reviews. Vol. 27. No. 19–20. P. 1791–1828.

31. Winton M. (2006) Amplified Arctic climate change: What does surface albedo feedback have to do with it? // Geophys. Res. Lett. Vol. 33. L03701. doi:10.1029/2005GL025244

32. Yamanouchi T. (2011) Early 20th century warming in the Arctic: A review. // Polar Science. Vol. 5. No. 1. P. 53–71.

Vladimir Klimenko is Full Professor and Head of Global Energy Laboratory at Moscow Power Engineering Institute. He received his Ph.D. degree in 1975 and D.Sc. degree in 1985 in thermal physics. His research interests are associated with energy and environment interaction, global climate change, palaeoclimatology, climate influence on social history, driving forces of the historical process. Main Publications: Climate of the Medieval Warm Epoch in the Northern Hemisphere (2001); Cold Climate of the Early Subatlantic Epoch in the Northern Hemisphere (2004); Climate: Lost Chapter of the World History (2009); A Composite Reconstruction of the Russian Arctic Climate Back to A.D. 1435 (2010).

Vladimir Matskovsky is Scientific Researcher at the Institute of Geography, Russian Academy of Sciences. He graduated in 2008 with diploma in computer science and received his Ph.D. in paleogeography in 2011. His main research interests are dendrochronology, dendroclimatology, and high resolution climate reconstructions. He participated in numerous expeditions to different parts of Russia. He is Principal Investigator of two research projects and the author and co-author of more than 20 papers and 1 monograph.

Dittmar Dahlmann is Full Professor and Head of the Department of East European History at the Rheinische Friedrich-Wilhelms-Universitдt, Bonn. He received his Ph.D. degree in 1983 and his Habilitation in 1994. His research interests are in the history of Siberia and in the history of Science in the 18th and 19th centuries. Main Publications: Sibiren vom 16. Jahrhundert bis zur Gegenwart (2009); Carl Heinrich Merck. Das sibirisch-amerikanische Tagebuch aus den Jahren 1788–1791 (2009, eds).

Alba Fuga
Laboratoire Sisyphe, UMR 7619, Université Pierre et Marie Curie Paris VI,
e-mail : alba.fuga@neuf.fr

ZONES D'INTERFAÇAGE GEOGRAPHIQUE ET METHODE DE COMPARAISON AUTOMATIQUE DE DONNEES

GEOGRAPHIC INTERFACE AREAS AND METHODS OF AUTOMATIC DATA COMPARISON

RÉSUMÉ. Dans le cadre de l'analyse d'un territoire sur le plan géophysique, et dans le but d'en identifier les ressources naturelles, de nombreuses informations sont acquises. Il s'agit de classifier, caractériser, et interpréter des mesures obtenues par campagnes de navigation sismique, par carottage, acquises dans des puits de forage, ou encore par campagnes de prélèvement d'échantillons.

La problématique qui accompagne cette analyse de territoire concerne d'une part la gestion des données complexes et volumineuses dans leurs lieux de stockage. D'autre part la question de l'aide à l'interprétation est posée lorsqu'il s'agit de classifier et comparer de la manière la plus automatique possible ces représentations et caractérisations du territoire. Dans ce contexte ont été développés la méthodologie et les programmes LAC (Logiciel Automatique de Comparaisons).

L'un des mécanismes mis en place dans cette méthodologie concerne l'interaction entre un système de filtrage à tamis de critères de comparaison et un système de seuillage pour définir une résolution de comparaison et de regroupement. Cette résolution représente un élément clé de l'analyse car elle permet de détecter des zones d'interfaçage, de frontière, ou de changement de milieu, tout en qualifiant un caractère plus ou moins progressif de ces frontières. Après une première description de la méthodologie LAC, nous voyons de quelle manière elle s'applique aux données de géosciences et comment on peut la décliner sur le plan géographique.

MOTS CLÉ: Ressemblance, métrique de similarité, groupe de similarité, résolution, seuil de tolérance, zone d'interfaçage

ABSTRACT. Numerous data are registered when a territory has to be analyzed in its geophysical configuration and behavior, in order to identify natural resources. All this information acquired through seismic navigation surveys, drilling, or sample withdraw, needs to be classified, characterized and interpreted.

This territory analysis process goes along with the management of complex and voluminous data. Automatic interpretation assistance is moreover needed to find a methodology that could optimize and automatize big geoscience data comparisons in order to automatically characterize a territory. In this context LAC (Logiciel Automatique de Comparaisons) methodology and programs have been designed and coded.

The interaction between comparison criteria filtering system and a threshold adjustment

system is one of the mechanisms involved in this methodology, in order to define a comparison and clustering resolution. This resolution is a key analysis element which makes geographic interface areas, border areas, or environment changes be detected. After a first description of LAC methodology, the way it is applied to geoscience data, and how it can be developed in the geographic field, will be explained.

KEY WORDS: Similarity, similarity metrics, similarity groups, resolution, tolerance threshold, geographic interface area.

INTRODUCTION : L'APPROCHE LAC DE COMPARAISON AUTOMATIQUE DE DONNÉES

La méthodologie générale est basée sur des algorithmes de classification automatique couplés à une série de mesures de similarité hiérarchisées.

L'objectif de la méthodologie LAC est de fournir un outil d'analyse de l'information territoriale et géophysique par la mesure de ressemblance, et par la réalisation de comparaisons suivant au plus près les raisonnements pouvant être faits par les experts métier.

La ressemblance peut être perçue comme le jugement ou l'évaluation de la proximité conceptuelle entre objets, selon une résolution donnée. On peut prendre l'exemple de la ressemblance en positionnement. Deux objets sont semblables en positionnement s'ils sont "suffisamment" proches, selon la distance euclidienne, orthodromie, ou loxodromie… L'adverbe "suffisamment" est relatif à la résolution à laquelle on juge de la ressemblance, ou encore au facteur de tolérance utilisé. On peut considérer que deux points de l'espace sont semblables si la distance euclidienne qui les sépare est inférieure à 1 unité de mesure. Il s'agit d'une notion extrêmement proche de la notion de limite en analyse mathématique. Deux objets sont proches s'ils tendent l'un vers l'autre. Ici, la différence est que l'on ne se place pas sur l'ellipsoïde, ou dans l'espace euclidien à 3 dimensions, mais on se place dans un "espace de similarité", c'est-à-dire un espace ayant autant de dimensions que le nombre de critères de comparaison, et régi par la métrique induite un l'arbre de décision.

Un arbre de décision est ici défini comme un arbre binaire, ou automate, permettant de savoir quelle métrique de similarité et quels facteurs de tolérance on applique si à l'étape précédente les objets comparés ont été identifiés comme similaires, et quelle métrique et facteurs on applique sinon. Un tel arbre permet la comparaison multicritères, aux facteurs de tolérance près. Il permet également de donner un indicateur signifiant le degré de ressemblance des objets comparés. Cet indicateur est relatif au cheminement de la ressemblance dans l'arbre. Cet arbre ou automate constitue lui-même un algorithme et donc une métrique de similarité évoluée, ou composée.

L'automatisation informatique de ces mesures de ressemblance et de ces comparaisons assure le croisement multicritères d'un grand nombre d'informations en peu de temps. Par exemple, le système croise en 5 minutes de comparaison 4000 lignes de navigation sismique. Une ligne de navigation sismique est un objet géo-scientifique complexe car mettant en jeu plus de 20 critères de comparaison hétérogènes pour la plupart.

LA MODÉLISATION ET LES CRITÈRES DE COMPARAISON

Le phénomène que l'on souhaite analyser, ou le territoire que l'on souhaite explorer est modélisable par un ensemble d'attributs et de caractéristiques. Certaines de ces caractéristiques constituent des critères pertinents de comparaison entre les différentes configurations d'un même phénomène sur ce territoire. Une acquisition est une mesure, un enregistrement, de l'un de ces critères de comparaison. Elle est une réalisation physique du critère. Cependant, comme toute mesure et tout enregistrement, elle a une nature et une unité de mesure. Par "donnée", on entend ici l'ensemble des informations, acquisitions

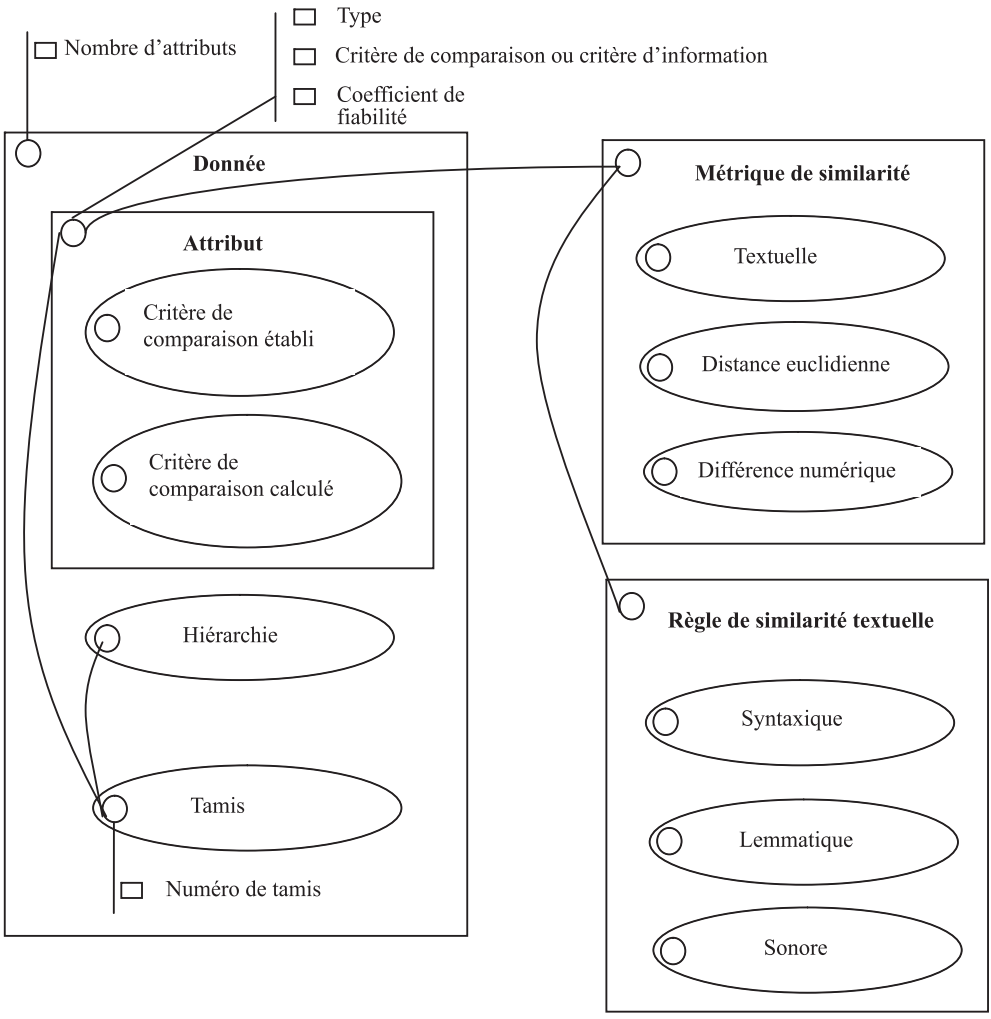

Fig. 1 : Schéma HBDS de la méthodologie LAC

directes ou déduites réalisant un modèle d'un phénomène physique, ou une configuration physique.

Dans l'approche LAC, la première phase de la méthode de comparaison est la modélisation de la donnée ou du phénomène. Ensuite, il est nécessaire d'identifier les différentes catégories d'attributs, en distinguant les attributs critères de comparaison des attributs de renseignement qui ne serviront pas à la comparaison des données.

Dans une deuxième phase méthodologique, les critères de comparaison établis ou calculés sont classifiés eux-mêmes. Il s'agit de les ranger par catégorie, par tamis. Les critères de la classification attributaires sont la fiabilité mathématique, la pertinence de comparaison (ou degré de caractérisation de la donnée), la robustesse du facteur de tolérance.

La fiabilité mathématique concerne la formule mathématique de calcul de l'attribut et son adéquation plus ou moins grande avec le phénomène modélisé. Par exemple, une longueur pour une ligne de navigation sismique peut être calculée soit par interpolation et abscisse curviligne, soit par sommation des segments entre points

de tir. L'abscisse curviligne est le moyen mathématique approchant le plus la réalité de la longueur d'une ligne, mais ce n'est pas forcément l'appareil mathématique utilisé, notamment s'il faut faire face à une problématique de performances temporelles des comparaisons et calculs d'attributs.

Le critère de pertinence de comparaison vise à ordonner les attributs selon leur capacité à caractériser le phénomène ou la donnée modélisée. Par exemple, pour une modélisation de cours d'eau, la couleur des pierres dans l'eau serait un critère moins caractérisant que sa profondeur ou son débit à des points précis, ou en moyenne.

Concernant la robustesse des facteurs de tolérance qui sont ces seuils de résolution nous permettant de savoir à partir de quelle proximité les objets sont suffisamment similaires, leur fiabilité peut dépendre de la zone géographique où est prise la donnée. Par exemple, les noms donnés aux objets géographiques peuvent être plus ou moins éloignés d'un nom standard selon le pays dans lequel ils sont saisis. Alors on devra prendre en compte dans le seuil de tolérance le pays d'acquisition des données. Pour l'exemple de modélisation d'un cours d'eau, le débit change en fonction de la saison, selon le climat de la zone géographique ciblée. Le seuil de tolérance choisi pour comparer des débits de cours d'eau n'est donc pas aussi robuste et générique qu'un attribut que serait le nombre de barrages sur le cours d'eau à une date donnée, par exemple.

Une fois que les attributs sont classés dans des tamis, et que les tamis sont eux-mêmes hiérarchisés, on peut aborder la question des métriques de similarité attributaire et élémentaire.

LES MÉTRIQUES ATTRIBUTAIRES DE SIMILARITÉ – SPÉCIALISATION EN FONCTION DES CRITÈRES DE COMPARAISON

A chaque nature d'acquisition correspondent une unité de mesure et une métrique. On peut considérer qu'une métrique de similarité est une formule mathématique, ou algorithme permettant de comparer deux objets selon un critère unique afin d'évaluer s'ils sont similaires ou non. La comparaison se fait au facteur de tolérance près. Un simple comparateur ">" (supérieur ou égal) peut constituer une métrique de similarité. Par exemple, pour comparer deux profondeurs totales de puits de forage, on utilise une simple soustraction métrique. Pour comparer deux positions géo-référencées, on utilise une distance euclidienne si on a à faire à des coordonnées planes, ou bien une orthodromie ou une loxodromie si on manipule des coordonnées géographiques.

De la même manière, on définit dans la méthodologie LAC un ensemble de comparateurs. Ils sont applicables aux métadonnées que représentent les conditions d'acquisition comme un nom de campagne sismique, un nom de ligne de navigation sismique ou des noms de documents et rapports techniques, d'avis donnés sur les conditions d'acquisition ou sur la fiabilité des mesures. Les comparateurs s'appliquent aussi aux métadonnées déduites, c'est-à-dire calculées à partir d'acquisitions. Il peut s'agir de préfixes, suffixes déduits, de noms d'auteurs extraits, d'enveloppes convexes, centroïdes, azimuts et autres éléments pouvant être déduits et calculés depuis les acquisitions. Ces comparateurs et métriques concernent donc aussi bien des données numériques, géométriques que textuelles.

Un ensemble de comparateurs peut donc être attribué à chaque tamis de critères de comparaison, en fonction de la nature et de la fonction des critères qu'il contient. Par exemple, afin de rechercher certains noms de roches dans des titres de documents divers, il est nécessaire :

- De disposer d'un dictionnaire de synonymes, ou abréviations connues de roches que l'on souhaite chercher

- De prendre en compte le fait que ces noms peuvent être écrits dans les titres avec des insertions de caractères spéciaux

– De prendre en compte qu'il arrive parfois qu'on trouve dans ces titres un système de numérotation avec la présence potentielle de zéros non significatifs

L'analyse de l'information dépend donc d'une part de la modélisation du territoire et du phénomène, d'autre part de métriques de similarité spécifiques aux différents attributs. Elle dépend également de trois autres éléments : du type de classification que l'on effectue, de la hiérarchie des critères de comparaison, et du paramétrage des seuils de tolérance pour les comparateurs. Par la suite, on portera l'attention sur la notion de résolution que contient cette méthodologie, ainsi que sur ce qu'elle implique en termes d'analyse de l'information.

TROIS STRATÉGIES DE CLASSIFICATION – PRINCIPE DE RÉSOLUTION

On peut distinguer dans cette approche trois types de regroupements : les couples, les groupes asymétriques, et les clusters. Chacune de ces méthodes est appropriée à une problématique spécifique. Tout comme l'élaboration de métriques de similarité sur mesure selon la nature et la fonction des critères de comparaison, on attribue une méthode de classification spécifique à une problématique donnée. L'approche LAC est donc une approche adaptative. On répertorie les différentes problématiques, et pour chacune, on préconise une configuration donnée de LAC.

Par exemple, dans certaines bases de données, les informations peuvent être lacunaires, c'est-à-dire que tous les attributs caractérisant une donnée ne sont pas renseignés. Comment traiter alors ces attributs vides ? Dans les métriques de similarité attributaire, on peut considérer que les deux attributs comparés dont l'un vide sont soit exactement similaires, soit exactement différents. Cependant, selon la position hiérarchique de l'attribut dans son tamis, et du tamis parmi les autres tamis, si les attributs lacunaires ne sont pas bloquants, cela peut causer une baisse de précision dans la comparaison. Il faut donc encore choisir le comportement à adopter par rapport aux données lacunaires selon le contexte, la configuration des données, et la problématique visée.

Les différentes problématiques envisagées jusqu'à présent dans le cadre de la gestion du territoire, de l'analyse des risques et d'une meilleure exploitation des ressources naturelles, sont :

– l'harmonisation des bases de données afin d'enlever des doublons et de ne garder que les données les plus précises

– la réconciliation d'informations et de différents supports

– la reconstitution et le rattachement documentaire

– le géo-référencement

– le croisement multicritère pour l'analyse et l'interprétation des phénomènes

Couples et réconciliation de sources

Les couples sont des regroupements deux à deux de données, pouvant suivre des contraintes de regroupement comme la règle "on ne doit jamais retrouver dans un même couple deux données provenant d'une même source". Ce type de procédé est nécessaire lorsqu'on l'on souhaite fusionner ou réconcilier des bases de données. Il peut servir aussi lors du chargement de nouvelles données dans une base de référence, pour savoir si les données à charger ne sont pas déjà contenues en base. Ce procédé est aussi utile pour savoir quelles sont les données qu'on veut comparer une base que l'on possède déjà aux métadonnées d'une base qu'on souhaiterait acheter, afin de voir quelles données il est réellement nécessaire d'acheter.

Fusionner des informations concernant une même zone géographique demande de résoudre les cas de recouvrement

d'informations. Parfois des acquisitions peuvent avoir été faites par différentes technologies, ou méthodologies, différents traitements, notamment d'analyse du signal, peuvent avoir été appliqués sur les données. Doit-on alors fusionner les différentes bases de données en réalisant simplement une union d'ensembles, ou doit-on les fusionner de manière plus sélective afin de ne garder que les informations les plus complètes, de la meilleure qualité ?

La seconde solution permet d'optimiser notre aptitude à lire et analyser, puis prendre des décisions sur ces données. La classification par couplage permet donc la réconciliation de différentes sources de données. Elle permet aussi de vérifier s'il n'y a pas eu perte de données lors de migrations de bases ou de changements de support de stockage de l'information.

Groupes asymétriques et rattachements

Les groupes asymétriques correspondent à une situation où l'on souhaite rattacher des informations par recoupements afin de former un puzzle complet des données dont on dispose. Par exemple, on peut posséder d'un côté des cartes géo-référencées d'une zone, d'un autre côté des identifiants de puits de forage, des noms de puits, des rapports techniques de forage, des rapports et études de zones à risques naturels. Toutes ces données et ces rapports peuvent être nombreux, volumineux, et la liaison des éléments se référant aux mêmes phénomènes ou objets physiques peut être quasi impossible de manière manuelle. Notre approche permet ici de se baser par exemple sur un puits de forage et de lui rattacher l'ensemble des documents techniques dans les titres desquels on retrouve le nom de ce puits approximativement écrit, ou ses coordonnées plus ou moins exactement saisies. Le terme "approximativement" fait référence aux seuils de résolution exposés plus haut. Nous pouvons alors rattacher à une zone connue pour un risque naturel spécifique tous les puits qui ont un positionnement, ou des caractéristiques permettant de considérer qu'ils sont rattachables à cette zone. On construit donc de manière successive des relations 1-N d'appartenance, c'est-à-dire un puits lié à plusieurs documents, une zone liée à plusieurs puits.

Clustering, propagation, harmonisation

Le troisième type de regroupement utilisé est la classification hiérarchique ascendante par densité. La notion de densité utilisée est basée sur la mesure de similarité élémentaire suivant l'approche LAC. Il s'agit d'une mesure de similarité sur les objets, les futurs éléments de groupes, avec tous les attributs.

Dans cet algorithme de classification, on attribue dès le départ à chaque donnée un numéro de cluster. Au début, elles ont toutes le numéro du cluster inexistant. Ensuite, on compare la première donnée de la liste aux autres. Si on trouve des données qui lui sont suffisamment similaires (une donnée suffit), alors on affecte à ces données le même numéro de cluster, différent du numéro du cluster vide. Lorsqu'on en a fini avec la première donnée de la liste, on continue avec la deuxième, "donnée courante", seulement si elle porte toujours le numéro du cluster inexistant, donc si elle n'a pas déjà été affectée à un cluster existant. Si une donnée est suffisamment similaire à une donnée déjà contenue dans un cluster, alors nous avons deux possibilités. Soit la donnée courante porte le numéro du cluster inexistant, et n'est pas dans un cluster avec

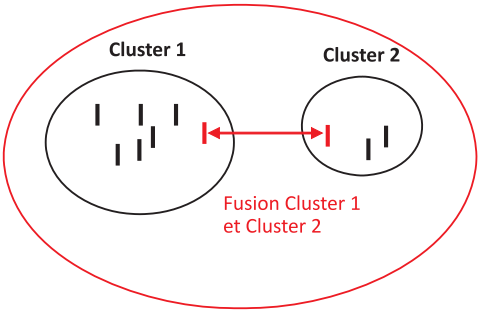

Fig. 2. Exemple de fusion entre deux clusters. Phénomène de "contagion"

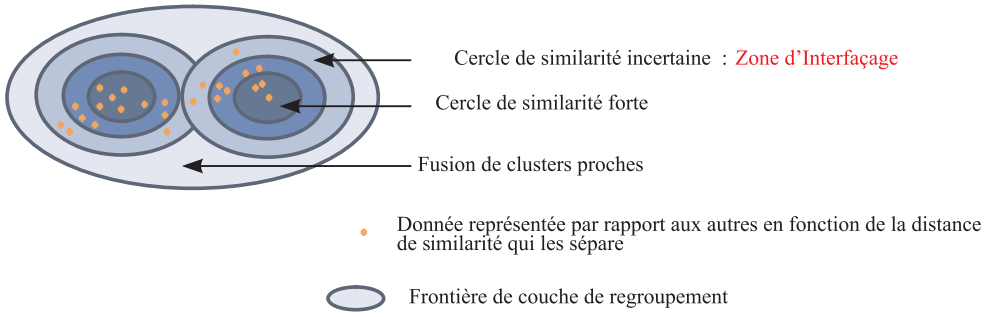

Fig. 3. Représentation de données dans un graphique de similarité, avec les contours de clusters formés selon différents vecteurs de similarité

d'autres données. On peut alors directement l'affecter au cluster de la donnée qui lui ressemble. Soit la donnée courante est déjà dans un cluster différent du cluster de la donnée qui lui est similaire. Il faut alors fusionner les deux clusters.

Quelles que soient les sources des informations et leur nombre, il s'agit de regrouper les objets similaires selon le vecteur de résolution. Il est possible de fusionner des groupes dont les données extrêmes sont au-delà du seuil de résolution, si d'autres données sont suffisamment proches. Ici on aborde une notion de continuité entre objets composites, dans le domaine de la similarité. Ces fusions peuvent se comporter comme des phénomènes de propagation par voisinage. Selon cette cartographie d'entités complexes et composites, il est possible de prendre, ou non, des décisions de fusion, d'intégration ou de séparation. Une autre possibilité est de choisir, ou construire un représentant d'un cluster, comme c'est le cas lorsqu'on raccorde en continuité deux lignes de navigation sismique si l'une des lignes possède des coordonnées de points de tir légèrement translatés.

La particularité de ces algorithmes de classification est leur couplage avec un système de filtrage qui correspond à la mise en tamis hiérarchisés des critères de comparaison dans les premières phases méthodologiques, ainsi qu'à l'affectation de métriques attributaires spécialisées à aux différentes natures de critères. La classification est automatique, ainsi que l'application du système de filtrage et des mesures. Par contre, il faut mettre l'accent sur le fait que la modélisation préalable du phénomène et la mise en tamis des critères dépendent d'un travail d'intelligence humaine.

Résolution et zone d'interfaçage

Le choix entre deux lignes de navigation sismique par exemple dépend de la résolution à laquelle on regarde ces lignes. Il s'agit de la résolution de similarité. Selon la méthodologie LAC, la similarité est mesurée de manière attributaire par les métriques de similarité spécifiques à chaque nature de critère de comparaison, mais également de manière élémentaire par association de ces mesures attributaires. La mesure élémentaire dépend d'une hiérarchie et d'un classement que l'on effectue entre les critères de comparaison, selon leur potentiel discriminatoire, et leur fiabilité.

On considère alors comme similaires deux objets dont la mesure de similarité est supérieure à un seuil de résolution pouvant être défini par l'utilisateur souhaitant analyser les données.

Ce seuil de résolution peut être défini comme un vecteur de seuils de résolution attributaire, chacun définissant une résolution attributaire sur un critère de comparaison du modèle. Par exemple, pour analyser une zone géographique sur laquelle

on a obtenu des traces de signaux à partir de géophones et sismographes, on pourra considérer que pour deux signaux similaires (même positionnement, mêmes longueurs d'ondes reçues), la trace la plus longue sera la plus complète, et la trace ayant le pas d'étalonnage le plus petit sera la plus précise. Si on considère que la précision est plus importante pour une étude de territoire, on considèrera que la trace la plus précise, même si elle est moins complète, prédominera.

Le paramétrage du vecteur de résolution permet de définir non seulement le moment à partir duquel on discrimine différents groupes, mais aussi de définir la limite d'interfaçage entre les différents groupes. Si l'on compare donc des données dans le but de les harmoniser, retirer les redondances, faire varier le vecteur de similarité permet de mettre en évidence des caractéristiques de dispersion de celles-ci, et de distinguer différentes cercles de certitude dans un même cluster.

En outre, il est nécessaire de remarquer que ces traitements appliqués à des données géographiques et géophysiques vont bien au delà du traitement de positionnement des données en deux ou trois dimensions. Dans cette approche, on est capable de simuler des phénomènes de regroupement en prenant en compte des paramètres comme des débits, des descriptions textuelles, des couleurs, des profondeurs, un âge, des types de roches et tout autre élément caractérisant la donnée.

Il s'agit d'un "positionnement" géographique étendu. Ce qui nous permet de reconnaître un objet, de le distinguer des autres est la représentation que l'on s'en fait, et notre manière de le placer, de le positionner par rapport aux autres. Dans cette approche, les coordonnées géographiques, projetées ou non, sont complétées par autant d'autres "coordonnées", critères de comparaison, qui nous permettent de construire une représentation plus proche du territoire ou du phénomène réel.

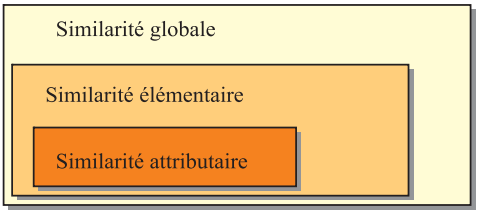

Fig. 4. Les trois échelles de mesure de Ressemblance

Ici, il est intéressant d'aborder la question de la visualisation des ces données complexes car constituées de nombreux attributs servant au traitement. La carte à deux dimensions serait un premier outil de représentation, mais très rapidement limité. En effet, si l'objectif d'un traitement est de retrouver les erreurs de positionnement géographique des données grâce à des comparaisons sur d'autres critères les caractérisant, alors sur une carte à deux dimensions, certains éléments appartenant au même cluster seraient "regroupés" de manière spatialement discontinue.

Ce type de représentation par carte répond à un besoin de placer les groupes les uns par rapport aux autres. Il s'agit d'un besoin d'une vision globale du traitement et des groupes. Dans le cas de la carte géographique classique, une représentation possible serait sorte une anamorphose en fonction des mesures de similarité entre les clusters. Il s'agirait d'adopter en premier le point de vue du groupe, de placer tous les objets du groupe les uns par rapport aux autres selon les mesures de similarité, comme si la similarité élémentaire (par opposition ou attributaire) était une "force d'attraction".

Une fois cette dispersion par cluster effectuée, il s'agirait de placer les clusters les uns par rapport aux autres selon des mesures de similarité entre clusters. Ces distances entre groupes sont également liées aux zones d'interfaçage entre lesdits groupes. Un autre intérêt de ce type de représentation peut être trouvé dans le fait que les zones d'interfaçage, zones frontalières sont alors représentées selon la dispersion des éléments et des groupes dans cet espace de similarité.

La question que l'on peut se poser concerne alors le lien faisable entre une carte

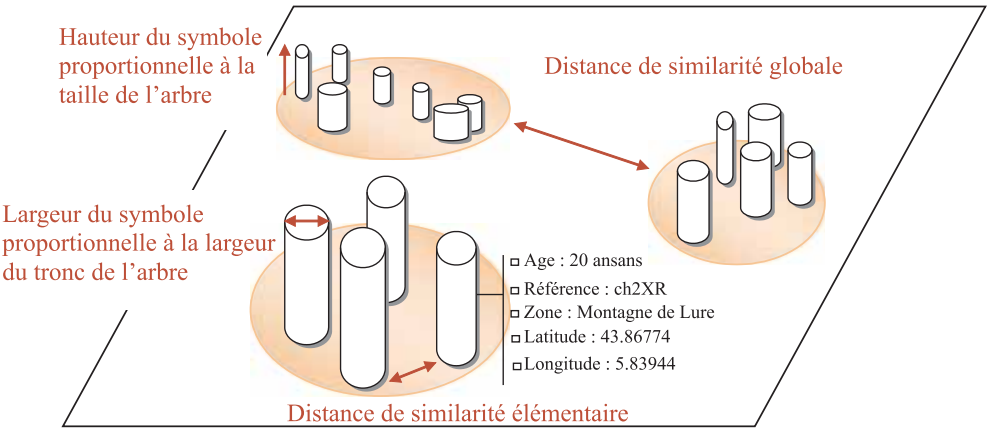

Fig. 5. Une possibilité de visualisation de clusters. Exemple sur des arbres que l'on a classifié selon leur taille, la largeur de leur tronc et leur positionnement géographique

géographique construite par projection de coordonnées, et une telle carte de similarité.

Le premier lien possible consiste en la réalisation d'une carte de similarité numérique en trois dimensions, où la troisième dimension permettrait l'affichage d'attributs nous permettant de faire le lien avec les cartes en projection géographique. Ces attributs seraient des toponymes, des coordonnées géographiques, les langues parlées dans les zones concernées, par exemple, l'idée étant pour le lecteur de pouvoir se repérer entre les différents modes de représentation.

CONCLUSION – L'APPLICATION À DES ZONES D'INTERFAÇAGE DE DONNÉES GÉOPHYSIQUES

L'approche LAC permet aujourd'hui d'harmoniser, réconcilier des bases de données géophysiques, et rattacher des informations les unes aux autres, dans le but d'un meilleur accès à la donnée, et à un gain de place de stockage de l'information. En l'appliquant sur des données géographiques, océanographiques et géophysiques, les croisements et classifications que l'on obtient peuvent permettre d'étudier l'évolution de limites et frontières naturelles entre différents écosystèmes, de repérer des caractéristiques identitaires prédominantes, des zones frontalières d'interfaçage plus ou moins progressives ou des variations brutales du territoire. Des méthodes de visualisation de ces zones et de ces traitements où la mesure de ressemblance à différentes échelles serait la règle de représentation sur ces "cartes de similarité". Ces méthodes de visualisation sont en cours d'étude car elles demandent la définition de stratégies de projection de la similarité en trois dimensions au maximum. ■

Alba Fuga – Ingénieure en Systèmes d'Information Géographiques, elle met actuellement en production le système expert qu'elle a conçu pour le Data Management chez TOTAL, basé sur la méthodologie LAC. Elle poursuit ses recherches en mesure de ressemblance entre données géo-scientifiques dans le cadre d'un Doctorat à l'Université française Pierre et Marie Curie.

Andrey A. Lukashov[1*], Stepan V. Maznev[2]
[1] Faculty of Geography, Lomonosov Moscow State University, Russia. 119991, Moscow, Leninskiye Gori, 1. Tel: (+7 495) 939 54 69; E-mail: smoluk@yandex.ru
[*] **Corresponding author**
[2] Faculty of Geography, Lomonosov Moscow State University, Russia. 119991, Moscow, Leninskiye Gori, 1. E-mail: stepusja-bdsm@mail.ru

MORPHOSTRUCTURE OF THE KODAR-UDOKAN SECTION OF THE BAIKAL RIFT ZONE

ABSTRACT. The morphostructure of the region is a natural result of active geodynamics in the eastern Stanovoe Upland. Extreme seismic conditions become apparent in rare devastating earthquakes (up to 10–11 in the Mercally scale), as well as in frequent slight ones. Seismic events affect topography and produce seismic deformations of different scale and morphology. Areal disturbances (like the New Namarakit Lake in the South-Muya Mountains origin) and, more often, local deformations (like destructions of the Kodar ridge rocky saddles or clamms [gorges] opening) are evident. Using morphotectonic analysis methods the morphostructural scheme of the Kodar-Udocan section of the Baikal rift zone (perhaps pull-apart basin) is done. In our model piedmont and mountain territories are divided in five level groups of blocks. Neotectonic movements' amplitude is estimated at 5000 m.

KEY WORDS: Chara basin, morphotectonics, active tectonics, block analysis, seismoalpine topography, seismic deformations.

INTRODUCTION

The Baikal rift zone is the most seismically active continental region in Russia (Fig. 1) [New seismic map..., 1996]. Dozens of $M_W \geqslant 4$ and hundreds of $M_W < 4$ earthquakes happen here every year [Earthquakes..., 2007; Earthquakes..., 2009]. Such tense seismic conditions reflect in impressive morphostructures in the Kodar-Udokan segment – one of the most active parts of the rift. The Kodar-Udocan section of the Baikal rift zone (perhaps, pull-apart basin [Explanatory dictionary..., 2002]) is located on its eastern flank. As is well known, in the Pleistocene and the Holocene, the Baikal rift zone was subjected to magmatogene activity [Active tectonics..., 1966]. The section includes the Chara (or Upper-Chara) basin, the Kodar and the Udokan ridges on its sides, and the interbasin tectonic sowneck between the Chara and the western Muya basins. We can consider the Kodar-Udokan section to be the outermost eastern pronounced rift segment. The issue of the eastern rift closing remains an open problem. Thirty kilometers easterly is the feebly marked Tokko basin; it gives us no reason to search for the rift closing in the Chara basin. In this paper, we concentrate on the tectonic aspect of the morphostructure evolution and are putting aside many issues concerning the morphological expression of the Quaternary volcanism in region.

GEODYNAMICS

The formation of the Baikal rift zone became possible because of the existence of the border between the thick (more than 50 km), cold, and strong pre-rift lithosphere of the craton and the fold belt lithosphere of not more than 35 km in thickness [Petit, Burov, Tiberi, 2008]. Rift development on the Siberian craton boundary is believed to be impossible without the mantle plume influence and an appropriate field of strain. The plume presence evidence is shown by a number

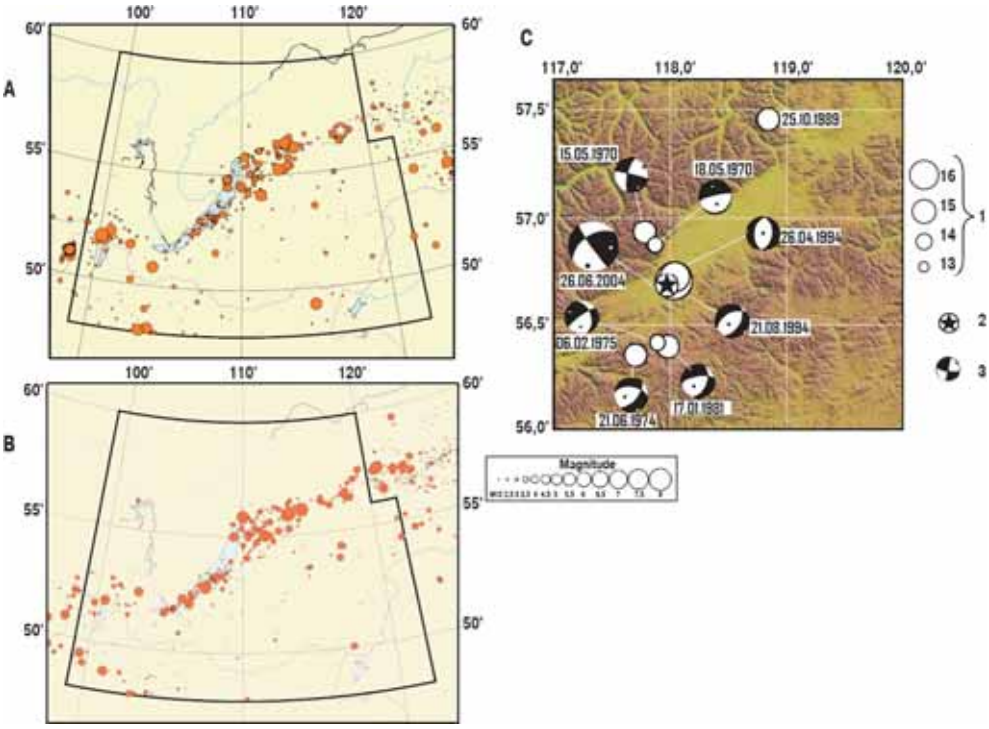

Fig. 1. Seismicity of the Baikal rift zone:

A – in 2004 [Earthquakes..., 2007; B – in 2007 [Earthquakes..., 2009] (earthquakes not lower than 33 km; the strongest in the year is marked by the star); C – epicenters of strong earthquakes in the Chara basin and adjacent ranges in 1960–2004 (1 – earthquake epicenter with date; 2 – the epicenter of the earthquake on 28 June 2004; 3 – focal mechanism in the lower hemisphere [Goljova et al., 2010])

of authors [Ufimcev, 2002; Logachev, 2003; Zorin, Turutanov, 2005 and others].

The asthenospheric upwelling zone traces along the rift axis under some basins of the north-east, including the Chara basin. Presumably, the upward plume part is located here, which provides for the Kodar-Udokan culmination of the Sayan-Baikal arc rise in the Stanovoe upland. Stress along the rift axis extends to its north-eastern flank. The Chara basin was forming under pulling stress created by a slipping constituent (, while its mountain border is a part of an arch formed during warming pahse. The Muya-Chara interbasin tectonic sowneck is a product of the inverse-compensational isostatic uplift [Ufimcev, 2002]. The seismic environment is the product of the regional geodynamic processes. Tectonic movements (including the latest period) control the basalt magmatism activity.

Active geodynamics manifests in rare devastating (reaching 10–11 points n the Mercalli scale), as well as in frequent small earthquakes (see Fig. 1). Seismic events in the Kodar-Udokan region (the strongest – Muyskoe in 1957 with $M_W = 7,8$, Nukzhinskoe in 1958 with $M_W = 6,5$, Kodarskoe in 1970 with $M_W = 5,6$, Charskoe-I in 1994 with $M_W = 5,8$, Charskoe-II in 1994 with $M_W = 6,3$, and some weaker ones) create a number of seismic deformations throughout the rift zone section. The Charskoe-III earthquake is the latest, typical for the region, and one of the strongest. It happened on June 28, 2004, and had a 5,1 point magnitude. Its focal mechanism demonstrates reverse strike-slip and strike-slip offsets in the north-western and north-eastern directions with fault planes. That corresponds to the local stress field [Giljova et al., 2010].

Fig 2. View of the Medvezhy pass from the Medvezhy stream valley. Dotted lines show the block-divider zone; arrows show pressure directions. Photo by E. Tokareva

The Medvezhy pass (H = 2200 m), a saddle between the Medvezhy stream and the Lednikovaya river valleys in the Kodar ridge, is one of the examples of the resent seismic deformations (Fig. 2). It is difficult to trace the block-divider in this area on a topographical map; the saddle has a U-shaped lengthwise profile with 30° slopes, while the adjacent slopes are notably steeper. Strongly brecciated biotite granites were found on the saddle; these rocks are the evidence of "dry" dislocation metamorphism in the tectonic displacement zone. It shows that the block-divider extends into this area. The topography around the saddle was altered after the 2008 earthquakes. The pass was fractured; the slope of the Ledinkovaya valley became steeper and harder for tourists. Such deformations confirm the presence of a relatively high-ranked block divider in the compressed and strained state.

In many respects, seismic events form large and small seismic dislocations and define the appearance of the Kodar ridges and valleys topography. Probably, the highest level of the Kodar belongs to a unique, i.e., seismic-alpine, mountain type. We noticed the active seismic destruction of a number of complex high-altitude climbing passes. Such destruction is very impressive in the peaked watersheds of the Upper and Middle Sakukane rivers (passes Pioneer – Fig. 3, Balitisky, Of Three Gendarmes, and others). The extraordinary sharpness of the landforms distinguishes the seismic-alpine topography from the classic alpine topography of the Alps, the Big Caucuses, the Pamir, and the Tan-Shan formed during numerous phases of anastomosing glaciation. The typical features of the landscape denudation complexes include widely spread steep (up to pendant) slopes, anomalous number of carlings and "gendarmes" on the ridges, and profound fragmentation of saddles that frequently are saw-like. At the lower elevations, the seismic-alpine topography is controlled by continuity of the gravitational trains in the lowest parts of river valleys, rocky glaciers, and stepped lengthwise stream profiles.

**Fig. 3. The easterly Pioneer pass view from the BAM peak (3072 m).
Fresh seismic deformations on the watershed of the Upper and Middle Sakukane.
Dotted lines show the block-divider zone; arrows show seismic cracks.
Photo by E. Chesnokova**

MORPHOSTRUCTURE

The Chara basin is a concave tectonic macrorelief landform partly filled with sediments (Fig. 4). Its bottom presents a predominantly subaerial accumulative plane influenced by mainly exogenous agents in tectonic submerge conditions [Geology and seismicity..., 1984]. Accumulative landforms in the basin bottom have glacial, fluvial, and limnic genesis. In several locations, differential tectonic movements in the basin uplift the bedrock to the surface and form individual hills.

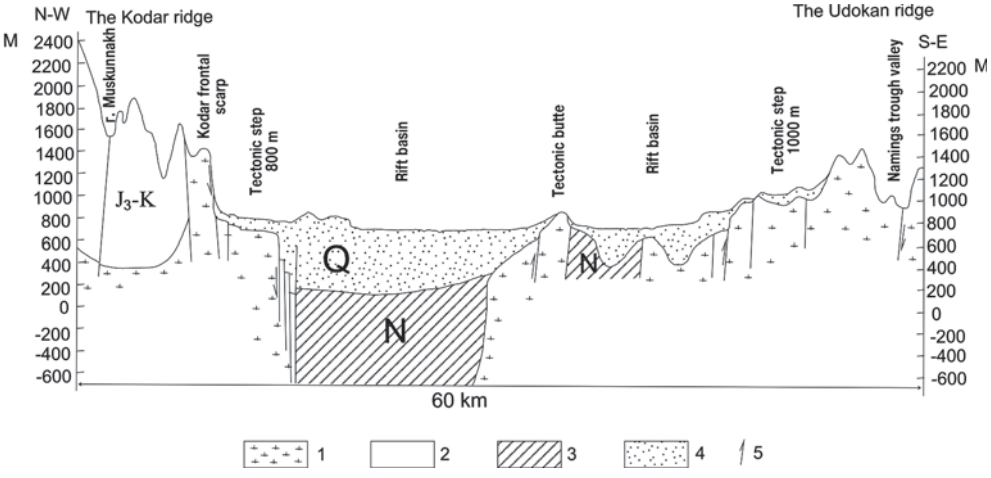

Fig. 4. Schematic geologic-geomorphic section across the Chara basin in the Apsat coalfield line [by Enikeev, 2009] with the authors' modification (position on Fig. 5).

1 – bedrock, 2 – mesozoic sedimentary deposits, including carboniferous, 3 – sandstones, conglomerates and boulder-pebble Neogene deposits, 4 – quaternary, mainly sandy fluvioglacial-alluvial and glacial deposits; 5 – fault kinematics

No boreholes reached the bedrocks in the central part of the rift (the deepest of them has 1180 m in face [Enikeev, 2009]); therefore, the maximal thickness of the sediments is unknown. Sedimentation of Lake Baikal is uncompensated; on the contrary, the Chara basin exhibits compensative warping. The large number of lakes in the north-eastern (downstream) part of the basin points to unsteady sedimentation. According to the foundation bedding depth assessed from geophysical data, the north-eastern part of the basin plunges faster than its south-western part.

Tectonic block structures that correspond to the lithosphere units of different ranks form mainly under the influence of vertical movements' effects, even assuming noticeable horizontal movements. Topography is the most clear visual demonstration of tectonic blocks identified using geomorphic, geological, and geophysical data.

A small-scale schematic map of the terrain structures contours (Fig. 5) shows the specific morphostructural features of the region. The Chara basin is the visible space-forming depression in the centre of the map. To the north-east and south-west of it, we can see tectonic morphostructures with the same (lower than 1000 m) altitude. In the north-east, there is the Tokko basin; in the utmost south-western part, there is the Sulban and Kouanda basins. The latter ones are separated by the extremely north-eastern spurs of the South-Muya Mountains (above 2250 m); we can also name these structures the Muya-Chara interbasin tectonic sowneck.

The Chara and Tokko basins are separated by a lower tectonic sowneck, just few meters higher than 1500 m. From the north, the Chara basin is bounded by the Kodar ridge, whose peaks are often over 2750 m (the dominant, Peak BAM, is 3072 m high). The Kodar has massive structure; its most important tops are situated rather close. We can isolate individual large blocks. In the Kodar ridge, the Upper-Sulban basin is well seen through block-dividers. The Kodar is bounded from the north by tectonic depressions with the Senj (north-west) and the Malaya Tora (south-east) rivers and altitudes not exceeding 1000 m. The Udokan-Kalar area is located in the south-eastern part of the scheme. The pattern of the terrain structure contours shows that the Udokan and Kalar ridges are difficult to separate. At the same time, neither of them looks as a united mountain range. The topographical maximums concentrate in the central part of the Udokan; however, it does not look like a large united massif. In comparison with the Kodar, the Udokan is more "descrete". In the Udokan-Kalar area there is the Upper-Kalar basin situated at the same level as the Upper-Sulban basin. Also, we can see the depression with the Kalar river in the outermost south-eastern part of the map that can be traced through block dividers.

The pattern of the terrain structure contours depends, undauntedly, on the block division and allows us to estimate the amplitude of the Neogene-Quaternary movements. Thus, in the zone of the Kodar fault between the Apsat and Middle Sakukane, this amplitude reaches about 1700 m; in the south-eastern periphery of the Chara basin, the amplitude of mutual displacement of the outermost blocks of the Udocan (estimated with the series of downthrows) reaches 1000 m. In the through block-dividers zones in the Kodar and Udokan ridges, throws with several hundreds meters amplitude were repeatedly found during field research and on topographic maps and recorded with remote sensing data.

The Olekma-Vitim mountainous country is a morphostructure of the first order; in the study area, it includes four morphostructures of the second order: the Kodar, the Udokan, and the South-Muya ridges, and the Chara basin [Lopatin, 1972]. Their general characteristics are presented below.

The Chara basin is a 120 km long Baikal-type basin. It is a tectonic depression elongated in the north-eastern direction and bounded

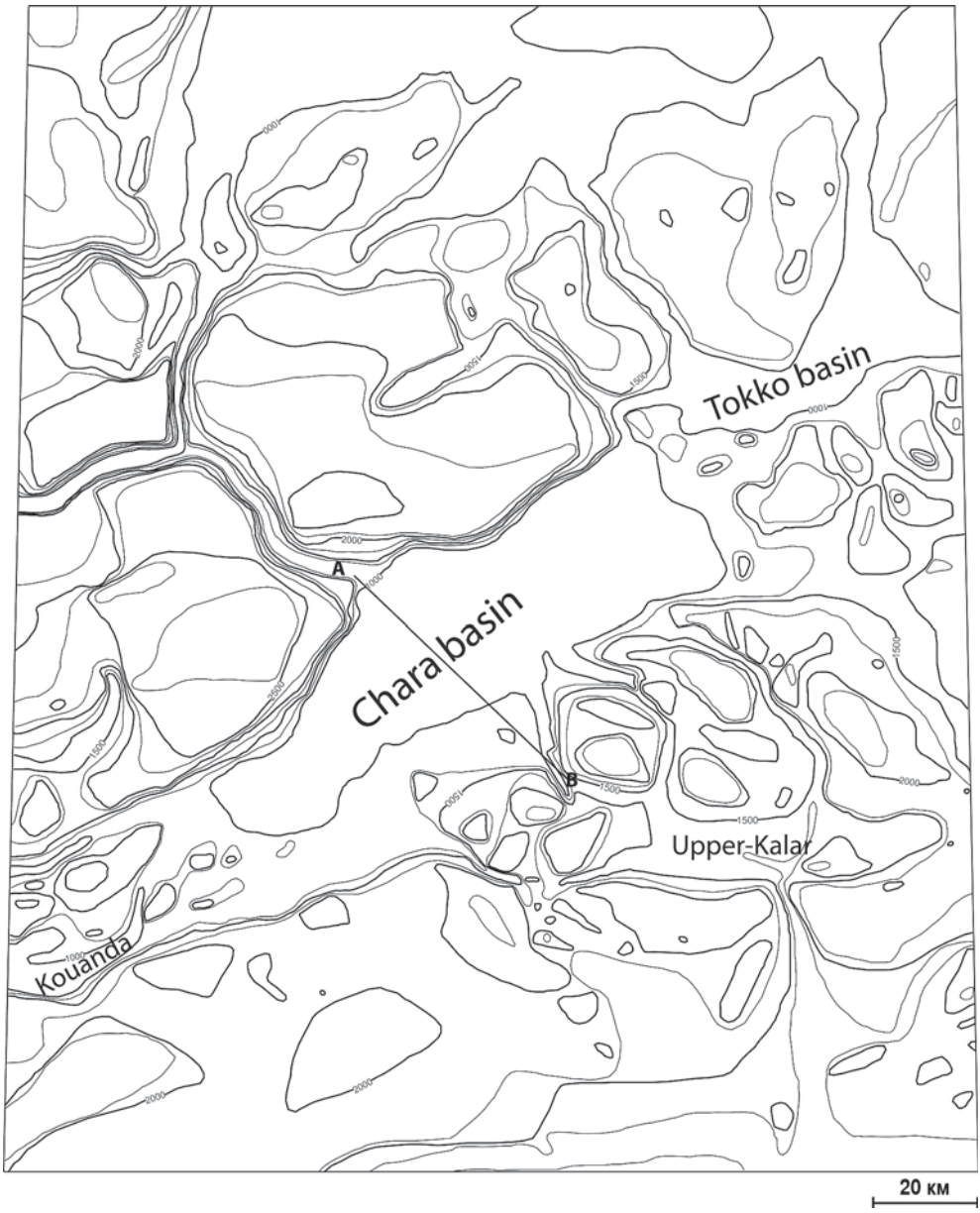

Fig. 5. Schematic map of the terrain structure contours (every 250 m). A–B – transect line (see Fig. 4)

by the Kodar and Udokan tectonic scarps flanks. The basin has an asymmetrical structure: the north-western (Kodar) side slope is much steeper, i.e., 35–60°; the mostly submerged foundation fragments are along this side. The bottom represents a predominantly subaerial accumulative plane as we have already mentioned above. However, the plane is squeezed between the mountain massifs and we can consider the direct structure/topography correlation. At the same time, in the bottom of the basin, there are bedrock protuberances that correlate with separated uplifted blocks and tectonic buttes. In the south-western part of basin, the South-Muya – Udokan junction, the inversionally uplifted tectonic step, is located. Probably, it was forming during

the uplift-submerge process [Ufimcev, 2002]. Step altitudes are 1000–1200 m, which is visible both on the map (see Fig. 5) and in the transverse geologic-geomorphic section (see Fig. 4).

The Kodar ridge is a complicated blocky construction. The transverse section shows the asymmetric structure with flat northern and steep southern slopes. In the north-eastern part, the ridge smoothly connects with the Baikal-Patomskoe and Olekma-Chara uplands; in the south, it abuts the Chara basin with a tectonic escarp. The Kodar is a tilted horst in a form of an asymmetric range. It is divided into a number of large blocks that consist of smaller cells.

The Udokan ridge is a complicated arch-blocky asymmetric structure. In the south-west, the Udokan arch becomes the Kalar ridge half-arch. That is why the northern slope is steeper than the southern. The northern macroslope is complicated by a series of small intramountain basins and grabens and has a stepped form. The steps are separated by tectonic escarps of east-north-eastern direction. The mountainous steps of the Udokan gradually transition into the piedmont steps of the Chara basin. The axled Udokan area is formed by several separated blocks and determines the blocky structure of range.

The considered part of the *South-Muya Mountains* is the eastern closing of the horst rise. The north-western ridge slope is a high-amplitude fault escarpment with 25–50° steepness. The north-eastern part of the mountains is very complicated. The entire width of the Kouanda-Sulban watershed is fractured with a great number of young faults [Active tectonics..., 1966]. The Sulban graben separates the mountains from the Kodar in the north; the Kouanda graben detaches Udokan in the south.

METHODS

Block morphotectonics analysis was done for a large-scale (detailed) study of the upper lithosphere and a further detailed endogenous topography investigation. The fundamentals of the methods are discussed in literature [Simonov, 1972, and others]. We used the assumption that beneath almost all streams, there are large faults and fracture densification. The initial principals consider block-divider delineation using only river network analysis. However, ruptures may become apparent not only in drainage systems but in some geomorphic and landscape characteristics too. Presence of long straightened river valley sections, their 90° bends, river interceptions, and seismogenic landforms (seismic deformations) support theoretically delineated block dividers**.**

The most impressive example is the frontal Kodar escarp that separates the ridge block (Kodar) from the Chara basin [Grachev, 1972]. Block dividers were also delineated using suture and tectonic lines and saddles. Large block dividers in mountainous areas correspond to rivers of highest order in the Horton-Straller system; through block-dividers – to river headstreams and their contact across the lowest cols. For extreme block tops analysis, we used five categories: innermost, descended, mid-high, uplifted, and most uplifted. We talk only about relative submerge or uplift. The result of the mountainous land block analysis is the delineation of 46 blocks of the second order; they are: 1) innermost – lower than 1700 m; 2) descended – 1700–1950 m; 3) mid-high – 1950–2300 m; 4) uplifted – 2300–2700 m; 5) most uplifted – above 2700 m (Fig. 6).

BLOCK ANALYSIS

In the topography of the Chara basin, of the Udokan, and especially of the Kodar, the morhotectonic mosaic structure can be seen. Sometimes, it defines the major orography features, in particular, in the Kodar glacier upland [Kovalenko, 2011].

One block on the Kodar has the highest altitudinal difference compared to the others and belongs to the "innermost" category. This

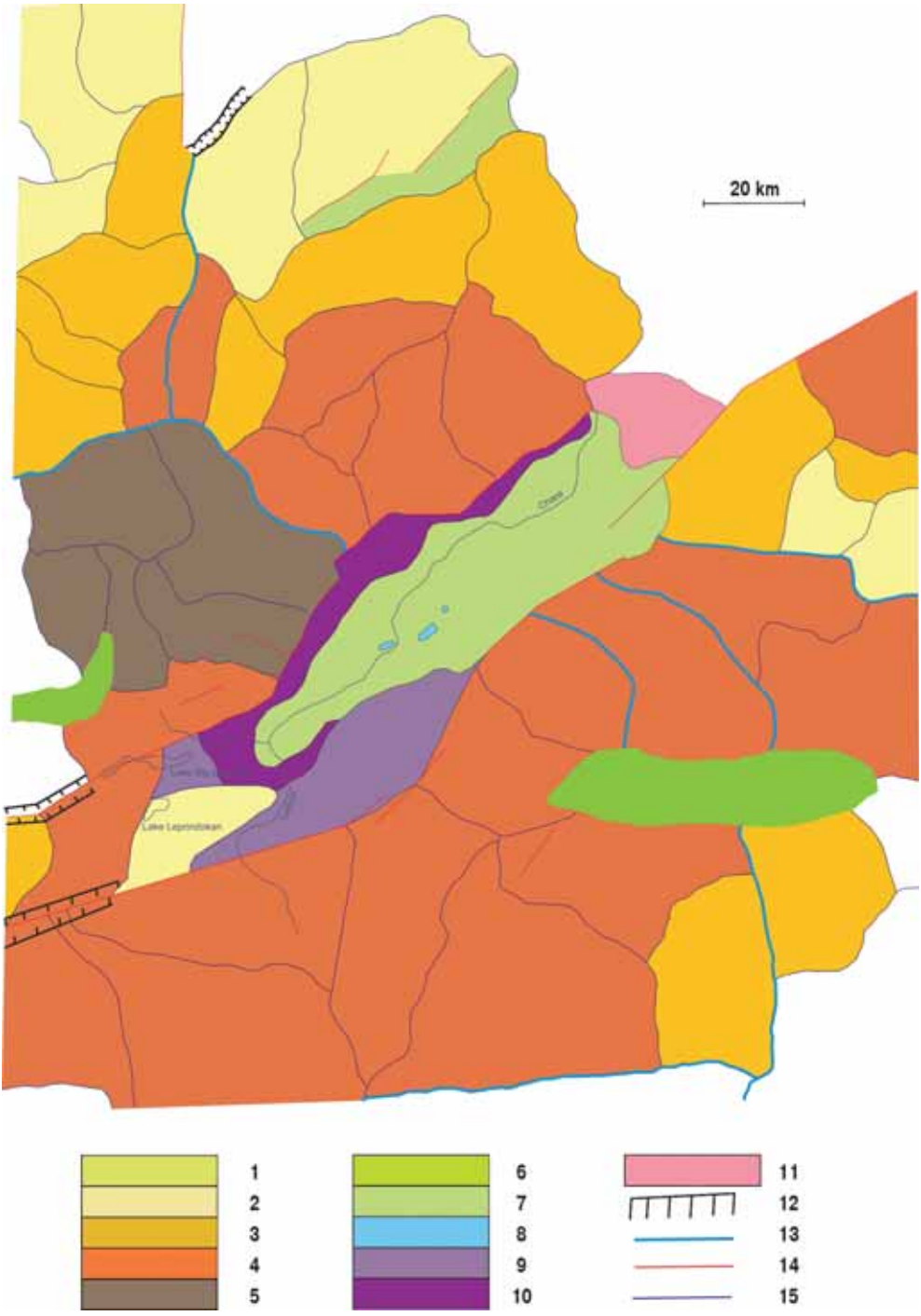

Fig. 6. Morphostructural elements scheme of the Kodar-Udokan segment of the Baikal rift zone. Block morphostructures motion tendencies:

1 – active submerge; 2 – temperate descend; 3 – comparative stabilization; 4 – temperate uplift; 5 – active uplift; rift basins bottoms: 6 – intramountain; 7 – intermountain; 8 – tectonic buttes; tectonic steps with altitude: 9 – near 1000–1200 m; 10 – near 800 m; 11 – small block fragmentation zone with denudation-tectonic topography; linear morphostructures (tectonic lines): 12 – frontal escarps of graben-like depressions, 13 – through the block-divider zone; 14 – large relief ruptures; 15 – ordinary block dividers

block has a depression, where the Malaya Tora River flows through. The depression is evident on the schematic map of the terrain structure contours (see Fig. 5). According to its morphology, the block belongs to the eastern Kodar periphery; its maximal altitude is higher than that of the Chara basin step elevation (1000–1200 m). The block is disjointed from the ridge body by distinct lineament zones; that is why we can consider it a plunged fragment of the ridge instead of the initial basin level.

Blocks with altitude below the average can be found in all studied ridges. They have features of mountain structure peripheries in the north of the Kodar, the east of the Udokan, and the east of the South-Muya Mountain. The blocks of middle height are situated at some distance from ranges axes areas, near the Olekma-Chara upland. Such blocks make a transition between descended and uplifted blocks like in the north-west of the Kodar.

Uplifted blocks have features of the central parts of mountains, but there are several outstanding blocks. The majority of blocks and all the uplifted block groups have contact with negative structures. This is the case in the central parts of the Kodar and the Udokan, in the Chara basin contact zone, in the north of the Udokan near the Tokko basin, in the west of the Kodar near the Upper-Sulban basin, and in the southern and central part of the Udokan near the Upper-Kalar basin. The highest block of the South-Muya Mountains is compressed between the grabens of the Sulban and the Kouanda. This is true for the most uplifted blocks. They group around the highest block in the Stanovoe upland and are situated between the Upper-Sulban and the Chara basins. Exactly in such contact zones, both direct and indirect signs of endogenous activity become clearly apparent, especially in cases when blocks are divided by a prominent fault zone.

The whole morphostructural scheme allows us to recognize that the differentiation exists not only between the main structural elements but also inside them. In uplifted and submerged blocks, contact zones, fault zones, and through block-dividers junctions we expect a great amount of endogenous activity to manifest morphologically. The presence of differently uplifted block morphostructures is also a sign of such activity.

N.A. Logachev [2003] estimates the sediment volume in the Chara basin at 2700 km^3. The area that now provides solid sediments to the basin is about 6600 km^2 wide. The total volume of the river valleys that surround the basin is about 1050 km^2, considering that these valleys were filled before the last activation period and the rest of the sediment material was brought from higher mountain levels. If we distribute the superfluous volume equally over the mountain watershed, we find less than 250 m of denudation in quaternary erosional period.

The extreme top of the Kodar is 3072 m high and the foundation bedding depth is not less than –600 m; Yu.A. Zorin [2005] estimates it at –1600 m level. Therefore, we can evaluate the bedrock surface altitude amplitude in the north-east of the Baikal rift zone at just under 5000 m (3072 + 1600 + 250 = 4922 m).

During the 1961–2010 field research in the Sulban, the Upper and Middle Sakukan in the Kodar, and the Lower Ingamakit in the Udokan we have repeatedly found seismogravitational collapses and landslides, "indents" and gaped clefts in massifs, seismotectonic cracks, and other morphological consequences of seismic processes (Fig. 7, 8). Great relief deformations in the form of lengthwise seismotectonic cracks can be seen in contact zones of different breaks with the main Kodar fault. Large seismic topography and structures deformations in a vaster area are shown in "Active tectonics..." by V.P. Solonenko [1966] and his co-authors. Therefore, we can see topographic signs of broad endogenous activity.

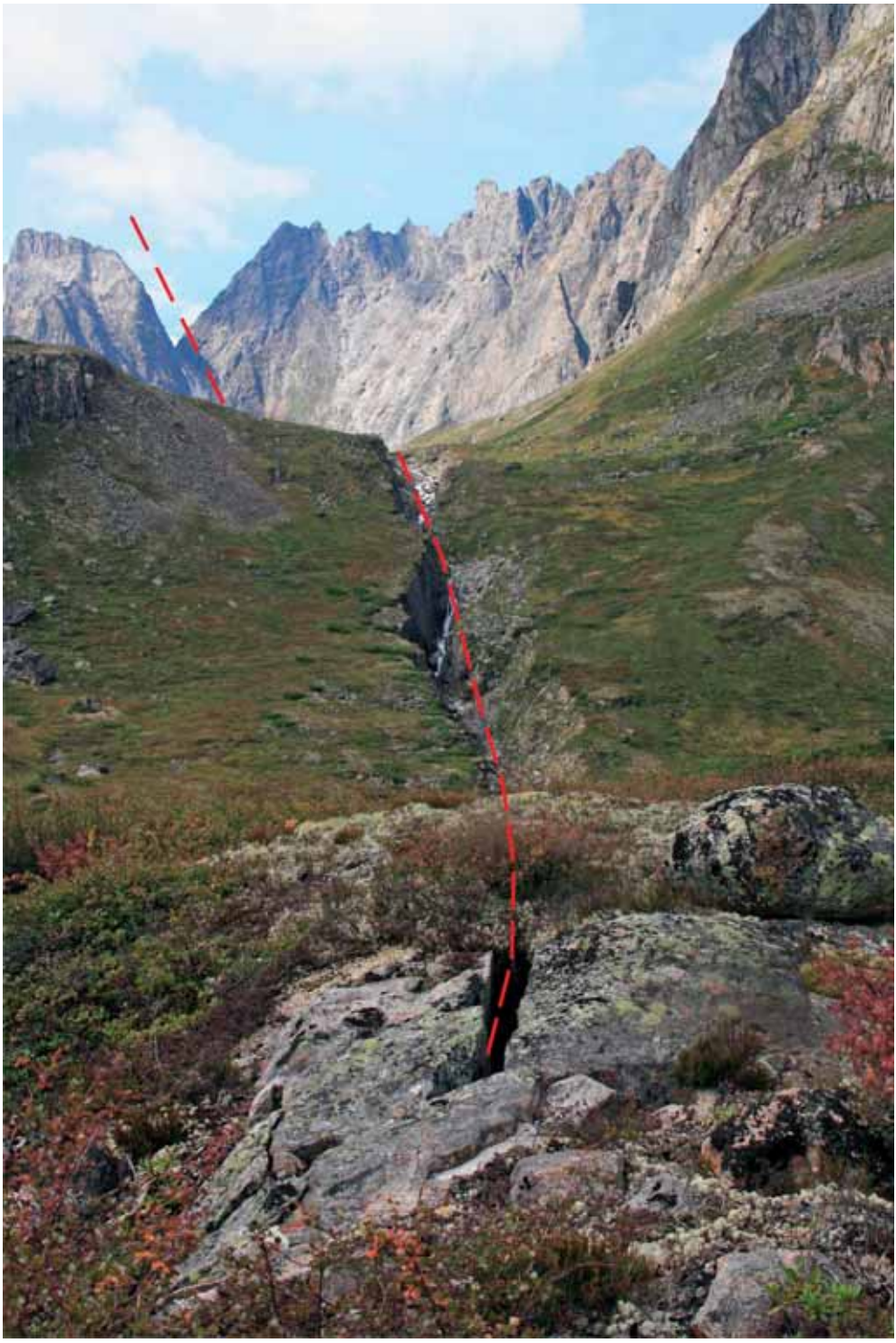

Fig. 7. 15-m deep seismotectonic narrow with the Uglovoy stream in the central part of the Kodar ridge. Dotted line shows the trace of the weakened zone.
Photo by S. Maznev

Fig. 8. The rocky canyon of the Uschelisty downstream in the Udokan ridge. Dotted lines show slopes of tectonic genesis in the canyon. Photo by S. Maznev

Presence of intramountain basins and differently uplifted morphostructures determines local denudation and accumulation areas. Naturally, mountainous lands remain a province of prevailing pulling down. Mainly, products of bedrock weathering transport by streams and rivers (historically – by glaciers) with through block-dividers. Such dividers are, per se, large tectonically weakened zones and crack frequency zones enlarged with glaciers and rivers. Such zones join through the low cols, and their tectonic genesis can be suggested. On the saddles of this kind, in tectonic gorges among river valleys in different phases of anastomosing glaciation, transaction-type glaciers were forming. As a consequence, presence of lakes and wetlands on pass saddles of through block dividers is typical.

The altitudes of block dividers are different on the sides of the rift axis. The pass saddles in the Kodar have elevetation of 900–1100 m; in the Udokan, it is 1200–1500 m. Such difference can be explained in the following way: in the Kodar, they are the result of the initial ridge division, but in the Udokan, they are the product of arch splitting and disintegration. In the Kodar, the largest block dividers split macroblocks with different tectonic movement rates, whereas in the Udokan, such lines occur due to stretch strain realization.

CONCLUSION

Active geodynamics in the Kodar-Udokan segment of the Baikal rift zone is naturally reflected in the morphostructures of the region. Fault slips take place regularly in seismic dislocations and new seismic deformations occur. Fresh fault escarpments, tearing off walls of collapses, and talus are current activity indicators in the region. In spite of the evident Pleistocene-Holocene volcanism weakening in the Udokan, we cannot speak about the seismotectonical activity decrease in the region. We can also see a widely spread topography reaction to stretch strain and to pressure stress in the south-eastern Kodar. ■

REFERENCES

1. Active tectonics, volcanoes, and seismicity of the Stanovoe Upland (1966) / Editor-in-Chief V.P. Solonenko. – Moscow: Nauka. 232 p. (In Russian).

2. Earthquakes in Russia in 2004 (2007). – Obninsk: GS RAN. – 140 p. (In Russian).

3. Earthquakes in Russia in 2007 (2009). – Obninsk: GS RAN. – 220 p. (In Russian).

4. Enikeev F.I. (2009) Pleistocene glaciations of the Eastern Transbaikalie and South-East of Middle Siberia // Geomorphology, №2, 2009, pp. 33–49. (In Russian).

5. Explanatory dictionary of English geological terms (2002). Vol. 2 / Editor-in-Chief J.A. Jackson. – Moscow: MCGK "Geocart", GEOS. 644 p. (In Russian).

6. Geology and seismicity of the Baykal-Amur Mainline zone (1984). – Novosibirsk: Nauka. 174 p. (In Russian).

7. Giljova N.A., Radziminovch Ya.B., Melnikova V.I., Radziminovch N.A. (2010) The Chara-III earthquake on June 28, 2004 with MSPS = 4,7, K_p = 13,5, I_0 = 6 (Pribaikalje) // Earthquakes of northern Eurasia in 2004, pp. 324–334. (In Russian).

8. Grachev A.F. (1972) Asymmetry of the Baikal rift zone (geophysical solution of geomorphologic problem) // Geomorphology and geophysics, pp. 95–106. (In Russian).

9. Kovalenko N.V. (2011) Behavior and evolution of small glacier forms. – Moscow: MAKS Press. 240 p. (In Russian).

10. Logachev N.A. (2003) History and geodynamics of the Baikal rift // Geology and Geophysics, vol. 44, №5, pp. 391–406. (In Russian).

11. Lopatin D.V. (1972) Geomorphology of the eastern part of the Baikal rift zone – Novosibirsk: Nauka. 116 p. (In Russian).

12. New seismic zoning map of the Nothern Eurasia (1996) / Khromovskikh V.S., Nikolaev V.V., Demjanovich M.G. et al. // Geophysical research in Eastern Siberia at the point of the 21st century – Novosibirsk: Nauka. Siberian publishers of RAS. P. 94–99. (In Russian).

13. Petit C., Burov E., Tiberi C. (2008) Strength of the lithosphere and strain localization in the Baikal rift // Earth and Planetary Science Letters, v. 269. P. 523–529.

14. Simonov Yu.G. (1972) Regional geomorphologic analysis. – Moscow: Moscow University Publishers, 1972. 254 p. (In Russian).

15. Ufimcev G.F. (2002) Morphotectonics of Eurasia– Irkutsk: Irkutsk State University Publishers, 2002. 494 p. (In Russian).

16. Zorin Yu.A., Turutanov E.H. (2005) Plums and geodynamics of the Baikal rift zone // Geology and Geophysics, vol. 46, №5, pp. 685–700. (In Russian).

Andrey A. Lukashov received his D.Sc. degree in 1990. Since 1993 he is professor of the Faculty of Geography, Lomonosov Moscow State University. His present research interests are connected with structural geomorphology, karst, geoecology, comparative planetology. Prof. Lukashov delivered a number of lecture courses at Russian and Ukrainian universities. He published over 180 works, including maps and 7 monographs. Main publications: Relief of planetary bodies. Introduction to comparative geomorphology (1996); Problems of theoretical geomorphology (2000, with co-authors); Structure, Dynamics and Evolution of Natural Geosystems (2000, with co-authors).

Stepan V. Maznev graduated from the Faculty of Geography, Lomonosov Moscow State University in 2011. He actively participated in expeditions at the Pasvik Nature Reserve, at Kamchatka Peninsula and Northern Transbaikal region. The main topic of his study is structural geomorphology. From 2011 he is engaged in engineering geology pioneering, he took part in investigations at the Caucasus, the Yamal Peninsula, Volgograd and Moscow regions and others. Now he is a geologist of the "Geologix" company.

Nikolay S. Kasimov[1], Dmitry V. Vlasov[2*]
[1] Faculty of Geography, Lomonosov Moscow State University, Leninskie gory, 1, 119991 Moscow, Russia; Tel. +7 495 939238, e-mail: secretary@geogr.msu.ru
[2] Faculty of Geography, Lomonosov Moscow State University, Leninskie gory, 1, 119991 Moscow, Russia; Tel. +7 926 7603742, e-mail: vlasgeo@yandex.ru
[*]**Corresponding author**

GLOBAL AND REGIONAL GEOCHEMICAL INDEXES OF PRODUCTION OF CHEMICAL ELEMENTS

ABSTRACT. This paper presents a geochemical assessment of the primary involvement of chemical elements in technogenesis in the world and individual countries. In order to compare the intensity of production of various chemical elements in different countries, the authors have introduced a number of new terms and parameters. The new term is "abstract rock" (AR) – an elemental equivalent, whose average composition corresponds to the average chemical composition of the upper continental crust. The new parameters are: "*conditional technophility of an element*" (T_Y), "*specific technophility*" (T_{YN}) "*regional conditional technophility*" (T_{YR}), "*specific regional technophility*" (T_N), and "*density of regional conditional technophility*" (T_S). T_Y equals to the tons of AR per year necessary for the production of the current level of the element. T_Y of different elements has been estimated for 2008–2010. The highest T_Y values are associated with C, S, N, Ra, and Au. T_Y of many micro- and ultramicroelements is of the order of $n \cdot 10^{11}$t. T_{YN} reflects the volume of AR per the world's capita. T_{YN} changes from the 1960s to 2010 indicates that the Earth's population is growing much faster than its demand for many chemical elements. T_{YR}, T_N, and T_S were used for the integrated assessment of technogenesis at the regional scale; they reflect the intensity of the technogenesis process at the level of individual countries and allow comparing countries with different levels of elements production, population, and areas. The T_N and T_S levels of the leaders in extraction of natural resources are below these values in other countries due to the large territories (Russia, USA, Canada, Australia, Saudi Arabia, Kazakhstan, Argentina, Bolivia, Venezuela, Colombia, Zambia, Mali, Libya, Mongolia, and Sudan), to the large population (Indonesia, Vietnam, the Philippines, Bangladesh, Nigeria), or to both high spatial and demographic dimensions (India, Brazil, France, Egypt, Thailand, Pakistan, Algeria, Tanzania, Congo (Kinshasa), Malaysia, and Morocco).

KEY WORDS: technogenesis, tehnophility, elements production, elemental equivalent.

INTRODUCTION

Extraction of chemical elements from different layers of the Earth – the lithosphere, hydrosphere, and atmosphere, their controlled and spontaneous incorporation in a man-made migration, which currently involves almost the entire globe, creation of new artificial and "alien" to the biosphere compounds, global anthropogenic scattering, and intense local concentration of elements in the cities and near deposits of natural resources generate increasingly more clearly manifested geochemical differences between different terrestrial macroregions, countries, and their parts. In the last quarter of the XXth century, N.F. Glazovskiy has formulated the idea of a new direction in environmental geochemistry – geochemical regional geography [Glazovskiy, 1976].

The methods of comparison of countries by the intensity of certain aspects of technogenesis[1] represent a ranking system with a large number of characteristics and a general principle of descending or ascending ranking. These methods include: the "geographical" method that primarily considers the common physical and economic-geographical characteristics of countries: area, population size and density, GDP, etc. [Tikunov & Tsapuk, 1999]; the "matter-energy" method that considers the levels of production of energy, mineral and other resources, and goods [Mineral..., 2012; Key world..., 2012]; the "geochemical" method that considers identification of the intensity of technogenic migration of elements and representation of the flows of goods as the flows of chemical elements between countries, regions, cities, etc. [Glazovskiy, 1976]; and the "environmental" method that involves calculation of a set of coefficients and indices. The latter includes the following approaches: "environmental price" utilizing basic indicators (GDP, gross domestic savings, net domestic product), adjusted for the valuation of natural resource depletion and environmental damage, and natural capital, e.g., genuine savings index (GSI), environmentally adjusted net domestic product (EDP), etc. [Вцhringer & Jochem, 2007; Bityukova & Kirillov, 2011]; "sustainable development" that includes the quality of life and environmental indicators – human development index (HDI), environmental sustainability index (ESI), environmental performance index (EPI), ecological footprint (EF), living planet index (LPI), absolute and proportional composite environmental rankings (aENV, pENV), etc. [Esty et al., 2005; Вцhringer & Jochem, 2007; Bradshaw et al., 2010; Bityukova & Kirillov, 2011]; "technogenic impact" that involves the grouping of countries, regions, and cities by the intensity of impact on the individual components of the environment, e.g., on the atmospheric air, with assessment of the total emissions from industry and vehicles [Bityukova et al., 2012] and emissions of individual elements or compounds, i.e., heavy metals, CO_2, CH_4, SO_2, NH_3, etc. [Pacyna & Pacyna, 2001; Nriagu & Pacyna, 1988; Denier van der Gon et al., 2009; Revised.., 2012; Bityukova, Kasimov, 2012]; or the integrated assessment of the anthropogenic impact considering several components simultaneously [Bityukova, 2010].

The "emission", "matter-energy," and "geochemical" approaches are the best methods for the evaluation of the intensity of technogenesis in the world and individual countries, because they allow identifying groups of countries with close parameters of direct and indirect impact on the environment. However, to date, these approaches have not utilized integral parameters.

In order to assess the involvement of chemical elements in technogenesis at the global and regional scales, it is necessary to know the value of the primary technogenic mobilization of the elements of the Earth's interior (extraction of different types of natural resources), abundance of elements (which directly influences the potential of their inclusion in the technogenic migration [average composition of the upper continental crust]), and geographical parameters that influence the magnitude of elements production (spatial and demographic dimensions of countries). Geology and endowment of mineral resources determine the distribution of the chemical elements production in different countries. But these factors are not discussed in the paper, because we focused on searching geochemical indexes which allow to compare countries with different levels of elements production, population, and areas.

Technophility (*T*) is an important notion for understanding the basic trends in the intensity of chemical elements extraction from the Earth's interior and their use in techcnogenesis. *T* represents the ratio of the annual primary production of an element in tons to its average concentrations in the Earth's crust [Perel'man, 1975]. *T* is an informational coefficient that reflects the level of chemical elements production

in different phases of the technogenic development of society. Some elements are extracted by mankind proportionately to their average content in the Earth's crust (Cd, Hg, U, Mo, Ti, and Zr), while for others, such dependency is lacking.

T of various chemical elements varies over time [Kasimov & Vlasov, 2012] and depends on the increasing or decreasing intensity of elements production and corrections in the previously calculated average composition of the Earth's crust. The work presented herein improves the earlier calculations of *T* with the new data on the production of Os, Sc, Rb, some platinum group metals, noble gases, rare earths, and information on the elements production in Africa and Central America [Kasimov & Vlasov, 2012]. The authors have calculated the mean values of the elements production for the three years (2008–2010), accounted for the impact of the global economic crisis on the mining industry, and used the information on the production of elements in almost all countries of the world and the latest data on the average composition of the upper continental crust.

MATERIALS AND METHODS

The production values of most chemical elements and their compounds were derived from the annual reports of the U.S. Geological Survey (USGS) averaged over 2008–2010 [Mineral ..., 2012; International minerals .., 2012]. In the absence of data for 2010, the information for 2007 averaged over 2007–2009 was used. The production levels of elements in the 1960s were obtained from [Perel'man, 1975], in the 1980s – from [Emsley, 1991], in the late 1990s and early 2000s – from [Mineral ..., 2012; Butterman et al., 2003, 2004]. The production of some elements was calculated from the values of production of the essential minerals.

Thus, the USGS data state that zirconium concentrates contain up to 49,8% Zr. They are also the only source of Hf – about 2% of the mass [Mineral ..., 2012]. Extracted spodumene $LiAl(Si_2O_6)$ contains 3,73% Li, lepidolite – 3,1–6,0% Li_2O. The oxide content of 40% was used to calculate the Ta_2O_5 and Nb_2O_5 contents from tantalite and columbite, respectively. Djalmaite can contain up to 15% UO_3. The mass of rare earth elements produced was calculated from their average content in the main ore mineral – bastnaesite: 49% Ce, 34% La, 13% Nd, 4% Pr, and 0,1% for other individual elements in this group [Haxel et al., 2002; Yang et al., 2009].

Data on the production of fossil fuels (coal, oil, and natural gas) were obtained from [International energy ..., 2012]. Barrels to tons conversion was done assuming a coefficient of 0,1364 and the density of natural gas of 0,765 kg/m^3. After reducing the data on fossil fuels production to the common unit of measure (tons per year), the mass of CO_2 and C content were calculated using the average calorific value coefficients and emission factors: for oil – 42,5 TJ/kt (i.e., TJ per thousands of tons) and 20 t C/TJ, respectively; for coal – 20 TJ/kt and 25,8 20 t C/TJ; and for natural gas – 43 TJ/kt and 15,3 t C/TJ [Revised ..., 2012].

Information on the production of Xe, Kr, Ne, Ar, Os, Sc, Po, Ac, Pa, Th, Cs, and Rb was obtained from [The world market.., 2012; Environmental, chemistry.., 2012; Butterman et al., 2003, 2004]; the data on the population size and area of individual countries and of the world as a whole – from [The world factbook, 2012]; and the data on the population of the Earth at different times of the last century – from [Kapitza, 1999].

The authors took into account only the main sources of production of elements; although many natural resources (sand, limestone) contain trace elements whose masses are generally very high, they are only "potentially" involved in technogenesis and are only "associated" with the production, without being its primary goal.

In Russia, the average contents of the elements in the Earth's crust calculated

by A.P. Vinogradov [Vinogradov, 1962] are often used, whereas only its upper part is a reservoir of natural resources used by mankind and the main source of most of the chemical elements involved in technogenesis. Therefore, when estimating the intensity of technogenesis, as well as in environmental and geochemical studies, it is feasible to apply the average composition of the upper continental crust calculated from the weighted averages of the chemical composition of rocks exposed at the Earth's surface [Clarke, 1889], or the average composition of fine-grained clastic sedimentary rocks, glacial deposits, or glacial loess [Goldschmidt, 1933]. R.L. Rudnick and S. Gao [2003] calculated average composition of the upper crust using both methods separately for macro- and microelements according to their solubility, correlation with La, and relations with other elements, for example, Rb/Cs.

The estimates of [Grigoriev, 2009] for some elements are very different from those of [Rudnick & Gao, 2003]; the concentrations are higher for S – 23 times, for Br and Cd – 7 times, for Cl – 4 times, for Au –3 times, and for B, Ca, Se, Ag, Sn, Sb, Gd, Ho, Lu, Ta, and Bi – 1,5–2 times; the concentrations for I is 3 times lower. The difference in the average concentrations in the upper continental crust of 1,5–3 times is not that significant for the assessments of the technogenesis intensity; therefore, this work relied on the average composition of the upper continental crust of R.L. Rudnick & S. Gao due to a larger list of elements included in their estimates. The average composition of the upper continental crust of [Grigoriev, 2009] were used for S, Br, Cd, and Cl.

For inert gases, Po, Rn, Ra, Ac, Pa, Rh, and Te, the concentrations in the upper continental crust have not been estimated; therefore, this paper used the average concentrations in Earth's crust in general [CRC Practical Handbook, 1989; Greenwood & Earnshaw, 1997; Vinogradov, 1962].

RESULTS AND DISCUSSION

Global estimates of the intensity of technogenesis

If technophility is multiplied by 100, then it has a physical meaning: the unit of T corresponds to the volume of extracted "abstract rock" (AR) (in tons) required for production of X grams of the element, where X is the value of the average concentration of element in the upper continental crust in g/t. In this case, AR corresponds to rock whose chemical composition equals to the average chemical composition of the upper continental crust. Hereafter, the authors are using the term "conditional technophility" (T_Y) to indicate the volume of extracted AR necessary for the production of a chemical element corresponding to its current level. The high level of contrast (from $n \cdot 10^3$ to $n \cdot 10^{13}$t) and temporal variability (large differences in production volume over time) of T_Y for different elements allows using this parameter as one of the general indicators of technogenesis.

The assessment of the total production of different types of natural resources, varying in composition, represents a problem in analysis of a number of aspects of technogenesis. For fossil fuels, this problem may be solved by converting the mass of fuel to an equivalent amount of CO_2 that can be released into the environment by burning, or by using the energy equivalent – by converting it to tons of oil equivalent [Revised ..., 2012]. The term "abstract rock" proposed herein is similar to the term "oil equivalent" and can be used for comparison of intensity of production of different chemical elements and for their overall accounting, i.e., it represents an elemental equivalent. Calculation of the sum of T_Y of chemical elements provides for assessment of their integrated involvement in technogenesis.

At the end of the first decade of the XXIst century, the largest T_Y was associated with C, S, N, Ra, Au, Xe, Kr, and He (Fig. 1). High T_Y of inert gases can be explained by the fact

Fig. 1. Conditional technophility of chemical elements (here and in Figs. 2–4, the data on elements production are for 2008–2010)

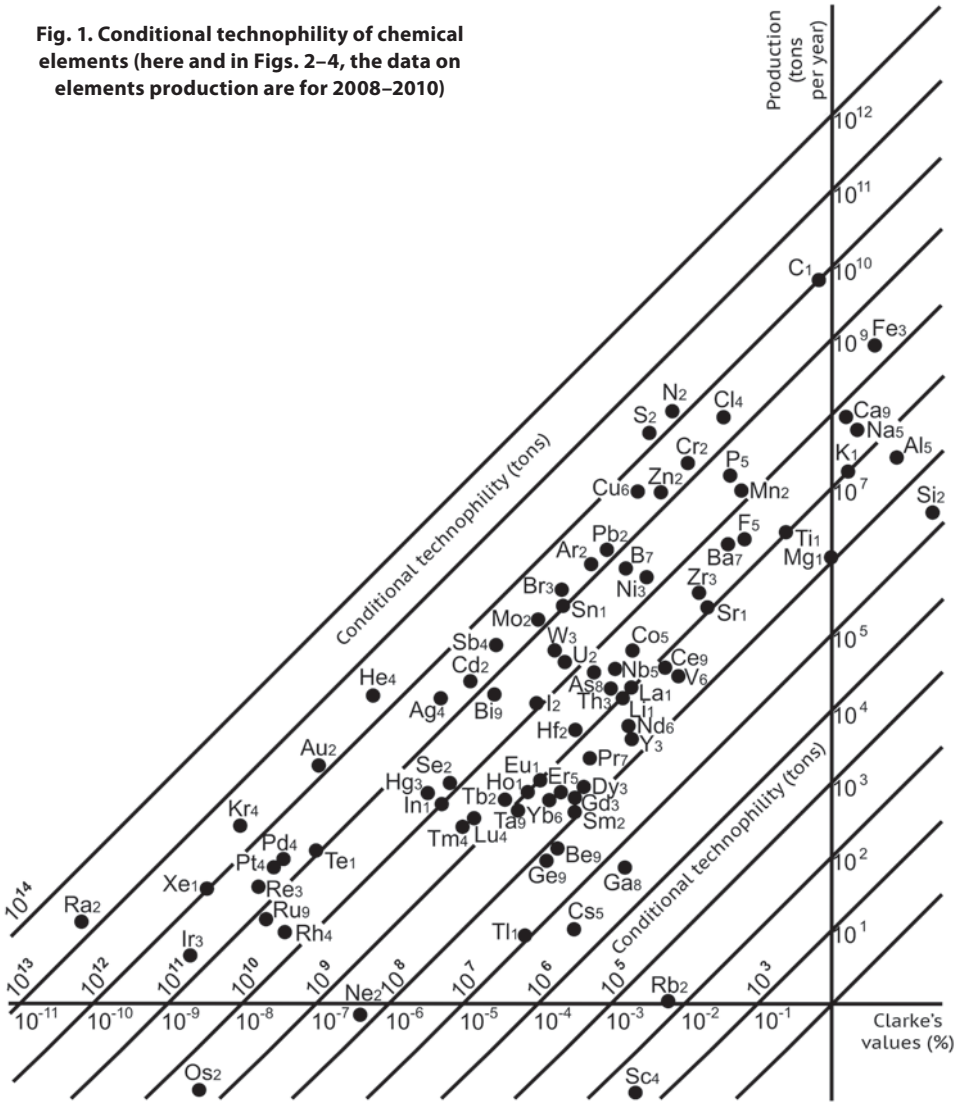

that the main source of their production is not the upper continental crust, but the atmosphere; therefore, it is more feasible to use the average composition of the atmospheric air. Under this approach, their T_Y values decrease by several times: about 100 times for He, while for Kr, Xe, Ar, and Ne – by 10000 times. Therefore, the data on the production of inert gases was not considered in the regional assessments of technogenesis. T_Y of some elements with very low average concentrations in the upper continental crust are not shown in Fig. 1: for Po it equals to $5 \cdot 10^{11}$t, for Ac – $2 \cdot 10^{9}$t and for Pa – $9 \cdot 10^{8}$t. T_Y of rare earth elements is $9 \cdot 10^{8}$t and varies from $4 \cdot 10^{9}$t for Lu to $2 \cdot 10^{8}$t for Sm.

Many micro-and ultramicroelements – Cr, Zn, Cu, Pb, Br, Sn, Mo, Sb, Cd, Ag, and some platinum group elements used for the production of various industrial products, spare parts, and car fuel, have T_Y of $n \cdot 10^{11}$t. The minimal T_Y (1000–10000t) is characteristic of Sc and Rb, the elements little used nowadays by mankind, but with relatively high concentrations in the upper continental crust. A more detailed explanation of the technophility parameter is given in [Kasimov & Vlasov, 2012]. Currently,

the most important from the technogenesis perspective are the elements with intensive production, i.e., C, Fe, S, N, Cl, Cu, Zn, Cr, Mo, and Sb.

Specific technophility (T_{YN}) represents change in AR production calculated per capita population (thousands tons per capita per year). This parameter can be used for comparison of the growth rate of the population and its demand for various chemical elements. In the mid 1960s, T_{YN} was equal to 6,4; it grew to 58,2 by the 1980s due to a sharp increase of the use of ultramicroelements that practically had not been previously used in the industry; then, it began to decline, reaching 47,2 in 2000 and 44,3 in 2010. This reduction in T_{YN} indicates that the world population in recent years is growing significantly faster than its demand for many chemical elements.

Regional intensity of technogenesis. Geochemical regional geography

Regional conditional technophility (T_{YR}) was incorporated in order to assess the technogenic contribution of 172 different world's countries to the total world's T_Y considering production of all chemical elements: $T_{YR} = \Sigma T_{Yi}$, where T_{Yi} is production of an *i*-chemical element in a country relative to AR (tons per year) (Fig. 2). This parameter represents an integral index of technogenesis at the regional level.

T_{YR} of the macroregions of the world varies from $3{,}6 \cdot 10^{11}$t in Central America to $1{,}4 \cdot 10^{13}$t in Asia (including Russia). Other countries occupy intermediate positions: Africa ($1{,}6 \cdot 10^{12}$t), Europe ($1{,}4 \cdot 10^{12}$t), North America ($1{,}3 \cdot 10^{12}$t), South America ($1{,}2 \cdot 10^{12}$t) and Australia and Oceania ($4{,}2 \cdot 10^{11}$t).

According to the values of T_{YR}, six groups of countries (with an order of magnitude step-difference between the individual groups) were isolated: *very high*, *high*, *intensive*, *medium*, *low*, and *very low* (Fig. 2).

Very high ($> 10^{12}$t). The leader of this group is Kyrgyzstan ($7{,}8 \cdot 10^{12}$t – Au, Hg, Mo, C, F, Sb, Na, Cl, and Ca); the group also includes China ($2{,}3 \cdot 10^{12}$t – practically all elements), South Africa, and Russia (each $1{,}1 \cdot 10^{12}$t– practically all elements).

High (10^{11}–10^{12}t). The group includes 21 "polyelemental" countries with a significant

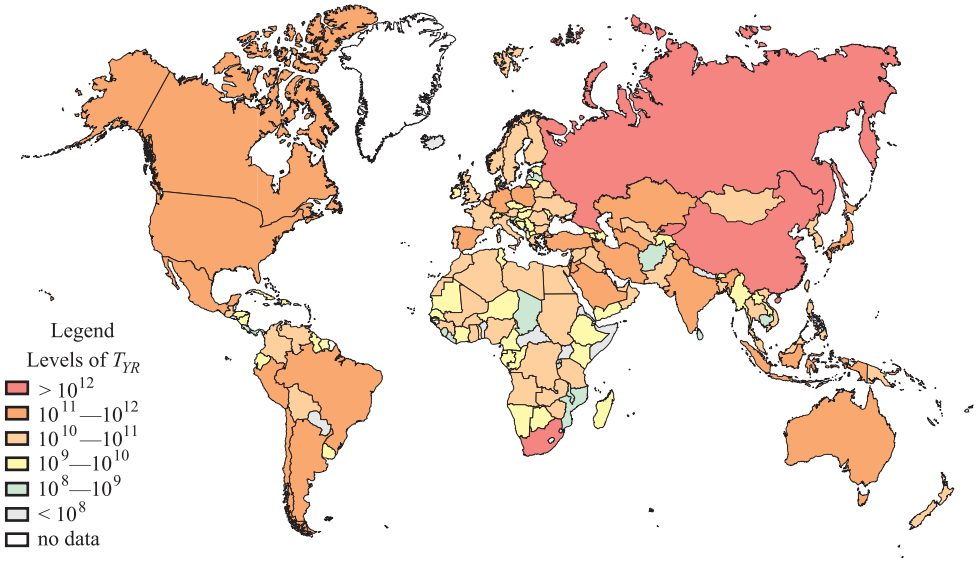

Fig. 2. Regional conditional technophility (T_{YR}) of different countries (tons per year)

production of a wide range of elements. In the descending order of T_{YR}, these countries are USA, Chile, Canada, Australia, Peru, Turkey, India, Mexico, Japan, Indonesia, Turkmenistan, Germany, Iran, Saudi Arabia, Kazakhstan, Poland, Brazil, Spain, Israel, Jordan, and Argentina. The main contribution to T_{YR} of these countries is provided by Na, Cl, Ca, Mg, S, N, P, B, Fe, Mn, heavy, non-ferrous, and precious metals. In addition, some of the countries have a large level of production of very toxic elements: As (Japan, Peru, Kazakhstan, Chile, and Iran), Hg (Peru, Mexico, Chile, and Argentina), and Sb (Canada, Australia, Japan, Peru, Kazakhstan, Mexico, and Turkey).

Intensive (10^{10}–10^{11}t). This group includes 55 "polyelemental" countries with a smaller list of produced elements. Many countries have high levels of C, S, Ca, Na, Cl, N, Si, Fe, Ag, Au, and non-ferrous metals production.

Medium (10^{9}–10^{10}t). This group has 53 countries with mining of either limited list of chemicals and high levels of their production, or a large number of elements with small production.

Low (10^{8}–10^{9}t). This group includes 20 countries that produce only some chemical elements: C, Ca, Na, Cl (almost all countries), Au (Mozambique, Rwanda, Burundi, Sierra Leone, Chad, Fiji, Costa Rica, Panama, and Liberia), Fe and Ti (Mozambique, Afghanistan, Sri Lanka, and Sierra Leone), Ta and Nb (Mozambique, Rwanda, and Burundi), S (Afghanistan, Latvia, and Malawi), Si (Mozambique, Sri Lanka, and Slovenia), Sn and W (Rwanda and Burundi), Ag (Fiji), U (Malawi), Mg (Latvia), P (Sri Lanka), Ba, Cr, and N (Afghanistan), and Be, Zr, and Hf (Mozambique).

Very low (< 10^{8}t). This group includes Uganda (Au, Be, C, Ca, Cl, Na, Nb, Sn, Ta, and W), Eritrea (Au, C, Ca, Cl, Na, Mg, and S), and the countries with mining of one to four chemical elements: Belize (Au, C, Ca, and Mg), Guadeloupe (C, Na, Cl, and Ca), Benin and Central African Republic (Au, C, and Ca), Paraguay (Ca, C, and S), Nepal (C, Ca, and Si), Iceland (Na, Cl, and Si), Barbados, El Salvador, and Haiti (C and Ca), Mauritius and Cape Verde (Na and Cl), Swaziland (C and V), Luxembourg (P), and Singapore, Puerto Rico, Netherlands Antilles, and Somalia (C).

In general, the expansion of the list of elements produced in a country is associated with the growth of its T_{YR}: the groups of intensive, high and very high T_{YR} include exclusively "polyelemental" countries, where a wide range of elements is produced, while the groups of low and very low T_{YR} include countries with mining of only isolated elements (C, Si, Na, Cl, Ca, Mg, N, P, S, Al, Fe, Mn, Ti, and heavy and precious metals).

Specific regional tehnophility and density of regional conditional technophility

For comparison between different countries by the intensity of technogenic or other parameters, it is feasible to use relative coefficients in addition to the absolute parameters. The relative coefficients should be calculated depending on the intended purpose in relation to population, area, or other physical, economic, or socio-geographical characteristics.

In order to estimate the per capita contribution to technogenesis of individual countries, the authors have calculated *specific regional tehnophility* (T_N), which is equal to the ratio T_Y/N, where T_Y is the volume of extracted AR in a country (t/yr) and N is the population of that country (persons) (Fig. 3). For the world as a whole, T_N is equal to 2,850 tons per capita per year. For the countries of the macroregions, T_N varies from 1,500 tons per capita per year in Africa to 15,400 tons per capita per year in Australia and Oceania. In North America, Asia, South America, Europe, and Central America, T_N is 3,800, 3,200, 3,100, 2,000, and 1,800 tons per capita per year, respectively.

Within the territories of relatively small countries, very rare elements can be produced (e.g., Nb and Ta in Rwanda, or Au

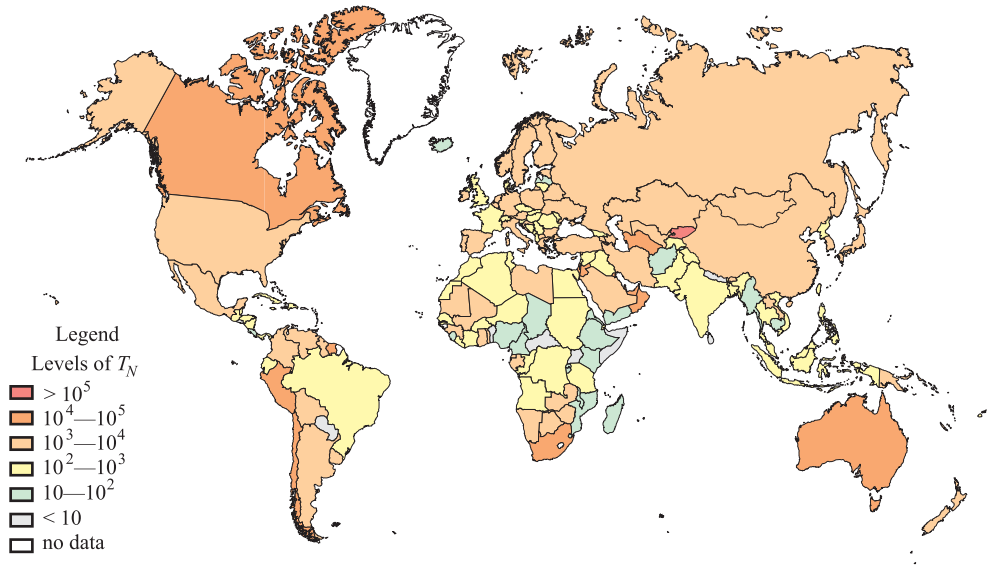

Fig. 3. Specific regional technophility (T_N) of different countries (tons per capita per year)

in Burundi, Togo, and Fiji). Therefore, their T_R values increase. In order to compare different countries with different levels of production of elements and area, *the density of regional conditional technophility of a country* (T_S) have been introduced; T_S equals to the ratio T_Y/S, where S is the area of a country (km^2) (Fig. 4). The world's level of T_S reaches 149 thousands t/km^2 per year. For the macroregions, T_S varies from 52,6 to 281 thousands t/km^2 per year in Australia-Oceania and Asia, respectively. T_S of Europe, Central America, South America, North

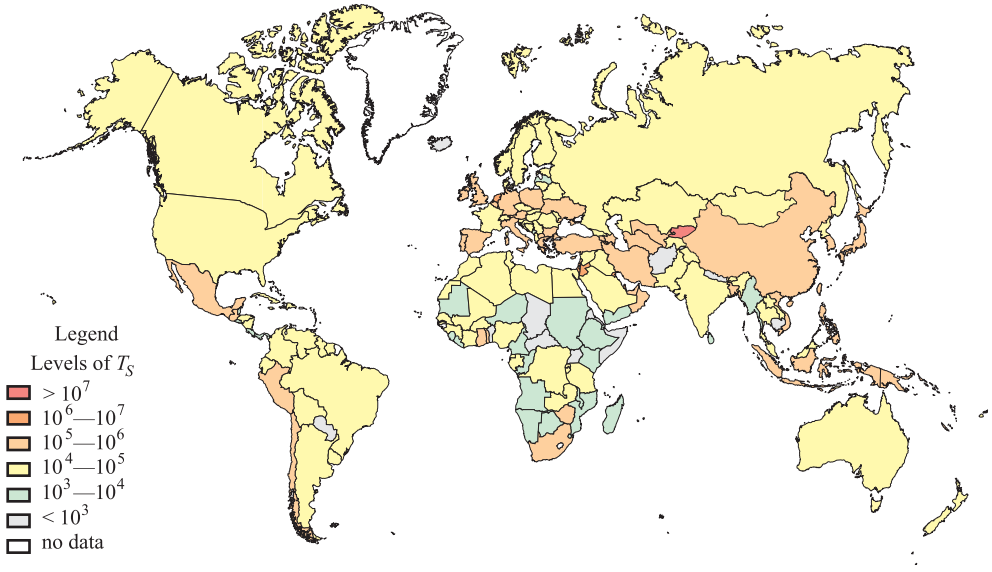

Fig. 4. Density of regional technophility (T_S) of different countries (tons per km^2 per year)

Table 1. The matrix array of the world's countries based on the intensity of technogenesis

Factor		Levels of TN (tons per capita per year)					
		Very low (<10)	Low (10–102)	Medium (102–103)	Intensive (103–104)	High (104–105)	Very high (>105)
Levels of TS (tons per km2 per year)	Very low (<103)	Cape Verde, Puerto Rico, Benin, Uganda, Nepal, CAR, Paraguay, Somalia, Haiti	Cambodia, Afghanistan, Eritrea, Chad, Iceland	–	–	–	–
	Low (103–104)	Sri Lanka, El Salvador, Mauritius	Burma, Ethiopia, Yemen, Netherlands Antilles, Cameroon, Costa Rica, Latvia, Sierra Leone, Malawi, Madagascar, Kenya, Swaziland, Mozambique	Montenegro, Angola, Panama, Djibouti, Sudan (with S. Sudan), Congo-Brazzaville, Liberia, Niger, Belize	Namibia, Mauritania, Botswana	–	–
	Medium (104–105)	–	Singapore, Rwanda, Burundi, Luxembourg, Nigeria	Denmark, Thailand, Czech Rep., D.P.R. Korea, Jamaica, Slovakia, France, India, Egypt, Malaysia, Albania, Romania, Hungary, Serbia, Georgia, Switzerland, Syria, Dominican Rep., Pakistan, Cuba, Tajikistan, Bosnia & Herzegovina, Guadeloupe, Fiji, Morocco, Moldova, Iraq, Burkina Faso, Honduras, East Timor, Tanzania, Tunisia, Nicaragua, Lithuania, Brazil, Slovenia, Senegal, Cote d'Ivoire, Algeria, Ecuador, Congo-Kinshasa	USA, Croatia, Norway, Equatorial Guinea, Belarus, Saudi Arabia, Kazakhstan, Russia, Sweden, Bolivia, Venezuela, Finland, Guinea, Estonia, New Zealand, Colombia, Zambia, Laos, Argentina, Uruguay, Bhutan Guyana, Mali, Libya, Gabon, Mongolia	Australia, Suriname, Canada	–
	Intensive (105–106)	–	–	Malta, Taiwan, Lebanon, Martinique, UK, Barbados, Bangladesh, Philippines, Indonesia, Vietnam, Guatemala	Belgium, R. Korea, Japan, Germany, Gambia, Turkey, Poland, Armenia, Austria, Brunei, Bulgaria, China, Spain, Ghana, Italy, Uzbekistan, Macedonia, Togo, Cyprus, Ireland, Greece, Mexico, New Caledonia, Portugal, Bahamas, Zimbabwe, Azerbaijan, Iran, Papua New Guinea, Ukraine	South Africa, UAE, Chile, Turkmenistan, Peru, Oman	–
	High (106–107)	–	–	–	Netherlands	Aruba, Qatar, Israel, Kuwait, Jordan	–
	Very high (>107)	–	–	–	Bahrain	Trinidad & Tobago	Kyrgyzstan

America, and Africa is 196, 133, 69,4, 66,9, 53,7 thousands t/km^2, respectively.

According to the values of T_N and T_S, the countries were combined into six groups (with an order of magnitude step-difference between the individual groups): *very high*, *high*, *intensive*, *medium*, *low*, and *very low* (Fig. 3 and 4). The *very high* ranking was assigned for the T_N values of higher than 10^5 tons per capita per year and for the T_S values higher than 10^7 t/km^2 per year. Eighteen groups of countries were isolated considering concurrently T_N and T_S (Table 1). Table 1 is a matrix array of T_N and T_S values that should be considered in combination.

The countries whose values of T_N and T_S depend on the intensity of production of chemical elements are located on the main diagonal of the matrix. Thus, low and very low T_N and T_S values are typical of small and medium-sized, in terms of population and area, countries where only some elements are produced (C, Ca, Na, Cl, S, Au, Si, Fe, Ti, and non-ferrous metals). Further increase of T_N and T_S occurs due to expansion of the list of produced elements and the intensity of their production.

Very high or *high* T_N and T_S are characteristic of relatively small, in terms of population and area, countries with intensive and medium level of production of chemical elements (Aruba, Israel, Kuwait, Jordan, Qatar, and Trinidad and Tobago), as well as of Kyrgyzstan that stands out as a country with the enormous T_{YR} reaching the level of T_{YR} for the major resource extraction countries, i.e., Russia, China, and South Africa.

The location of the countries in the cells next to the main diagonal may occur in the following cases: if production of chemical elements is comparable with the intensity of technogenesis in the countries of the main diagonal, the countries with a greater or smaller populations are located in the matrix to the left or to the right of the main diagonal, respectively, while countries with greater or smaller areas are located above or below the main diagonal. However, the values of both T_N and T_S for different countries in the cells adjacent to the main diagonal do not differ significantly. For example, for Russia, USA, and Kazakhstan with intensive chemical elements production, the level of T_S is *medium* because of the giant territories. On the other hand, The Netherlands, by the reason of small territory, is set into the group with *high* T_S. That is why the authors suggest considering such countries in the *intensive* T_N–T_S group.

Countries that are not in the adjacent to the main diagonal cells have "*very high*" T_S due to a small area (Bahrain), *low* levels of T_N, or *high* levels of T_S due to the low density of the population of about 3 persons per km^2 (Australia, Canada, Suriname, Namibia, Mauritania, and Botswana).

Analysis of Table 1 and Figs. 2–4 allows identifying countries with significant absolute elements production and with high levels of relative parameters of technogenesis, i.e., with *intensive*, *high*, and *very high* T_{YR}, T_N, and T_S: Kyrgyzstan, China, South Africa, Chile, Peru, Turkey, Mexico, Japan, Turkmenistan, Germany, Iran, Poland, Spain, Israel, Jordan, Uzbekistan, R. Korea, Trinidad and Tobago, Ukraine, Qatar, Italy, UAE, Ghana, Netherlands, Papua New Guinea, Zimbabwe, Kuwait, Oman, Bulgaria, Austria, Belgium, Greece, Bahrain, and Portugal. The leaders in the production of various minerals with the giant absolute levels of technogenesis have low relative regional parameters: Russia, USA, Canada, Australia, Saudi Arabia, Kazakhstan, Argentina, Bolivia, Venezuela, Colombia, Zambia, Mali, Libya, Mongolia, Sudan (with South Sudan) – because of large territories; Indonesia, Vietnam, Philippines, Bangladesh, Nigeria – because of significant population; while India, Brazil, France, Egypt, Thailand, Pakistan, Algeria, Tanzania, Congo (Kinshasa), Malaysia, Morocco (with Western Sahara) – because of both high spatial and demographic dimensions.

Thus, the proposed integral parameters allow comparing the relative intensity of technogenesis of the countries with very different demographic and spatial dimensions. They account for a wide range of chemical

elements and are effective in identification, for example, of small countries with high levels of elements production, or on the contrary, of large countries with low levels.

CONCLUSION

The "geochemical" approach provides for comparison of certain aspects of technogenesis intensity in different countries and represents analysis of various factors and indices, among which the most useful are tehnophility and its derivatives.

For concurrent comparison of the intensity of production of chemical elements, the authors have introduced the concept of elemental equivalent, i.e., "abstract rock" whose average chemical composition coincides with the average chemical composition of the upper continental crust. The authors have also introduced new parameters. "*Conditional technophility*" (T_Y) represents the number of tons of AR per year, necessary for production of the current level of an element. Because of the high level of contrast and temporal variability, T_Y is a useful indicator of the level of technogenesis in different countries. Calculation of the sum of T_Y for different chemical elements allows assessing their integral involvement in technogenesis. The highest T_Y values are associated with C, S, N, Ra, and Au. T_Y of many micro- and ultramicroelements is of the order of $n \cdot 10^{11}$t. T_Y is minimal for Sc and Rb that, though they have relatively high concentrations in the upper continental crust, are little used by mankind so far.

"*Specific technophility*" (T_{YN}) reflects the volume of AR per the world's capita. Analysis of the changes from the 1960s to 2010 indicates that the Earth's population is growing much faster than its demand for many chemical elements.

In order to integrally assess the regional aspects of technogenesis, the authors have also used: T_{YR}, T_N, and T_S – "regional conditional technophility," "specific regional technophility," and "density of regional conditional technophiliy," respectively. These parameters indicate the intensity of involvement of a range of chemical elements in technogenesis, depending on the population and physical size of a country. The highest T_{YR} is associated with Asia and Europe, while the lowest – with Central America and Australia-Oceania.

Considering T_N and T_S concurrently, it was possible to isolate 18 groups of countries that differ in the lists of produced chemical elements and in the intensity of the primary mobilization of the elements in technogenesis. *Low* and *very low* T_N and T_S values are typical of small and medium-sized, in terms of population and area, countries where only individual elements are produced; *high* and *very high* T_N and T_S values – of small countries with intensive and medium levels of production of chemical elements (Aruba, Trinidad and Tobago, Kuwait, Qatar, Israel, and Jordan), as well as of Kyrgyzstan with its enormous volume of elements production.

The authors have isolated the countries with high levels of the absolute and relative parameters of technogenesis: in Asia – Kyrgyzstan, China, Japan, Turkmenistan, Iran, Israel, Jordan, Uzbekistan, R. Korea, Qatar, UAE, Papua New Guinea, Kuwait, Oman, and Bahrain; in Europe – Turkey, Germany, Poland, Spain, Ukraine, Italy, Netherlands, Bulgaria, Austria, Belgium, Greece, and Portugal; in Africa – South Africa, Ghana, Zimbabwe; and in South America – Chile, Peru, Mexico, and Trinidad and Tobago.

The relative indicators of technogenesis of the leaders in extraction of natural resources are below these values in other countries due to the large territories (Russia, USA, Canada, Australia, Saudi Arabia, Kazakhstan, Argentina, Bolivia, Venezuela, Colombia, Zambia, Mali, Libya, Mongolia, and Sudan), to the large population (Indonesia, Vietnam, the Philippines, Bangladesh, Nigeria), or to both high spatial and demographic dimensions (India, Brazil, France, Egypt, Thailand, Pakistan, Algeria, Tanzania, Congo (Kinshasa), Malaysia, and Morocco). ■

REFERENCES

1. Bityukova V.R. (2010) Evolution of regional structure of ecological situation in Russia 1990–2008. *Ecology and industry of Russia*, N 10, pp. 4–7 (in Russian with English summary).

2. Bityukova V.R., Kasimov N.S. (2012) Atmospheric pollution of Russia's cities: Assessment of emissions and immissions based on statistical data. *Geofizika*, Vol. 29, N 1, pp. 53–67.

3. Bityukova V.R., Kasimov N.S., Vlasov D.V. (2011) Environmental portrait of Russian cities. *Ecology and industry of Russia*, N 4, pp. 6–18 (in Russian with English summary).

4. Bityukova V.R., Kirillov P.L. (2011) Methods of complex estimation of the regional defferences under the ecological stress in Russia. *Regional studies*, N 2 (32), pp. 56–69 (in Russian with English summary).

5. Bцhringer C., Jochem P. (2007) Measuring the immeasurable – A survey of sustainability indices. *Ecological Economics*, Vol. 63, Iss. 1, pp. 1–8.

6. Bradshaw C.J.A., Giam X., Sodhi N.S. (2010) Evaluating the relative environmental impact of countries. *PLoS ONE*, Vol. 5, Iss. 5, e10440.

7. Butterman W.C., Brooks W.E., Reese R.G. Jr. (2004) *Mineral Commodity Profiles. Cesium* [online]. USGS, Open-File Report 2004–1432. Available from: http://pubs.usgs.gov/of/2004/1432/2004-1432.pdf [Accessed 02.12.2012].

8. Butterman W.C., Reese R.G. Jr. (2003) *Mineral Commodity Profiles. Rubidium* [online]. USGS, Open–File Report 03–045. Available from: http://pubs.usgs.gov/of/2003/of03-045/of03-045.pdf [Accessed 02.12.2012].

9. Clarke F.W. (1889) The relative abundance of the chemical elements. *Phil. Soc. Washington Bull.*, XI, pp. 131–142.

10. CRC Practical Handbook of physical properties of rocks and minerals (1989). Edited by R.S. Carmichael. Boca Raton: CRC Press, 741 p.

11. Denier van der Gon H.A.C., Visschedijk A.J.H., van der Brugh H., Droge R., Kuenen J. (2009) *A Base year (2005) MEGAPOLI European Gridded Emission Inventory* [online]. MEGAPOLI Project Scientific Report 09-02, MEGAPOLI Deliverable Report D1.2. Available from: *http://megapoli.dmi.dk/publ/MEGAPOLI_sr09-02.pdf* [Accessed 17.06.2013].

12. Esty D.C., Andonov B., Kim C., Townsend J., Srebotnjak T., Campbell K., Li Q., Zhang B., Goodall M., Gregg K., Martinez M., Levy M., de Sherbinin A., Anderson B., Saltelli A., Saisana M., Nardo M., Dahl A. (2005) *Environmental sustainability index* [online]. Environmental Performance Measurement Project. Available from: http://www.yale.edu/esi/ [Accessed 17.06.2013].

13. Glazovskiy N.F. (1976) Technogenic migration of nitrogen, phosphorus, potassium and sulfur on USSR territory. *Vestnik Mosk. yn-ta, Ser. 5, Geor.*, N 4, pp. 32–44 (in Russian).

14. Glazovskiy N.F., Glazovskaya M.A. (1981) Environmental geochemistry and regional geography, pp. 104–120. In: Issues of Geography. Regional Geography: condition and tasks. Vol. 116. Moscow: Mysl' (in Russian).

15. Goldschmidt V.M. (1933) Grundlagen der quantitativen Geochemie. *Fortschr. Mineral. Kirst. Petrogr.*, N 17, pp.112. (in German).

16. Greenwood N.N., Earnshaw A. (1997) Chemistry of the Elements. Oxford: Butterworth-Heinemann, 1600 p.

17. Grigoriev N.A. (2009) Chemical element distribution in the upper continental crust. Ekaterinburg: Ural Branch of RAS, 382 p. (in Russian with English summary).

18. Emsley J. (1991) The Elements. Oxford: Clarendon Press, 251 p.

19. Environmental, chemistry & hazardous material news, careers & resources (2012) [online]. Environmental chemistry. Available from: http://environmentalchemistry.com/yogi/periodic/ [Accessed 02.12.2012].

20. Fersman A.E. (1934) Geochemistry. Leningrad: Khimteoret, 354 p. (in Russian).

21. Haxel G.B., Hedrick J.B., Orris G.J. (2002) Rare Earth Element – Critical resources for High Technology [online]. USGS, Fact Sheet 087–02. Available from: http://pubs.usgs.gov/fs/2002/fs087-02/fs087-02.pdf [Accessed 02.12.2012].

22. International energy statistics (2012). U.S. Energy Information Administration [online]. Available from: http://www.eia.gov/cfapps/ipdbproject/IEDIndex3.cfm [Accessed 02.12.2012].

23. *International minerals statistics and information* (2012). U.S. Geol. Surv. [online]. Available from: http://minerals.usgs.gov/minerals/pubs/country/ [Accessed 02.12.2012].

24. Kapitza S.P. (1999) Essay on the theory of human population growth: how many people lived, lives and will live on the Earth. Moscow: Nauka, 239 p. (in Russian).

25. Kasimov N.S., Vlasov D.V. (2012) Technophility of chemical elements in the beginning of the 21st century. *Vestnik Mosk. yn-ta, Ser. 5, Geor.*, N 1, pp. 15–22 (in Russian with English summary).

26. Key world energy statistics (2012). International Energy Agency [online]. Available from: http://www.iea.org/textbase/nppdf/stat/12/kwes.pdf [Accessed 02.12.2012].

27. *Mineral commodity summaries* (2012). U.S. Geol. Surv. [online]. Available from: http://minerals.usgs.gov/minerals/pubs/mcs/ [Accessed 02.12.2012].

28. Nriagu J.O., Pacyna J.M. (1988) Quantitative assessment of worldwide contamination of air, water and soils by trace metals. *Nature*, Vol. 333, pp. 134–139.

29. Pacyna J.M., Pacyna E.G. (2001) An assessment of global and region emissions of trace metals to the atmosphere from anthropogenic sources worldwide. *Environmental Reviews*, N 9, pp. 269–298.

30. Perel'man A.I. (1975) Landscape geochemistry. Moscow: Vyshaja Shkola, 342 p. (in Russian).

31. *Revised 1996 IPCC Guidelines for National Greenhouse Gas Inventories: Reference Manual* (2012). IPCC [online]. Available from: http://www.ipcc-nggip.iges.or.jp/public/gl/invs6.html [Accessed 02.12.2012].

32. Rudnick R.L., Gao S. (2003) Composition of the continental crust. In: Treatise on geochemistry. Vol. 3: The Crust. Edited by H.D. Holland and K.K. Turekian. Elsevier Science, pp. 1–64.

33. The world factbook (2012). CIA [online]. Available from: https://www.cia.gov/library/publications/the-world-factbook/ [Accessed 02.12.2012].

34. The world market of noble gases. (2012) New chemical technologies. Analytical portal of chemical industry [online]. Available from: http://www.newchemistry.ru/printletter.php?n_id=7855 [Accessed 02.12.2012] (in Russian).

35. Tikunov V.S., Tsapuk D.A. (1999) Sustainable development of territories: cartographic and GIS support. Moscow–Smolensk: Izd-vo SGY, 176 p. (in Russian).

36. Vinogradov A.P. (1962) The average content of chemical elements in the main types of igneous rocks of the Earth crust. *Geochemistry*, N 7, pp. 555–571 (in Russian).

37. Yang X.-Y., Sun W.-D., Zhang Y.-X., Zheng Y.-F. (2009) Geochemical constraints on the genesis of the Bayan Obo Fe–Nb–REE deposit in Inner Mongolia, China. Geochim. et *Cosmochim. Acta*, N 73, pp. 1417–1435.

Nikolay S. Kasimov, Professor of the Lomonosov Moscow State University and Full Member of the Russian Academy of Sciences, received his PhD in Geography studying landscape geochemistry of fault zones in 1972 and gained Doctor of Science for research in paleogeochemistry of steppes and deserts landscapes in 1983. Since 1987 he is the Head of the Department of Landscape Geochemistry and Soil Geography and since 1990 – Dean of the Faculty of Geography at the Moscow State University. His current research interests are: geochemistry of urban landscapes in the cities of Russia and the world, their assessment and classification, elaboration of geochemical principles for GIS of cities and regions and geochemistry of aquatic landscapes. He leads Russian-Dutch projects related to the study of changes in the coastal zone landscapes of the Caspian Sea. At the Moscow State University he delivers courses of lectures: "Landscape geochemistry" and "Geochemistry of natural and anthropogenic landscapes". He also gave lectures at the universities of Sofia, Havana, Barcelona and Cambridge. In 2000 he was awarded by the Russian government for the development of a system of environmental education in the universities of Russia and in 2004 for the elaboration of environmental and natural resource atlases of Russia. He is the author of about 300 scientific works, including: Landscape Geochemistry, 1999 (co-author A.I. Perel'man); Landscape Ecogeochemistry, 2013.

Dmitry V. Vlasov studied Geoecology at the Moscow State University, graduated in 2012 and obtained the Specialist's degree (Diploma). Since October 2012 he is a PhD student and Junior Researcher of the Department of Landscape Geochemistry and Soil Geography of the Faculty of Geography, Moscow State University. The focus of his studies is in urban geochemistry, techogenesis and biogeochemistry. Main publications are "Environmental portrait of Russian cities", "Technophility of chemical elements in the beginning of the 21st century", "Geochemistry of snow cover within the Eastern district of Moscow" (all in Russian with English summaries, with co-authors).

Olga Solomina[1*], Olga Maximova[1], Edward Cook[2]
[1]Institute of Geography Russian Academy of Sciences, Staromonetny-29, Moscow, Russia, 119017; Tel: +7-495-959-00-34, Fax: +7-495-959-00-33,
e-mail: olgasolomina@yandex.ru
[*] **Corresponding author**
[2] Lamont-Doherthy Observatory, Palisades, New York 10964 USA;
Tel: 845-365-8618, Fax: 845-365-8152, e-mail: drdendro@ldeo.columbia.edu

PICEA SCHRENKIANA RING WIDTH AND DENSITY AT THE UPPER AND LOWER TREE LIMITS IN THE TIEN SHAN MTS (KYRGYZ REPUBLIC) AS A SOURCE OF PALEOCLIMATIC INFORMATION

ABSTRACT. We present here the results of spruce (*Picea schrenkiana Fish. et May.*) tree-ring research in the Tien Shan Mountains, Kirgiz Republic. We explore the connection between climatic parameters and spruce ring width and maximum density at the upper and lower tree limits and provide two reconstructions: the May–August temperature reconstruction from 1626 to 1995 based on a multi-site composite maximum density chronology from the upper tree limit and the drought index reconstruction from 1680 to 2000 based on the lower tree limit regional ring width chronology. The ring width chronologies from the upper and lower tree limits show a strong similarity. They both depend to a large extent on moisture availability. The maximum density chronology does not correlate with them: it depends on different climatic parameters, namely on the summer temperature. The correlations of the reconstructions with CRU TS3 temperature and precipitation grid point data confirm the results of the modeling using the meteorological data from the nearest stations. The 20th century does not look unusual in the context of the last three hundred years in the Tien Shan Mountains, either in terms of the drought occurrence and severity or in summer temperature changes. However the reconstruction does not encompass the last decade when the summer warming in Tine Shan has been especially prominent. In contrast, some change in precipitation is indicated with the 19th century being drier in the Issyk Kul region compared to the 20th century.

KEY WORDS: Tree rings, ring width, maximum density, summer temperature and drought index reconstructions, upper and lower tree limits, Tien Shan.

INTRODUCTION

Tree-ring based reconstructions are among the most reliable sources of high resolution paleoclimatic information. This kind of information is especially important in the remote mountain regions with poor meteorological networks. The Tien Shan Mountains in Kyrgyzstan is one of those regions. Meteorological observations in Tien Shan began in 1879 at the Karakol meteorological station, near Issyk Kul lake shore, but most of stations were established in the second half of 20th century only. Spruce forests, which are wide spread in this region, provide important dendrochronological

material for potential dendroclimatic reconstructions. The spruce trees can be up to 700–800 years old and form clear annual rings. The study presented here aims to synthesize the achievements of spruce tree-ring research in the Tien Shan Mountains, namely to explore the connection between climatic parameters and spruce ring width (RW) and maximum density (MXD), and to reconstruct climatic parameters at the upper and lower tree limits in the Tien Shan Mountains in the Krygyz Respublic.

STATE-OF–THE-ART

Two kind of trees – juniper (*Juniperus sp.)* and spruce (*Picea schrenkiana Fish. et May.*) growing in the Tien Shan Mountains attracted most attention of dendrochronologists since 1960–1970s. Studying the juniper forests at the Northern slope of the Alaisky Range, Mukhamedshin [1977] discovered trees more than thousand years old. He demonstrated the general correspondence of the juniper ring width to summer temperature. Solomina and Glazovsky [1989] obtained similar results for juniper in the Issyk Kul area. However, these first attempts were based on poorly replicated chronologies, short meteorological series used for calibration, and weak correlations of ring width and meteorological parameters. Graybill et al. [1990] and Glazirin and Gorlanova [2005] sampled juniper in the vicinity of meteorological stations aiming to identify the climatic signal more clearly, but their results were similar: they identified weak correlations with climate. Later, Esper et al. [2002] constructed the longest juniper chronology (since AD 618) for one site in southern Kyrgyzstan. Due to the lack of statistically significant correlation between ring width and meteorological variables, they calibrated the juniper ring width against the maximum density chronology of spruce, which in turn correlates with July-August summer air temperature. The similarity between these series with others from Tien Shan and Karakomum provided evidence that the chronologies contained a regional climatic signal as well. Esper et al. [2003] used the "Regional Standardization Curve" to preserve the long-term temperature trend in the reconstruction based on the juniper ring width chronologies constructed in the Alai Mountains in the southern part of Kirgiz Republic.

In the early 1980s Borscheva [1981, 1983] published the results of her studies of *Picea Schrenkiana* ring width in Zailiiiskii Alatau along an elevational transect – 1400 m (lower spruce tree limit), 2200 and 2600 m (ecological optimum), and 2800 m (upper spruce tree limit). She discovered that the early wood ring width of spruce even at the upper tree limit depends mostly on the fall-winter-spring precipitation preceding the growth season. In the narrow shaded valleys the ring width also depended on the summer temperature [Borscheva, 1981]. At the lower tree limit the ring width depends on the combination of temperature and precipitation during the vegetation period [Solomina et al., 2007]. The ring width is influenced by the climatic parameters of several years preceding the growth [Borscheva, 1981]. Spruce RW chronologies from the Issyk Kul area [Solomina and Glazovsky, 1989] were also used to reconstruct an index of glacial activity. Recently, tree-ring (spruce) reconstructions of air temperature [Solomina et al., 2006] and drought index [Solomina et al., 2007] covering the last few centuries were published, but all of these publications are in Russian and were not internationally peer reviewed.

SPATIAL DISTRIBUTION AND ECOLOGICAL PREFERENCES OF *PICEA SCHRENKIANA* IN TIEN SHAN MOUNTAINS

Picea schrenkiana grows in the Kyrgyzky, Zailiisky, Kungey and Terskey Ala-too, Koeliu, Sarydzhaz, and Atbashi regions, as well as in the western Tien Shan. The optimum for Tien Shan spruce growth is attributed to the area with the mean annual air temperature from –2 to 2°C, annual precipitation from 500 to 700 mm, and an elevation range of 1400 to 3600 m asl. In the lowest part of its range, spruce grows on north-facing slopes, in the mid part on west- and east-

facing slopes, and in the uppermost part on south-facing slopes [Kozhevnikova, 1982]. This distribution suggests that at the upper tree limit the growth of spruce is limited by temperature. The soil moisture plays an important role in the spruce ecology. Spruce requires abundant water, but in the uppermost part at the northern slopes the thin soil layers can become too wet due to great amount of precipitation and low evaporation [Kozhevnikova, 1982].

MATERIALS AND METHODS

From 2000 to 2009 we collected tree-ring samples (cores and disks from dead trees) of spruce (*Picea schrenikiana*) from 15 high elevation and 9 low elevation sites in the Central Tien Shan in Kyrgyz republic (Fig. 1). We also used in this study the collections of ring width and density measurements (3 sites) from the International Tree-Ring Data Bank (Karabatkak, Sarykungey and Saryimek valleys) contributed by F. Schweingruber.

All samples were analyzed using the standard dendrochronological methods [Fritts, 1979; Cook and Kairiukstis, 1990]. Where possible we selected for sampling the trees standing apart from each other, without visual disturbances and wounds, and from the sites with homogeneous orographic, soil and other meso- and microclimatic characteristics. The coordinates of the selected sites were fixed with by GPS and mapped (see Fig. 1). We used COFECHA [Holmes, 1983] for evaluating the quality of the cross-dated series and used ARSTAN [Cook, 1985] to detrend the series and build the local chronologies. The growth trends were approximated by negative exponential or linear curves and the resulting tree-ring indices were calculated as the division of each annual ring width by its respective fitted growth curve value (see Cook and Kairiukstis [1990] for details). The individual detrended series were then averaged in local chronologies. The same procedure was used to detrend the MXD series of F.Schweingruber. Due to the unsufficient number of samples of the subfossil wood we were not able to use RCS detrending [Briffa and Melvin, 2010].

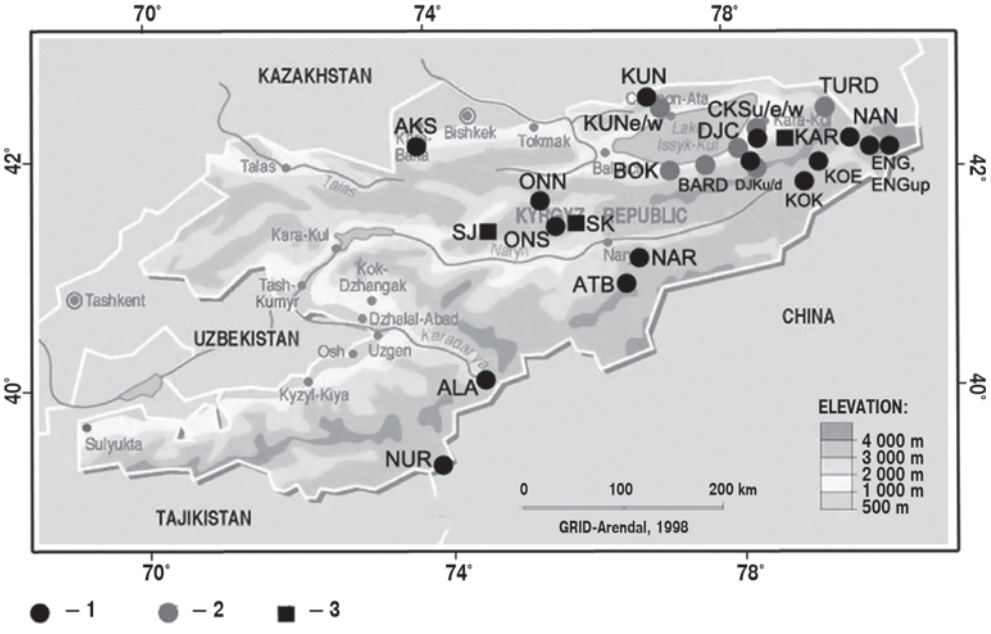

Fig. 1. Map of tree-ring sites: 1 – Upper tree limit, RW, 2 – Lower tree limit, RW, 3 – Upper tree limit, MXD (from the International Tree-Ring Data Bank contributed by F. Schweingruber)

We used DENDROCLIM [Biondi and Waikul, 2004] and correlation analyses to estimate the factors that influence both ring width and density. For this analysis, mean monthly temperature and total monthly precipitation measured at meteorological stations located near the sampling sites were used. In some cases due to the lack of meteorological stations at the high elevation we had to use records from elevations lower than 2000 m. The missing values in the meteorological time series were replaced by the medians of the same series. We could not calculate the response for the sites AKS and ATB due to the insufficient length of meteorological series.

RESULTS

Upper tree limit. Ring width. The correlation analyses demonstrates the high similarity of all 18 RW site chronologies from various locations in the Tien Shan Mountains., which is a sign of a common signal influencing the growth pattern at this large territory. In order to combine the site chronologies we used both correlation and principal component analyses. The similarity of sites by the first PC shows that there is a common factor explaining 50% of ring width variability. The 2nd and 3d PC explain 25 and 10% of the variance respectively. Based on these analyses three groups of chronologies were identified: 1 – AKS, ATB, KUN, ONS, ONN, NAR, CKSU; 2 – ENG, KOE, NAN; 3 – DJKU, KOK. The chronologies tend to group by the vicinity of their location, though this rule has some exceptions. For instance, DJKU does not correlate with any neighboring site except for the KOK. KUN has a high correlation with ATB, ONS, ONN, CKSU, though they are located far away from this site. ATB correlates well with even remote sites.

As soon as all samples cross-date well and the local chronologies correlate with each other they all can be averaged in a regional chronology – TSH UP (Fig. 2*)*. The earliest part of the chronology (AD1301-1360) was cut out due to the poor replication. According to the EPS-test (> 0,85) the remaining chronology is reliable from 1360 to 1460 and from 1510 to 2006.

In general the correlation of the meteorological variables with the ring-width chronologies is not high. This can be partly explained by the remote location of many meteorological stations from the tree-ring sites, but also by a complexity of climatic signal embedded in the spruce tree-rings in Tien Shan**.** In the Fig. 3 one can see that there is a tendency for positive correlation between ring width and total precipitation in August, October, November, December of the previous year. The correlation with temperature is less consistent: there is a negative correlation with the April–May temperature as well as with the summer months of the previous year. Temperature in

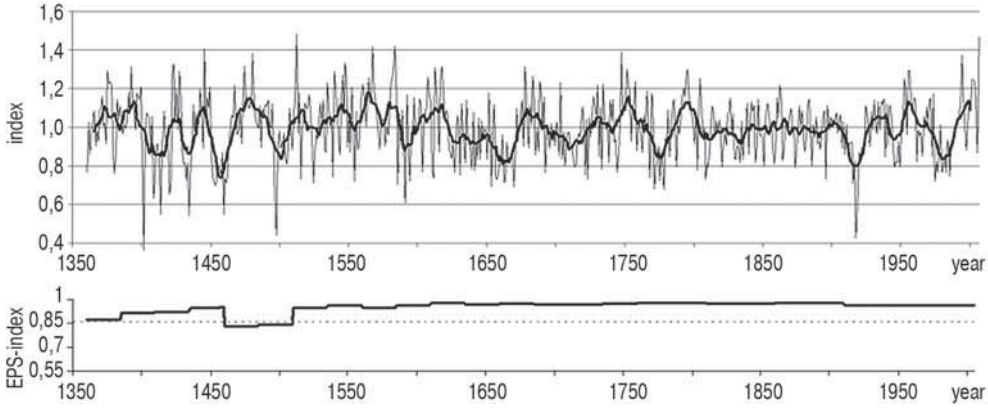

Fig. 2. Regional RW spruce chronology (TSH UP) and its EPS index

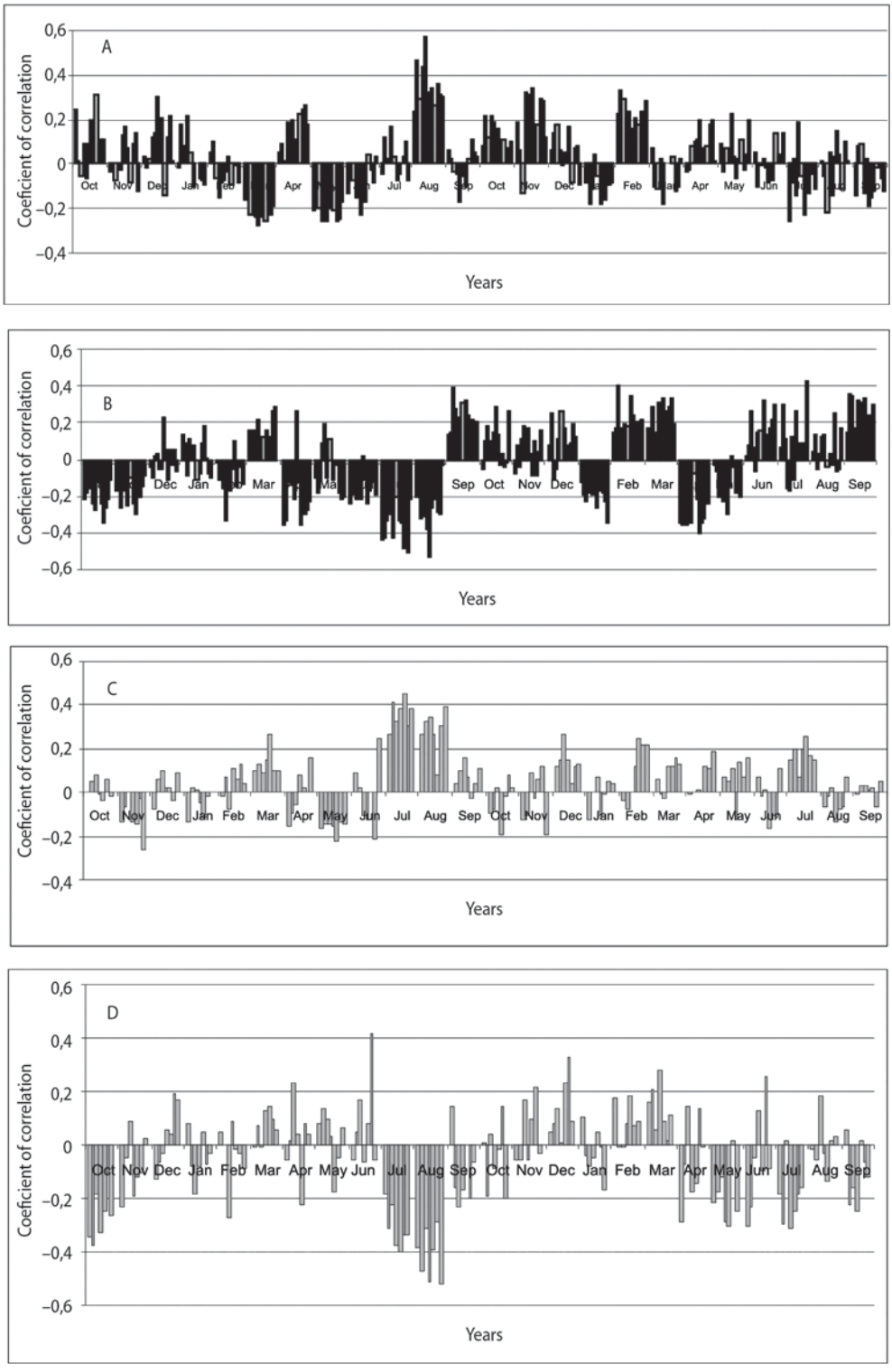

Fig. 3. Correlation functions: the correlation of ring width site chronologies (upper tree limit) with the monthly sum of precipitation (a) and monthly temperature (b) measured at the nearest meteorological stations. (c) and (d) – the same for the lower tree limit site chronologies. Significant at 95% level are coefficient of correlation exceeding 0,35

Table 1. The largest and narrowest tree rings at the upper tree limit

Largest rings		Narrowest rings	
year	ring width	year	ring width
1474	1.45	1451	0.61
1480	1.53	1452	0.67
1512	1.59	1453	0.65
1567	1.38	1454	0.67
1582	1.44	1457	0.64
1583	1.56	1459	0.54
1651	1.35	1496	0.54
1677	1.38	1497	0.45
1747	1.45	1535	0.66
1751	1.30	1538	0.65
1795	1.34	1549	0.62
1804	1.30	1591	0.65
1955	1.30	1771	0.65
1956	1.33	1917	0.49
1994	1.34	1918	0.60

June-September is to the contrary favorable for the growth at the upper tree line.

The low growth anomalies are identified in our regional chronology in 1970–80s, in the early 20th century, in the second quarter 19th century, in 1770–80s, in the late 17th – early 18th centuries, in the mid 17th century, and in the end of 16th century (see Fig. 2). The positive growth anomalies occurred in the mid 20th century, in the late 18th – early 19th centuries, in the middle of 18th century, and in the early of 17th century, in the late 16th – early 17th centuries, n the middle of 16th century. In the Table 1 we list the narrowest and largest rings.

Upper tree limit. Maximum density. The maximum density chronologies for KAR, SK, SJ demonstrate a very high similarity both at the level of interannual and decadal variability. This similarity means that a strong climatic signal is forcing maximum density formation. The correlation between the sites is high despite of long distance between them (r = 0,7–0,75). The response functions for all three sites are also similar [Solomina et al., 2006]. The maximum density significantly correlates also with April-September, but with lower coefficient of correlation when comparing with a shorter window for May–August (r = 0,63 and r = 0,79, respectively). The correlation is significant and negative with the sum of annual precipitation (r = –0,56).

The high similarity and correlation of the KAR, SK, SJ maximum density chronologies permit them to be averaged into a single chronology lasting from 1626 to 1995 and including 58 cores. According to the EPS-test (> 0,85) the chronology is reliable over the period AD 1650–1995. This regional Dmax chronology correlates (r^2 = 0,62) with the May-August temperature measured at the Chon-Kizil-su meteorological station (1948–1987). The correlation with the longer record from Tien Shan meteorological station (1930–1995) decreases, but remains significant at 99% level (r = 0,41). The three offsets of the growth in the years 1694, 1696, and 1698 look like local disturbances, but they reveal themselves in both SJ and KAR chronologies which are located more than 200 km apart from each other and even at the different mountain ranges. For this reason we consider them as a sign of a climatic signal.

The subdivision of the meteorological records into calibration and verification periods (1965–1995 and 1930–1964) shows that the correlation with May–August temperature remains significant for both intervals (r = 0,51 and 0,48 respectively). The highest correlation is observed for the period of 1950s–1980s.

According to our reconstruction (Fig. 4) the low May–August temperature in the Tien Shan occurred in the second half of 17th century, in the middle and the end of 18th century, in 1810s, 1830s, 1880–90s, 1950–60s and in 1980s. According to these data extremely cold years are 1664, 1674, 1676, 1694, 1996, 1698, 1722, 1755, 1761, 1783, 1803, 1813, 1816, 1841, 1869, 1920, 1957, 1972, 1989; warm extremes are 1705, 1708, 1716, 1720, 1727, 1732, 1747, 1807, 1822, 1878, 1881, 1916, 1926, 1933, 1944, 1978, 1984, 1994, 1995.

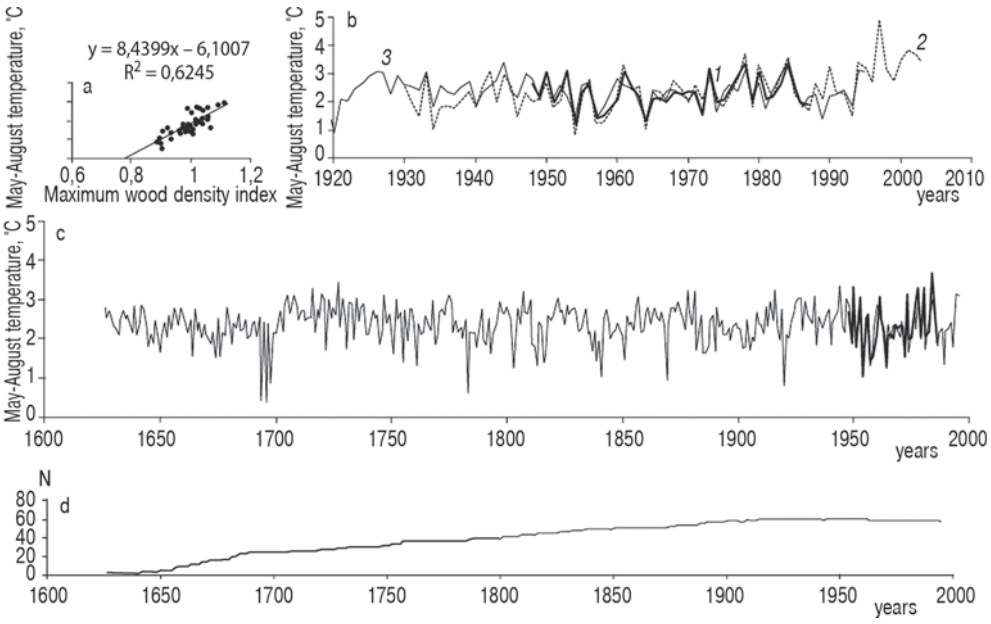

Fig. 4. Reconstruction of May–August temperature by maximum late wood density (mean of three chronologies SJ, SK, KAR):

(a) linear regression and coefficient of correlation of May–August temperature and indices of maximum density chronology; (b) May–August temperature measured at the Chon-Kizil-su meteorological station and adjusted to the elevation of 3600 m (for the comparison with Tien Shan station) (1), measured at the Tien Shan station (2), reconstructed by the maximum density on the base of linear regression coefficient (3); (c) May-August temperature, measured at the Chon-Kizil-su station and adjusted to the elevation of 3600 m and reconstructed by maximum density for 1626–1995; (d) number of samples N in the chronology used for the reconstruction

Maximum density of spruce at the upper tree limit does not correlate with the ring width. This is also clear from the response function, which shows that the DMAX is responsible mostly for the summer temperature, while the ring width is more influenced by the moisture supply.

Lower tree limit. Ring width. For the lower tree limit we analyzed 9 individual site chronologies. The length of the spruce tree-ring series at the lower tree limit is short for two reasons. Firstly, the spruce wood is intensely used for the building activity near the places where the population is concentrated. Secondly, the trees are almost always rotten inside at these sites and the remaining solid wood portion has relatively few rings in it. Thus the chronologies from living trees here rarely exceed the instrumental period (one century) and therefore are not very valuable for the paleoclimate reconstructions. In order to extend their length we sampled old buildings in the area. They are the Svetly Mis Monastery, the school in Pokrovka village, one of the first Russian house of Kolomiitsv in Teplokliuchenka village, and the house of Tien-Shan Physical Geography research station in Chon Kizil-su valley [Solomina et al., 2007]. We cross-dated the building samples with the living tree chronologies. With the exception of the last building all houses are located near the Issyk Kul shore at the elevation 1600–1800 m asl and most probably were built from the wood of the trees growing in the vicinity. Due to the late colonization of this region (19th century) we did not expect to extend the chronology far back more then a few more decades. The correlation of all individual samples with the living trees chronologies of the same valleys (CKS and KUN) is statistically significant. All samples of wood we used were around 200 years long and allowed the extension of the chronology back to AD 1680 (Fig. 5). According to the EPS-test (> 0,85) the chronology is reliable from 1750 to 2005.

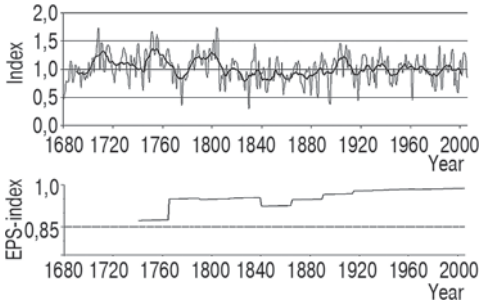

Fig. 5. Ring width regional lower tree limit chronology of spruce (TSH DOWN) and its EPS index

All local and regional average chronologies of the Issyk Kul area correlate with one another. The significant correlations also extend to the chronologies from the Zailiisky Alatau region except for the lowest chronology located at the elevation 1400 m a.s.l. [Borscheva, 1981]. It is of interest that this chronology also weakly correlates with the other sites in the same Talgar valley [Borscheva, 1981].

The correlation functions for the local RW chronologies from the lower tree limit are displayed at the Fig. 3 (c, d). The pattern of correlation function is generally similar to the upper tree limit (Fig. 3, a and b): both temperature and precipitation is July and August of previous year are most important for the tree growth. However the influence of the warm period temperature of the current year at the lower tree limit is negative.

We tested the correlation of the ring width with several modifications of the drought index combining the two parameters [Bitvinskas, 1974]. The highest correlations that we found are with the drought coefficient which includes both temperature and precipitation for the warm period for the current and previous year (June-September):

$$Q = P_1 + P_0/(T_1 + T_0)/2,$$

where P_0 (T_0) u P_1 (T_1) – precipitation (temperature) of June–September of the current and the previous years.

Using the longest Przhevalsk meteorological station (1887–1988) over its full length, the correlation of the regional low elevation chronology (TSH DOWN) with the drought coefficient is 0,41 (0,59 for five years running mean). The correlation is higher in the beginning of the records (for 1887–1959 R^2 = 0,50), but it decreases since the late 1950s.

We extended the Przhevalsk records from 1887 to 2000 using two neighboring meteorological stations Pokrovka (Kyzil-su) and Cholpon-Ata. We had to exclude the years (1986 and 1988–1990) from the Pokrovka time series because they demonstrate anomalous high precipitation in July–September exceeding two standard deviations and this anomaly is not recorded at other stations of the region. The drought coefficient based on these records correlates with the Przhevalsk drought index (r = 0,69) as well as with drought index reconstructed by tree-ring data for the period 1951–2000. However in the last case the correlation is not high (r = 0,34). The correlation between ring width and drought coefficient in the second half of the 20th century did not disappear, but it did weaken.

Thus, low precipitation and high temperature during the warm season limit the growth of *Picea Schrenkiana* at the lower tree limit. This allowed the reconstruction of the drought index for the the period 1750–2005 (Fig. 6). According to this reconstruction the droughts in the Issyk Kul region occurred in 1774–1775, 1828–1829, 1856–1857, 1873–1874, 1879–

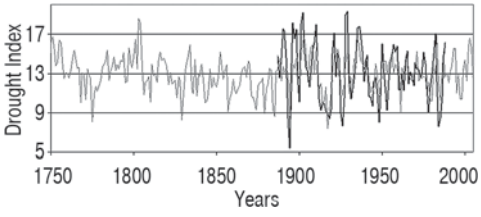

Fig. 6. Drought Index calculated from meteorological data (black) and reconstructed by tree rings (gray)

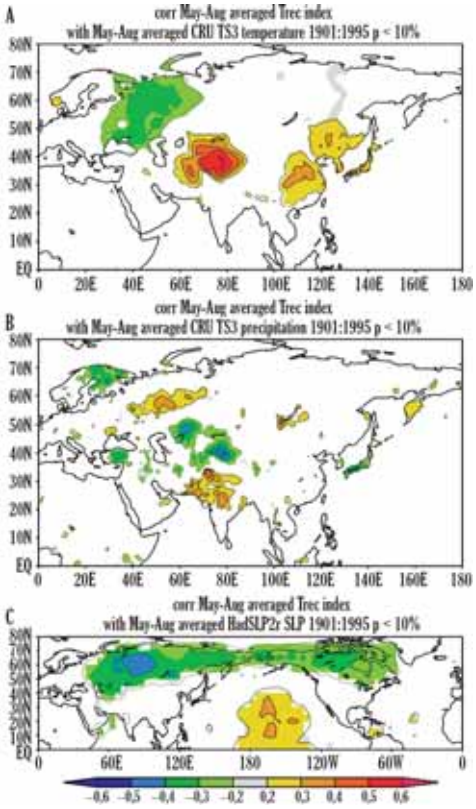

Fig. 7. Correlation maps of the May–August temperature in the Tien Shan Mts with CRU TS3 grid point parameters of the same period (a) temperature, (b) precipitation, (c) sea level pressure

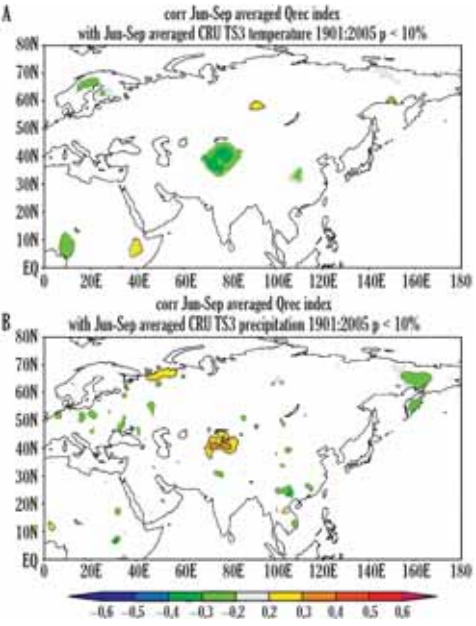

Fig. 8. Correlation maps of the June-September Drought index in the Tien Shan Mountains with CRU TS3 grid point parameters of the same period (a) temperature, (b) precipitation

1880, 1884–1885, including those during the instrumental period in 1894–1895 and 1916–1917. The longest drought occurred in 1768–1769/1774–1775. The tree ring based reconstruction demonstrates a lower interannual variability than the meteorological data due to lost variance due to regression, although it reproduces well the chronologies of the droughts. In general the 19th century was drier in the Issyk Kul region that the 20th century. The 20th century does not look unusual in terms of drought occurrence over the last three and a half centuries.

Spectral properties of the reconstructions. Spectral analyses of the two reconstructions presented above, namely for the May–August temperature and June–September Drought index was carried on using the online wavelet software http//paos.colorado.edu/research/waveleth. It shows a certain similarity in the spectral characteristics of both series with two significant peaks around 16–32 and 60–80 years. There is also some sign of consistent inter-annual variability in both series in the ENSO frequency (2–7 yrs) band, but there is little evidence for a strong teleconnection between ENSO and climate in the Tien Shan region.

Correlation maps. Using KNMI Climate Explorer [http://climexp.knmi.nl/], reconstructed May–August temperatures in the Tien Shan Mountains show a strong positive correlation with the CRU TS3 grid point temperature data especially over its northeast part of the region (Fig. 7a). The negative correlation of this reconstruction with CRU TS3 precipitation data over the same period is also observed (Fig. 7b). This is consistent with anti-correlation of summer temperature and precipitation in this region identified earlier basing on meteorological time series [Diurgerov et al., 1995]. A negative correlation of the reconstructed

May–August temperature with the HadSLP2 sea level pressure (same archive) over the large area of the high latitude from Siberia to the North America is a distinct pattern of the hemispheric significance (Fig. 7 c). The negative correlation means that during the negative anomaly of atmospheric pressure over Siberia warm air is advected from the southwest into its eastern periphery and brings hot summer weather to the Tien Shan Mountains.

The correlation fields of the June-September Drought Index reconstruction are somewhat smaller in space, but also consistent with the results on ring-width climatic response at the lower tree limit reported above. There is a positive correlation of our drought reconstructions with the precipitation and negative correlation with temperature in Tien Shan Mountains (Fig. 8 a, b).

DISCUSSION

We have shown that the ring widths of spruce in the Tien Shan Mountains depend mostly on moisture supply. For the upper sites the most important periods are precipitation of August, October–December and February, while at the lower sites the correlation is higher with July-August precipitation. Both conclusions generally agree with those of Borschova [1983] who used a more limited data set for both tree-ring and meteorological data. For the upper tree limit Borschova [1983] identified the October-May precipitation signal in the early wood ring width of spruce at the upper tree limit in Zailiisky and Kungey Alatau (for 5 years smoothed values). The summer precipitation of a previous year is important for both upper and lower tree limit sites. As the inner Tien Shan region is rather dry, thus making spruce quite sensitive to moisture supply [Kozhevnikova, 1982], the drought signal in ring width in spruce chronologies is logical.

At the upper tree limit one should also expect summer temperature to limit radial growth as well. This is indirectly supported by the results of Kozhevnikova [1982], who claimed that the poor soils at the northern slopes at the upper tree limit contain too much moisture, which can negatively influence tree growth, while high air temperature would on the contrary contribute the growth. None of our sites are south-facing, however, and we therefore suspect that they do not represent the potentially possible upper tree limit. Thus, the signal in their ring width is more typical for the lower-elevation belt of spruce forests. The actual real spruce forest is also lowered by anthropogenic and geomorphic activity. Use of the high elevations for pasturage is the traditional occupation of the local population, and the shepherds use wood to make fires and build huts. At the same time, the sheep are very efficient in destroying the natural vegetation. Avalanches, mud and debris flows, slope movement are also important natural agents in lowering the natural upper tree line.

The lower tree line in the Tien Shan is probably even more disturbed, but here human activity clearly dominates the natural processes: for centuries the spruce trees were used for building and heating. Most our sites in the lower locations are between 2000 and 2400 m a.s.l., while Borscheva [1983] was able to sample a much lower site at the elevation 1400 m a.s.l. At this site the ring width was limited by summer precipitation in a similar way to our cases, but with higher correlation between the ring width and meteorological parameters. At the elevation 2000–2400 m a.s.l. the signal becomes more mixed: the growth depends not only from the precipitation, but integrates also the influence of the temperature of spring, summer and early fall. This combination of integrated temperature/precipitation signal is typical for the semi-dry areas [e.g. Cook et al., 1999].

The individual samples and chronologies from the upper and lower tree limits cross-date against each other successfully. The combined chronologies from both locations

also show a lot of similarity especially at the level of interannual variations. This might be explained as a common influence of moisture supply on tree growth of both locations (see figure 3). Wang, Ren and Ma [2005] came to the same conclusions studying the ring width of *Picea schrenkiana* in the adjacent territory of the Tien Shan Mountans along an altitudinal gradient from 1600–1700 to 2600–2700 m a.s.l. They found the correlation between the sites and the decreased response with the increasing of the elevation of the sites. These authors showed that precipitation was the most important factor limiting tree radial growth even at the upper tree limit in the arid Tian Shan Mountains. Esper et al. [2007] found a high degree of similarity among juniper ring-width chronologies along the altitudinal gradient by analyzing 28 juniper sites in the Tien Shan and Karakorum mountains (correlation between the upper and lower tree limit sites is up to 0,72 for the period as long as 1438–1995). These authors suggested that the tree growth might be forced by solar radiation controlled by cloud cover changes, but did not prove this hypothesis.

The maximum density chronology does not correlate with either upper tree limit or low tree limit chronologies, clearly demonstrating a different climate signal. It depends on a different climate influence from ring width, which is the summer temperature. Similar relations of maximum density with summer temperature have been reported for the trees of different species growing at the upper [Schweingruber et al., 1988, Esper, 2002, 2003, Buentgen et al., 2010] or northern tree limits [Briffa et al., 1998, 2002].

There are very few reconstructions for the northern periphery of the Tien Shan region available for the comparison with our data. Most reconstructions of climatic parameters come from Tibet and Himalaya with substantially different climate largely influenced by monsoon activity. Wilson et al. [2007] used the ring width and density data from the ITRDB for their temperature reconstructions for the Kyrgiz territory. These included two of the three sites we used here to model the May–August temperatures. In the Wilson et al. [2007] study the RW and MXD chronologies were utilized separately as potential predictors in a stepwise multiple regression against gridded June–July mean temperatures. The reconstruction explained 36% (r = 0,61) of the gridded temperature variance. In our case the calibration was with a longer window (May–August temperature) measured at the Chon-Kizil-su meteorological station, and the variance explained is higher ($r = 0,79$, $r^2 = 0,62$) as in Wilson et al. [2007]. The correlation between the two reconstructions is high (r = 0,66, for 1775–1995). In contrast, the Esper et al. [2003b] June–September temperature reconstruction was based on a *Juniperus turkestanica* regional RW chronology, which correlated with the Fergana meteorological station in eastern Uzbekistan (r = 0,46). The correlation with our temperature reconstruction is insignificant, but it is also not significantly correlated with the Wilson et al. [2007] reconstruction mentioned above, although for some periods the two curves show a similar pattern.

CONCLUSIONS

Spruce ring width variations over a large range of elevations in the Tien Shan Mountains depend mostly on moisture availability. At the upper elevations of the mountains, cold period precipitation plays the most important role for spruce growth, while at the warmer and drier lower elevations, the combination of warm period temperature and precipitation is more important. In contrast, MXD correlates positively with the summer temperature in a highly consistent and significant way. Overall, the spatial agreement between the chronologies supports the conclusion that significant external forcing of growth due to climate is occurring.

We have also presented here a drought index reconstruction for 1750–2000 based on the lower tree limit chronology constructed for the Issyk Kul area. The best fit model includes

the sum June–September precipitation of previous and current years divided to the average temperature of the same period. The reconstruction accounts for 41% of the variance in observed drought index over 1887–1988. According to this reconstruction the 19th century was drier in the Issyk Kul region than the 20th century.

A summer temperature reconstruction was also presented here that is based on maximum wood density at the upper tree limit. The reconstruction accounts for 62% of the variance in the observed temperature data over 1951–2000. The significance of this correlation allows the reconstruction of May–August temperature from 1650 to 1995.

The correlation of the reconstructions with the CRU TS3 grid point data confirms the results of the modeling using the meteorological data from the nearest stations. We also identified a teleconnection pattern of the May-August temperature reconstruction in Tien Shan and the low pressure in the high latitudes in Siberia.

The reconstructions shows a certain similarity in the spectral characteristics with two significant peaks around 16–32 and 60–80 years.

According to these results the 20th century does not look unusual in the context of the last two hundred years, either in terms of frequency of drought occurrence or in terms of severity. The summer temperature reconstruction allows for a longer context over the past three and a half centuries. Again in this context the temperature variations of the last century do not look unusual, though they do not encompass the last decade when the summer warming in Tine Shan became especially prominent.

ACKNOWLEDGEMENTS

E. Cook was supported at the Lamont by National Science Foundation award ATM 04-02474. Lamont-Doherty Earth Observatory Contribution Number 0000, O.Solomina – by a RAS Program P4. ■

REFERENCES

1. Biondi, F. and Waikul, K. (2004) DENDROCLIM2002: AC++ program for statistical calibration of climate signals in tree-ring chronologies. Computers & Geosciences 30: 303–311.
2. Bitvinkas, T.T. (1974) Dendroclimatic research. Leningrad Gidrometeoizdat (in Russian).
3. Borscheva, N.M. (1981) Picea Schrenkiana ring width chronologies for Zailiiskiy Alatau mountains. Tree-ring chronologies of Soviet Union 2: 17–23 (in Russian).
4. Borscheva, N.M. (1983) Dendroclimatological analysis of *Picea Schrenkiana* radial growth in the Northern Tien Shan Mountains. Abstract of PhD Sverdlovsk (in Russian).
5. Buentgen, U., Frank, D., Trouet, V., Esper, J. (2010) Diverse climate sensitivity of Mediterranean tree-ring width and density. Trees 24: 261–273 DOI 101007/s00468-009-0396-y.
6. Briffa, K.R., Osborn, T.J., Schweingruber, F.H., et al. (2002) Tree-ring width and density data around the Northern Hemisphere: Part 1, local and regional climate signal. The Holocene 12 (2): 737–757.
7. Briffa, K.R., Jones, P.D., Schweingruber, F.H., Osborn, T.J. (1998) Influence of volcanic eruptions on Northern Hemisphere summer temperature over the past 600 years. Nature 393: 450–455.
8. Briffa, K.R. and Melvin, M. (2011) A Closer Look at Regional Curve Standardization of Tree-Ring Records: Justification of the Need, a Warning of Some Pitfalls, and Suggested Improvements in Its Application in M K Hughes, H F Diaz, and T W Swetnam, editors Dendroclimatology: Progress and Retrospects Springer Verlag 113–145.

9. Cook, A.R. (1985) A time series approach to tree- ring standardization. PhD Disser tation. University of A rizona. U SA . Tucson, 171.

10. Cook, E.R., Stahle, D.W., Cleaveland, M.K. (1999) Drought Reconstructions for the Continental United States. J of Climate 12: 1145–1162.

11. Cook, E.R. and Kairiukstic, L.A. (1990) Methods of dendrochronology: applications in the environmental sciences. Dordrecht, Netherland, Kluwer Academic Publishers.

12. Diurgerov, M.B., Kunfkhovich, M.G., Mikhalenko, V.N., et al. (1995) Tien Shan Glaciation Moscow (in Russian).

13. Esper, J., Frank, D.C., Wilson, R.J.S., Buentgen, U., Treydte, K. (2007) Uniform growth trends among central Asian low- and high-elevation juniper tree sites. Trees 21: 141–150 DOI 101007/s00468-006-0104-0.

14. Esper, J., Schweingruber, F.H., Winiger, M. (2002) 1300 years of climatic history for Western Central Asia. The Holocene 12 (3): 267–277.

15. Esper, J., Shiyatov, S.G., Mazepa, V.S., Wilson, R.J.S., Graybill, D.A., Funkhouser, G. (2003) Temperature-sensitive Tien Shan tree ring chronologies show multi-centennial growth trends. Climate ynamics 21: 699–706.

16. Fritts, H.C. (1979) Tree rings and climate. London-New York.

17. Glazirin, G.E., and Gorlanova, L.A. (2005) Experience of dendroclimatic researches of junipers on Western Tien Shan. Proceedings of NIGMI 5 (250): 24–42.

18. Graybill, D., Shiyatov, S., Burmistrov, V. (1990) Recent dendrochronological investigations in Kirghizia, USSR. Tree Rings and Environment 123–127.

19. Holmes, R. (1994) Dendrochronology program library – users manual. Laboratory of Tree-Ring Research, Tucson, Arizona.

20. Holmes, R.L. (1983) Computer-assisted quality control in tree ring dating and measurments. Tree-ring Bulletin 44: 69–75.

21. Kozhevnikova, N.D. (1982) Biology and ecology of Tien-Shan spruce Frunze, Ilim.

22. Mukhamedshin, K.D. (1977) Juniper forests in Tien Shan and their importance as a forest resources Frunze, Ilim.ORIG.

23. NOAA Paleoclimatology: http://wwwncdcnoaagov/paleo/treeringhtml.

24. Schweingruber, F. (1988) Tree rings: basics and applications of dendrochronology. RPC, Dordrecht, Holland.

25. Solomina, O., Schweingruber. F., Nagornov, O., Kuzmichenok, V., Yurina, Yu., Mikhalenko, V., Kunakhovich, M., and Kutuzov., S. (2006) Reconstruction of summer temperature and ablation of glaciers in Central Tien Shan for the period of AD 1626–1995 using maximum ring density of spruce (Picea Schrenkiana). Data of Glacialogical Studies 100: 104–113 (in Russian).

26. Solomina, O.N., Abilmeizova, B., Griaznova, V.V., Yershova, I.V. (2007) Tree-rings drought index reconstruction in Near Issyk-Kul area, Tien Shan, Kyrgyz Republic for AD 1680–2005. Problems of ecological monitoring and ecosystem modeling 21: 183–202 (in Russian).

27. Solomina, O.N., Glazovsky, A.F. (1989) Tree-ring of Tien-Shan spruce and glacier variations on the northern slope of Terskey Alatau range. Data of Glacialogical Studies 65: 103–110 (in Russian).

28. Wang, T., Ren, H., Ma, K. (2005) Climatic signals in tree ring of Picea schrenkiana along an altitudinal gradient in the central Tianshan Mountains, northwestern China. Trees 19: 735–741 DOI 101007/s00468-005-0003-9.

29. Wilson, R., D'Arrigo, R., Buckley, B., Buentgen, U., Esper, J., Frank, D., Luckman, B., Payette, S., Vose, R., and Youngblut, D. (2007) A matter of divergence: Tracking recent warming at hemispheric scales using tree ring data. J Geophys Res 112 D17103, doi:101029/2006JD008318.

Olga Solomina – Expert in climate change, glacial morphology, leoclimatology. Deputy director of the Institute of Geography RAS. Author of more than 100 scientific papers including those published in the high rating journals (Nature Geoscience, Quaternary Science Reviews, the Holocene, Climate in the Past). Lead author of the 4th and 5th IPCC Assessments.

Olga Maximova – expert in dendrochronology, climate and glaciological reconstructions. PhD thesis: Tree-ring based hydrometeorological reconstructions for last centuries for Tien Shan (Kyrgyzstan). Participated in scientific expeditions in Tien Shan mountains (Kyrgyzstan), Russian Plain, North Enisey region, Transbaikal region and North Mongolia.

Edward R. Cook – Ewing Lamont Research Professor. Specialist in tree-rings, biology and paleoenvironment, Director of Tree-Ring Laboratory in Lamont-Doherty Earth Observatory in Columbia University, USA. One of the most eminent experts in tree-ring climate reconstructions (http://www.ldeo.columbia.edu/user/drdendro).

Ekaterina V. Lebedeva[1*], Dmitry V. Mikhalev[2], Josй E. Novoa Jerez [3], Mariya E. Kladovschikova[4]
[1] Institute of Geography Russian Academy of Sciences, Moscow, Russia; Staromonetny per., 29, 119017; Tel: +7-910-416-66-89, Fax: +7-495-959-0033, e-mail: Ekaterina.lebedeva@gmail.com,
***Corresponding author**
[2] Faculty of Geography, Lomonosov Moscow State University, Moscow, Russia; Leninskie Gory, 1, 119991; Tel: +7-903-259-05-92, e-mail: mikhalev@kapitelproekt.ru
[3] University of La Serena – CEAZA, La Serena, Chile, Colina El Pino s/n, Casilla 599; Tel: 056-51-204396, e-mail: jnovoa@userena.cl
[4] Institute of Geography Russian Academy of Sciences, Moscow, Russia; Staromonetny per., 29, 119017; Tel: +7-926-577-40-43, e-mail: masisuanka@mail.ru

GEOMORPHOLOGIC HAZARD AND DISASTERS IN THE SOUTH AMERICAN ANDES[1]

ABSTRACT. Geological-and-tectonic and physiographical features of the South American Pacific coast caused high intensity of morpholitogenesis including disaster-like way of some geomorphologic processes. Their complex, interaction, and intensity of conductive factors increase the risk of disaster. The Andean terrain morphology and rock lithology, precipitation type, and vegetation status are the main drivers that influence the character and high potential intensity of the geomorphologic processes. The enormous hydrometeorological events, frequent seismic shocks, volcanic eruptions, and human impact cause disasters development. A schematic map of disaster and hazardous processes for the Central sector of Andes was compiled. 16 areas with different spectra of the dominant catastrophic processes were identified. The South American Andes extension allows drawing out principles of geomorphologic disasters of these continental marginal mountains in various natural zones – from temporal to subequatorial latitudes, which are characterized by the individual unique heat-moisture rate, which governs both typical and extreme geomorphologic processes. An important feature of the study area is the asymmetric distribution of geomorphologic processes within coastal and inland slopes of the mountain system, as well as latitudinal zoning of this distribution.

KEY WORDS: Geomorphologic hazard and disasters, South American Andes, intensity of geomorphologic processes, seismic and volcanic activity, unbalanced precipitation, mass movements of debris

INTRODUCTION

Geomorphologic disaster is considered to be a process which unbalances the geomorphologic system and leads to step or sudden change of its state [Aleksandrov, 1996; Ananiev, 1998; Phillips, 2011]. This change is the result of accumulation of substance and/or energy critical mass. Any process in one or another regional range could manifest a disaster, however, in this case its quickness, development, and impact (e.g. the volume of displaced material) would be incomparable to ground processes, i.e. common processes within a given territory. Geomorphologic disasters could be caused by immediate (e.g. volcanic eruption) or step-by-step (sea-level change) environmental transformations driven by

[1] The reported study was partially supported by RFBR, research project №12-05-00900 a.

natural and human factors (e.g. slope plant destruction).

Also, there are geomorphologic hazards (or extreme, critical display of processes) that coincide with short-run but serious deviation from the norm of typical (ground) processes and cause the transformation of certain elements in geomorphologic system [Ananiev, 1998; Korotkiy et al., 2011].

Actually, these specific environments act as some "triggers": they set and/or promote geomorphologic processes that change ground values for critical situations or disasters. These could be endogenous (e.g. earthquakes), exogenous (extreme volume or rate of precipitation, etc.), and human-caused factors and their combination.

Obviously, the character and rate of process activation largely depend upon specific nature of terrain: e.g., common ground mountainous processes may be disastrous for plain lands. Also, resistance of terrain complexes to natural and human-caused processes is of great concern. Lithological composition of rocks, vegetation, weathering kind, precipitation regime, and other physical-and-geographical conditions are of great importance. It is especially true for high contrast terrain territories with large number and high speed of terrain-forming processes where disaster risk is very high and causes significant damage to population and economic activity. The development of vulnerable regions and application of complex production technology increase the risk of natural hazard.

According to Swiss Reinsurance Co [http://inosmi.ru/infographic/20111226/181319543], global financial loss from natural disaster amounted to $226 billion in 2010 and a record figure of $350 billion in 2011. Finam.info states that all disasters in 2010 caused nearly 304 thousand deaths worldwide – maximal since 1976. Haiti earthquake is topping the list of the most lethal disasters – more than 225,5 thousand deaths. The most expensive natural disaster is associated with the Chinese earthquake with loss of $30 billion. According to World Bank, the Japanese earthquake of a 9,0 magnitude followed by the tsunami on March 11, caused the maximal loss of $122–235 billion [http://finam.info/need/news2478800001]. Therefore, the study and prediction for both natural and anthropogenic catastrophic geomorphic processes is a very important task.

Continental marginal mountains, including the South American Andes, are characterized by supreme terrain contrast, mosaic structure of surface and crust, and rich complex of modern endogenous processes – volcanism, seismicity, and vertical movements [Tectonic Evolution, 2000; The Andes, 2006; Charrier R. et al., 2013, etc.]. Climate patterns of these territories caused by ocean and continental air masses interaction also play the significant role in exogenesis. So given regions are characterized by diverse variety of terrain-forming processes, their high speed, and, sometimes, disasters.

Stress conditions of geomorphologic systems and processes, i.e., their potential disbalance [Gotvanskiy, Lebedeva, 2010; Lebedeva, 2013] require research of continental marginal mountains of areal and temporal specific nature of geomorphologic hazards and disasters. This issue is addressed in this paper.

The paper is based on the authors' field study records, results of photo- and satellite interpretation, literature, and map data analysis.

MAIN GEOLOGICAL-AND-GEOGRAPHICAL FEATURES OF THE REGION

The total length of the South American Andes is 9000 km; average altitude is 4000 m; and top altitude – Aconcagua – is 6962 m. There are two or even three subparallel mountain ranges within different areas. The total width is 500 km; in the Central Andes (between 18° and 20° S), where high-altitude

Altiplano plateau is situated, it reaches 750 km. This paper highlights the Central (Peruvian and Bolivian) Andes, the Southern (Chile-and-Argentine) Andes, and also the southern part of the Northern (Ecuadorian-and-Venezuelan) Andes.

The South American Andes, primary, is the result of Alpine orogeny; tectonic movements continue until present. Faults, volcanism, and recent lifting played an important role in the alpine fold-block structure forming. The main morphostructures are characterizes by submeridional extension, while crossover tectonic dislocations are indefinite [Tectonic Evolution, 2000, etc.].

High seismicity is indicative for young mountains as the Andes are. About 570 earthquakes with magnitude of more than 7 and focus of up to 100 km were instrumentally recorded before 2013 [http://www.ncedc.org/anss/catalog-search.html]. Coastal parts of Southern Columbia and Northern Ecuador, Central and Southern Peru, and coastal Chile to the north of Valdivia are most seismic and characterized by earthquakes with a magnitude of 8 and more. Detailed analysis of earthquakes frequency and energy distribution in the Pacific part [Levin, Sasorova, 2009] showed that the maximal seismic activity corresponds to two narrow latitudinal intervals, i.e., 20–25°S and 30–35°S. In these areas, the number of earthquakes and their energy are an order of magnitude greater than, for example, in the 40–45°S interval. The Eastern Andes are much less seismic, though even there, specifically, near Mendoza, San-Juan, and Salta (Argentina), the earthquakes reach 7–8 points on the Richter scale; these cities were destroyed many times in the past [Alvarado, Beck, 2006].

A seismofocal zone is traced along the west side of the South America; it is separated by lateral faults into several sections with unlike steep dip. Easy dip sections (the Peruvian and the Central Chilean Andes) are characterized by lack of quaternary and modern volcanism, while steep dip sections (the Central and the South volcanic mountains) are characterized by intense modern volcanism [Zhidkov, 1985; Cembravo, Lara, 2009; Tilling, 2009]. Three volcanic zones are located in the Andes with more than 200 active volcanoes – 197 of the Holocene age and 5 of the Pleistocene age with modern thermal activity [http://www.volcano.si.edu/world].

The Andes is a continental divide and most important South American climatic barrier that separates the Pacific and the Atlantic affected areas. Situated within 5 climatic belts (equatorial, subequatorial, tropical, subtropical and temperate) it is characterized by a sharp contrast in precipitation on the eastern and western slopes [Lukashova, 1958; Garreaud, etc., 2009]. The western slopes have low moisture availability between 5° and 28°S: while the northern part of the Central Andes (Peru) catches 200–250 mm annually, this amount decreases and does not exceed 50 mm annually in places southward (north of Chile) – the Atacama desert lies here – the most dry desert in the world. Desert landscapes are traced up to 3000 m A.S.L. and higher. Semidesert or steppe landscapes prevail above 3000 m (within the Altiplano plateau) – so-called dry puna with more than 250 mm annual rainfall only occasionally. Softening action of Lake Titicaca within surrounding lands mitigates temperature fluctuations and makes them less contrast compared to other parts of plateau. The eastern slopes of the Andes catch 3000–6000 mm annual rainfall brought from the Atlantic Ocean [Garreaud et al., 2003]. As for modern glaciation, it is too irregular because of the various climatic environments. At this rate, the snow-line in Ecuador and Peru ranges from 4000 to 5000 m and rises to 6300–6500 m in the Altiplano with its dry air and high insolation and winds – e.g. being at the top in the world [Troshkina, Kondakova, 2000].

Subtropical climate of the Chile-and-Argentine Andes (between 28° and 38°S) brings more moisture compared to the subequatorial and tropical zones. Southwards, annual rainfall values increase

from 350 (Santiago) to 750 mm (Valdivia) within western slopes, while eastern slopes become more rainless. Increasing south rainfall, along with a reduction in mean annual temperatures, leads to a gradual lowering of the snow line and valley glaciers are forming there.

Near 37–38°S, subtropical climate of western slopes gradually transitions to oceanic climate of middle latitudes: annual amount of rainfall increases; in-season humidity differences decrease. Southward 37°S, eastern slopes catch more precipitation although precipitation is lower than that of the western. Precipitation of the southern-most part of the Andes – Tierra del Fuego – (up to 3000 mm annual) bears is more like drizzle and snow in mountains. The Patagonian Andes environment is most favorable for glacier formation. The snow-line decreases to 1000–1200 m; areas of the continental ice sheet are located here – the South and North Patagonian glacier plateaus with extended outlet glaciers.

FACTORS THAT CAUSE EXTREME EVENTS AND DISASTERS

Therefore, various parts of the Andes are situated in different geological-and-tectonic and physiographic conditions that impact geomorphologic processes, including geomorphologic hazard and damage.

Active "provocateurs" of extreme (critical) geomorphologic situations are seismic and volcanic processes. Earthquakes provoke large movements of debris within slopes (Fig. 1) with volume equal to several cubic kilometers, glacial slides, avalanches and mudflows, and volcanic processes.

During seismic events, fractured zones "come to life" first – zones of rock breaking and advance rock fracturing; often, vertical movements of the land mass are recorded [Enman, 1973; The Andes, 2006]. The zones of big faults intersection – the so-called "morphostructural knots" [Zhidkov, 1985; Rantsman, Glasko, 2004] – are of high activity. Earthquakes with focuses in coastal areas or sea shelf provoke tsunami. Coastal areas of the Central Chile and Central and Northern Peru are most vulnerable. For example, near La Serena city (the Koquimbo bay, Chile) 37 tsunami were recorded during 1562–1995 with a peak of 14 m (1922) [Novoa et al., 1995]. The 1996 tsunami affected 400 km along the Peruvian coast – from Chimbote in the north to San-Juan in the south. It was found that the 24–26 m high destructive tsunami were provoked by the earthquakes in 1586, 1687, 1746, and 1828 within this coastal area. Numerous tsunami in this area are explained by vertical movements of the crustal blocks related to the Nazka plate subduction under the South American plate [Pararas-Carayannis, 1974]. However, distant seismic events sometimes influence the coast: tsunami of 2 m high, which have destroyed the La Serena city seafront (12.03.2011), were caused by the Japanese earthquake.

Volcanic activity can also cause the earth tremor and tsunami, but in mountainous areas, hazards are related to ash falls, lava floods, the lahars, and debris avalanches. The most powerful eruption of the region took place in 1600 in Peru: the total volume of Huayanaputina pyroclastic material reached near 11 cubic kilometers with 1000 km of blow radius. The subsequent lahar passed more than 100 km and reached the Pacific Ocean. Two eruptions of total volume 9,5 and 8 cubic kilometers took place in Chile in the XXth century [Tilling, 2009].

But even relatively small eruptions could be damaging, like the Nevado del Ruiz (Columbia, 5398 m) eruption in 1985 with the total volume of about 0,05 cubic kilometers. Lahars (mudflow with volcanic genesis) were formed due to the melting of snow cover and the glacier; one of them destroyed Armero city, causing more than 23 thousand deaths. Lahars traces were recorded on 32 active volcanoes; notably, the Cotopaxi (Ecuador) volcano has 22 traces of lahars that took place during the XVIth–XIXth centuries [Perov, 2012].

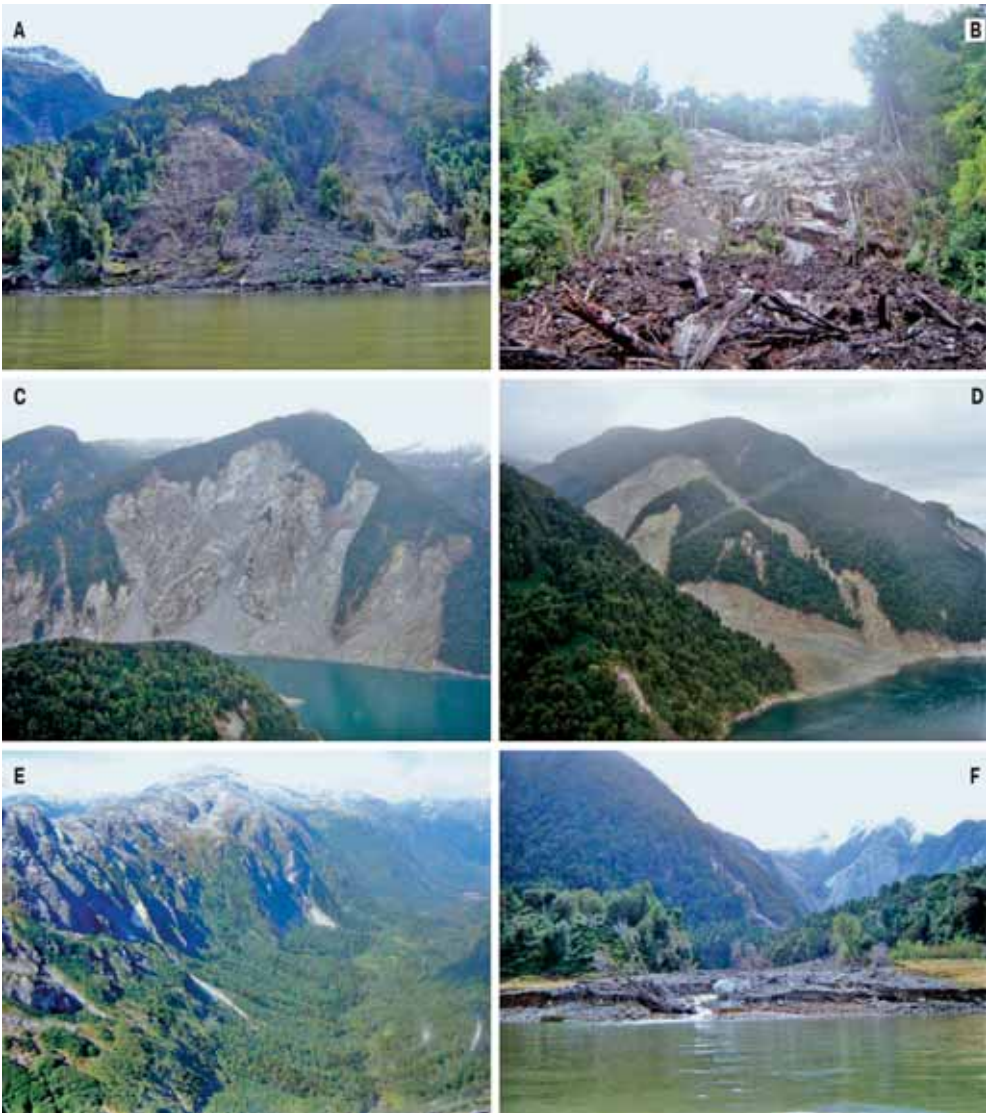

Fig. 1. Examples of the different types of earthquake-induced landslides in the Aysén Fjord area (Chile).

A – shallow soil slides, B – shallow soil–rock slide, C – rock slide in front of Mentirosa Island, D – rock slide and avalanche in Punta Cola area, E – rock falls, F – debris flow (Sepulveda et al., 2010)

Annually, several eruptions of different power usually take place in the Andes. For example, eruption of the small Chaiten volcano (1122 m, Chile) lasted almost two years: it started in May of 2008 after more than 9 thousand years of inactivity. The estimated volume of pyroclastic material was 0,17 cubic kilometers; slope lava and pyroclastic flows formed. There were also 3 lahars; one of them destroyed most part of the same-name town situated in the Rio-Blanca River mouth (Fig. 2); however, citizens were evacuated.

Geomorphologic instability and active terrain-forming processes are caused by the *topography* itself – high altitude and highly dissected steep-side mountains. The range of amplitudes within the studied territory, from the coast to the water-divide part of the Andes, is extremely high: 7000 m for 150 km in the central part of Chile and more

Fig. 2. Lahar traces on the Chaiten streets (Chile, February 2010). Hereinafter all photos without author index belong to E. Lebedeva

than 6000 m for 100 km in Peru. Two to three kilometers of gullies of some river valleys (both – western and eastern slopes of the Andes) cause the split of the interstream areas, rock-falls, instability of valley slopes to even long-distance earthquakes [Ufimtsev, 2011]. Deep valley cut-ins can provoke long-living landslides in hydrologically and lithologically favorable environment, e.g., the so-called "Lluta collapse" in the northern part of Chile, where landslides have been active during 2,5 million years [Novoa, 2013].

Other significant exogenous drivers are temperature and moisture conditions within the Andes slopes [Garreaud, 2009]. Air temperature decreases and precipitation increases with altitude in the same climatic zone. For example, precipitation increases from 0 to 400 mm/year in the Northern Chile (18–22°S) and to 700 mm/year in the Southern Peru (14–18°S) when moving from the coast to 4500 M.A.S.L. [Garreaud et al., 2003]. Southward in the Aconcagua and Maipo River basins (32–34°S), with every thousand meters of altitude, precipitation increases by one-half [Garreaud, 1992]. For example, precipitation increases from 240 to 1000 mm with altitude in the Aconcagua River basin [Golubev, 1969]. Each latitudinal and longitudinal zone is characterized by specific altitudinal zonality range. This is reflected not only in spatial change of natural complexes, but also in change of the exogenous processes specific for these complexes and, above all, of the consequences of these processes [Montgomery et al., 2001].

Topography and temperature and humidity conditions greatly influence gravitation, fluvial, glacial, eolian, and other geomorphologic hazards and disasters. This is reflected on the schematic map of modern exogenous processes in the area between the Ecuadorian and central part of the Chile-Argentine Andes [Kladovschikova, 2008].

In high humidity conditions, both fluvial and slope processes are active due to surface waterlogging: landslides, mudslides, solifluction, and mudflows. Mudflow hazards are indicative for the most part of the Andes (Fig. 3). The prevalent type of mudflow northward of 45°S is rain mudflows, whereas, southward and near the modern glacial mass, it is snow and glacial mudflows, and near active volcanoes, it is lahar mudflows [Perov, 2012]. The period of the most mudflow hazard within 6–30 S in the Andes is local summer;

Fig. 3. Mudflow cone in the River Santa tributary inflow (Cordillera Blanca western slope, Peru)

for 30–40° S, it is local winter; and southward, it is local spring and summer [Budarina et al., 2000]. Mudflows appear on the Western (near Antofagasta, Chile) [Novoa, 2013] and on the Eastern Andean slope (Rio Grande basin, Jujuy province, Argentine [Garreaud, 2009]). Often, mudflows descending along tributaries, pond up the main stream with fans forming storage ponds and creating favorable conditions for bigger mudflow descent when the ponds overflow [Marcato et al., 2009].

The annual precipitation is not so much important for the fluvial and slope hazard as the precipitation rate. Even in case of the low total precipitation, an extremely unbalanced (seasonal) precipitation provides for high intensity of certain events, which results in geomorphologic damage. The schematic representations presented in Fig. 4 clearly illustrate that more than 75% of precipitation, i.e., 300 mm, is typical for local summer (December–February) in Northern Chile, where precipitation is under 400 mm/year. By comparison, the typical precipitation in the Titicaca Lake basin is under 700 mm/year, and a little more than 50% of this volume is accrued in the summer months, i.e., relatively comparable data are around 350–400 mm [Garreaud et al., 2003].

More unbalanced precipitation is documented on the Eastern Andean slope in the Kolanguil River basin (San Juan province, Argentina), where annual average of precipitation is less than 100 mm. Once in 5–6 years, from 40 to 50 mm of rain falls in this area during one precipitation event, according to a 30-years observation cycle; the intensity of rain reaches 104 mm/hour [Angillieri, 2008]. A similar intensity of rainfall (about 100mm/hour) is recorded on the coast of Peru [Nicholson, 2011]. As a result of such heavy rains, dry streams are filled up with water, damage floods are formed, active erosion and redeposition of channel and slope debris take place.

Physical weathering is active in arid climate where a large volume of desegregated

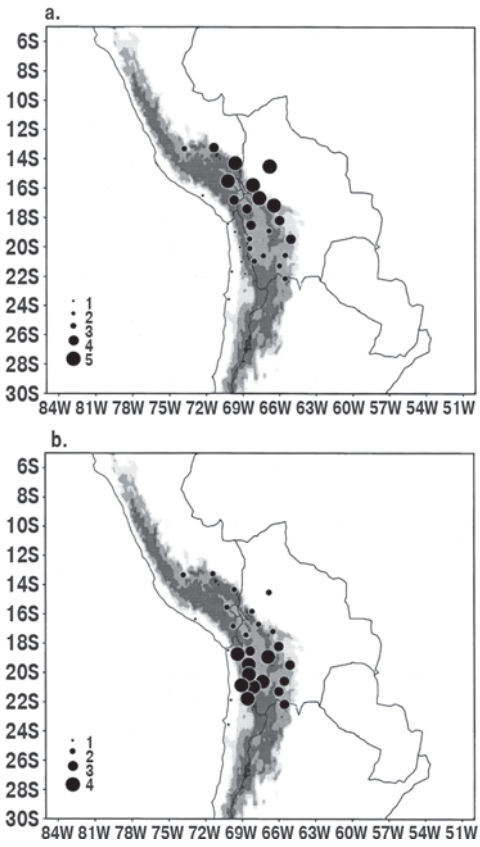

Fig. 4. Terrain elevation (shaded) and rainfall over the central Andes and adjacent lowlands. Shading begins at 2000 m and gets darker every 1000 m.

(a) Rain-gauged annual mean rainfall (mm) – size of the symbol indicates the amount of rainfall: 1 – 0–100, 2 – 101–200, 3 – 201–400, 4 – 401–700, 5 – over 701.

(b) As panel (a), but the size of the symbol indicates the fraction of annual mean rainfall (%) concentrated in the austral summer months (December, January and February): 1 – below 50, 2 – 50–60, 3 – 60–75, 4 – above 75 [by Garreaud R. et al., 2003]

rocks occurs on steep slopes not fixed with vegetation (Fig. 5). Excessive fissuring of rock zones and presence of weakly coupled volcanic rocks are conductive too. This causes extended rockslides and potential for huge debris mass-moving processes. Deficit of precipitation prevents these processes from realization, but debris avalanches appear in volcanic regions, as on the Parinakota volcano (Chile) eruption with collapse of a part of its cone [Novoa, 2013]. In case of disastrous heavy rains, debris begins to move. Giant landslides, up

Fig. 5. Rockslides in the area of Cristo Redentor (Chile-Argentinia border). The right low angle indicates the road tunnel entrance

to several cubic kilometers, take place on slopes, lock river-streams, and form storage ponds. Sometimes, the material can almost completely overlay river terraces.

Generally, in steep-side terrain conditions, intensity of debris mass-moving increases together with precipitation, however, increase of vegetation density reduces the impact. That is why slopes above tree-line are potentially hazardous. Hazards in periglacial conditions could be relevant to glacier dynamic (surge of glaciers), especially to glacial lakes and their failure.

Glaciers are more dynamic in the tropical part of the Andes and provoke negative geomorphologic processes there. For example, glaciers grow due to the influence of the Atlantic humid air mass on the Huaskaran massif (Peru). Geomorphologic disaster driven by glaciers are less common in Chile and Argentina (Aconcagua massif) due to smaller glacier dynamic as a result of much dryer the inlet Pacific and Atlantic air mass. Ice appears more like a "conserver" rather than a "provocateur" of geomorphologic disasters in temperate climate (the Patagonia plateau glacier) according to [Stillwell, 1992].

The Chilean-Argentinean and Patagonian Andes are the areas of frequent avalanche disasters [Troshkina, Kondakova, 2000]. Avalanche danger is high in all seasons here, and in the mountains of Peru, Bolivia, and Ecuador, – only in very snowy winter. Water-and-snow flows and avalanches can be triggered by even very weak seismic tremors, i.e., only 1–3 points, but volumes of seismogenic avalanches are usually larger than normal [Kazakov, 2000].

Every 25–30 years or less frequently, El-Nico acts with a tremendous force along the coastland of Peru and Northern Chile. During this period, west winds bring humid air masses that cause abundant precipitation within the otherwise dry coastland and mountains resulting in disastrous floods with run-off rise of up to 1000–3000% [Ananiev, 1999].

Generally, the 100 km-wide alongshore Pacific area is exposed to El-Nico; floodings is a normal occurrence in the valleys of the western Andean slope and the alongshore lowlands. Below normal precipitation is characteristic of the Altiplano during this time [Garreaud et al., 2003]. Flooding often happen in the intermountain basins, flat interstream areas (Altiplano), and valleys of the eastern Andean slope, where Atlantic air masses bring precipitation from January to March (Fig. 6). Heavy rains intensify fluvial and slope processes: landslides and creep of ground, vertical and lateral erosion, and mudslides. Observations in deep valleys on the western (Colca River, Peru) and on the eastern (Tarija River, Bolivia, and Quebrada de Humahuaca, Argentina) Andean slopes showed that huge landslides were most common during the periods of heavy rains coming after severe droughts [Codron, Cervera, 2000]. Urban and economic destruction and giant debris fans at foot-hills are the result of rainfall floods.

Arid areas face *deflation and eolian accumulation*. These processes occur frequently within the Pacific coastlands of Chile and Peru, in the Andean desert foothills in north-west Argentina, and on the Altiplano (Fig. 7) and the Ecuadorian paramo. Strongest winds (20–40 m/s) are typical for the Patagonian plains. One can often see drifty sand moving up the slopes in the form of yellow streams, sometimes turning into

A

B1

B2

Fig. 6. Flood consequences (Feb–Mar 2010).

A. Bolivian Altiplano: overflown river flooded the Tupisa-Uyuni road.

B. Peru: houses crashed by flood: 1 – the Urubamba River upper flow (the Amazon River basin), 2 – the River Santa upper flow (Pacific ocean basin) – the lateral erosion activation

sand flows, covering roads and buildings [Novoa, 1993]. Often, there are land spouts and dust storms, causing significant wind erosion [Nicholson, 2011].

Geomorphologic disasters impact adversely human life and economic activity;

Fig. 7. Permanently moving eolian sands choke up Pan American Highway (north of Peru)

however *economic activity* also provokes negative geomorphologic processes. For example, dam failures cause devastating consequences of flooding; moreover, increase of the population density and violation of environmental management rules increase pressure on the environmental and geomorphologic stress. Many negative processes intensify in urban areas. For example, 3 of more than 30 streams crossing Quito (Ecuador) are associated with frequent mudflows. They are caused not only by heavy rains, but also by garbage damps in their basins [Novoa et al., 1988]. During long rains, suffusion becomes active near lines of communications; funnel holes are formed within the bodies of road embankments. First of all, intense flow and landslides respond to anomalous hydrometeorological events and are active during rains within built-up and cut slopes. This is typical for

A B

Fig. 8. Processes activation on cut slopes after rainfalls (Peru, March 2010):

A – earthflows at the northern part of Cuzco city,
B – landslide-earthflow blocked the road in the Urubamba River basin

spontaneous urban development in poor outskirts situated on steep slopes (Fig. 8).

Roads and line structures are also associated with adverse impact on runoff and slope processes, resulting in events from landslides and rockslides to tropical solifluction. Mining is loosely controlled in the region and more often managed in violation of control measures [Porter, Savigny, 2002]: mining causes soil erosion, deflation, ground subsidence, ground and subsoil water level change and pollution, and slope processes activation.

Agricultural activity, e.g., slope deforestation and loss of growth as a result of overgrazing (the last one is typical for dry territories), also promotes increase of negative geomorphologic processes. Plant destruction and change of natural associations to monoculture systems create conditions for ground mass movement, erosion leading to badlands, gullying, deflation, and wind deposition [Codron, Cervera, 2000].

DISASTER LOCALIZATION

The summary of the world geomorphologic damage data [Geomorphologic hazards, 2010] shows that there are three drivers of geomorphologic hazard in mountains: tectonics, climate conditions (first of all, volume of precipitation and intensity), and human impact. The Andes are not the exception. Often it is difficult to mark the lead driver because all event-causing geomorphologic processes and their effects are interrelated. However, the efforts are under way.

Providing an overview of natural disasters in the Latin America, D. Stillwell [1992]

Table 1. Geomorphologic hazards and disasters within the Transandean track – the north of Argentina – the north of Chile (according to [Porter, Savigny, 2002])

Region	Natural hazards and disasters	Enhanced anthropogenic factors
Pampean Plain	Surface and linear erosion, deflation	Deforestation, plowing, grazing
Subandian ranges	Landslides, fluvial processes, lateral erosion, gullying	Line facilities construction, mining
Eastern Cordillera	High seismicity, modern land uplift 1–4 mm per year, landslides, locking of flows as a result of mass ground displacement, disastrous floods	Line facilities construction
Puna (Altiplano)	Seismicity, active volcanism, high potential of corrosion	Open- and underground uncontrolled mining
Western Cordillera	High seismicity, gravitational processes	Line facilities construction
Atacama	Active rupture tectonics, disastrous floods, mudflows, high potential of corrosion	Open- and underground uncontrolled mining
Chilean Pacific coast	Tsunami	

concludes that the maximum of various wide-scale negative events is specific to Peru in the XXth century; Chile comes fourth in the list. Peru also tops the list according to the number of fatalities from earthquakes and huge landslides. This is due to location of the country at the joint of active continental plates, providing high tectonic, seismic, and volcanic activity and effect of the El-Nico phenomena.

J.E. Novoa [2013] has analyzed regional confinedness of damaging mass-movement on the Chilean slopes and marked the main factors. According to his findings, geomorphologic damages within the northern and central parts of Chile are caused, primary, by enormous hydrometeorological events (El-Nico). The negative effect of deforestation is strongly marked in the central and southern parts of Chile. Seismic events influence also grows stronger in the northern part. According to S. Zavgorodniaya's findings [1996], primary seismic-and-tectonic and volcanic processes govern the extreme character of geomorphologic processes within the territory of Ecuador. The role of landscape-and-climate conditions increases within plains and foothills.

M. Porter and K. Savigny [2002] undertook a study of natural disasters for the purpose of laying a pipeline along the following transect: from the Pampean Plain, through the Subandian ridges in Argentine, Eastern and Western Cordilleras parted by the Bolivian Altiplano, and, then, through the Atacama to the Pacific coast of Chile. According to this study, we have isolated the reported geomorphologic processes of the subregions (Table 1).

We also carried out analysis of geomorphologic hazards and disasters confinedness to the main Andean parts: slopes, valleys, flat interstream areas, submountain and intermountain plains with low hills, the Pacific coast, and large lakes (Table 2). The above-mentioned data and our own observation results allowed us to compile a sketch map of the Central Andean part zoning considering special aspects of geomorphologic hazard and damage development (Table 3, Fig. 9). Sixteen areas with different spectra of the dominant catastrophic processes were identified.

Then, we can deduce that slopes, valleys, submountain and intermountain plains, and the Pacific coast are characterized by specific range of geomorphologic hazard, broadly speaking, by active denudation caused, primary, by a wide range of erosion and gravitational processes. As a result, large volumes of debris are moving towards submountain plains and the ocean trench. High seismicity of the territory is conductive to processes intensity increase.

Central parts of vast flat interstream areas develop apart from the main base level

Table 2. Localization of hazards and disasters driven by natural and human impact

Triggering factors	Localization of hazards and disasters within main Andean areas				
	Coasts (including big lakes)	Piedmont and intermountain plains	Valleys	Slopes	Plain interstream areas (Altiplano, Puna etc.)
Earthquakes	Tsunami, shore front uplifting	Formation and bursting of dammed basins, landslides, mudflows	Formation of dammed lakes, bursting of natural and man-made dams, mudflows	Mass moving of debris – rock falls, landslides, detaches; avalanches	Formation of cracks, faulting of mass fragments, detaches
Volcanic eruptions	Coastline and bathymetry changing, tsunami	Ash falls, formation and bursting of dammed lakes, lahars	Ash falls, formation and bursting of dammed lakes, lahars	Ash falls, lava and pyroclastic flows, lahars, debris avalanches, mass moving as a result of deforestation	Ash falls, lava and pyroclastic flows, formation and bursting of dammed lakes, lahars, ground subsidence
Surge of glaciers	Mini-tsunami as a result of icefall, plucking	Formation and bursting of dammed basins, mudflows, debris accumulation	Formation and bursting of dammed basins, mudflows	Avalanches, mudflows	Formation and bursting of dammed basins, mudflows, cryogenic processes
Heavy precipitation	Floods, storm surges, abrasion	Floods, erosion, suffusion, mudflows, accumulation, bogging	Floods, erosion, suffusion, mudflows, local accumulation	Mass moving of debris – landslides, creep; active erosion	Floods, erosion, suffusion, mudflows, accumulation, bogging
Increase of wind	Storm surges, abrasion, land spouts, dust storms, eolian flows	Gravity winds, dust-storms, eolian flows	Gravity winds	Eolian flows	Land spouts, dust storms
Human impact	Abrasion, accumulation	Erosion, suffusion, mudflows, deflation	Erosion, suffusion, mudflows	Mass moving of debris, erosion	Erosion, suffusion, deflation (including land spouts, dust storms)

defining specific range of associated processes. These are not only various examples of denudation (particularly, erosion and deflation) but also accumulation related to local flooding, local river network transformation, and change of volcanic and glacier dynamics in some cases. Gravitational and seismic-and-gravitational processes and erosion leading to deep canyons and badland are active peripherally.

Analysis revealed that certain geomorphologic processes are not so hazardous by themselves, but their combination and interaction and intensity of conductive factors increase the risk of disasters [Lebedeva, 2013]. Frequently, a chain of extreme processes and their sequence and combination lead to huge disasters e.g., the Yungay event (Chile), where seismic shock caused a landslide followed by a mudflow. There is also the Parraguirre event in the Colorado valley (Santiago region), where rocky slide transformed into debris avalanche that, in turn, after 5 km, transformed into mud-and-stone flow because of melting of included ice; the height of flow frontal wave reached 20–30 m [Novoa, 2013]. The 1987 earthquake in Ecuador caused numerous slumps in the Cordillera Real, and heavy rains caused disastrous mudflow in the Salado-Coca valley resulting in transport of 0,08 cubic kilometers of debris, pipe line, and highway destruction within 100 km. The Hosefina landslide in the Paute valley in 1993, was also complicated [Zavgorodniaya, 1996]: it was caused by both heavy precipitation and human impact (slope cutting in case of cropping).

The Chaiten eruption in 2010 was responsible not only for descent

Table 3. Explanatory notes for the map of geomorphologic hazards and disasters in the Central part of the Andes (from 50 to 280S), scale 1:8 000 000

Natural hazards and disasters	Background geomorphologic processes	Terrain type
Regional processes 1. The Andean Western mega slope		
1.1. Floods, tsunami, abrasion, erosion, accumulation, bogging, suffusion, land spouts, dust storms, eolian accumulation	Deflation-and-accumulation together with nonroutine alluvial-and-proluvial accumulation	Coastal lowland plains (up to 200 m)
1.2. Tsunami, abrasion, floods in valleys, erosion, accumulation, gravitational processes, land spouts, dust storms, eolian flows	Deflation-and-corrasion processes together with gravitational and nonroutine alluvial-and-proluvial processes	Low coastal ranges (200-500 m)
1.3. Abrasion, tsunami, floods in valleys, erosion, badlands' forming, accumulation, gravitational and seismic-and-gravitational processes, eolian flows, land spouts	Deflation-and-accumulation together with non-routine proluvial processes	Coastal low- and medium-altitude (up to 1500 m) residual ridges and bald mountains, high (1500-3000 m) intermountain basins
1.4. Abrasion, erosion, accumulation, gravitational and seismic-and-gravitational processes, eolian flows, land spouts	Active erosion together with gravitational processes and deflation	Deep dissected ranges (up to 2500-3000 m), parts of low-mountains, residual ridges and hills
Regional processes 2. The Andean central body		
2.1. Lahars, lava and pyroclastic flows, ash falls, gravitational processes, including debris avalanches, rock falls, erosion, gullying, subsidence, badlands' forming, land spouts	Pyroclastic and lahar sedimentation together with gravitational processes	Slopes and foots of lost and active volcanoes
2.2. Gravitational and seismic-and-gravitational processes, including avalanches, glacial falls, gravity winds	Glacial plucking and accumulation	Above snow line
2.3. Gravitational and seismic-and-gravitational processes, erosion, mudflows	Landslides, rock falls together with alluvial-and-proluvial and mudflows	Short various directed hills and ranges (600-3000 m)
2.4. Gravitational and seismic-and-gravitational processes, including landslides, rock falls, detaches, avalanches; erosion, mudflows	Rock falls, landslides together with erosion and mudflows	High (up to 4000 m and more) ranges and rock massifs
2.5. Erosion, solifluction, gravitational and seismic-and-gravitational processes, accumulation, floods, land spouts, dust storms	Erosion together with gravitational and cryogenic processes, solifluction	The northern part of the Altiplano (3000-4000 m)

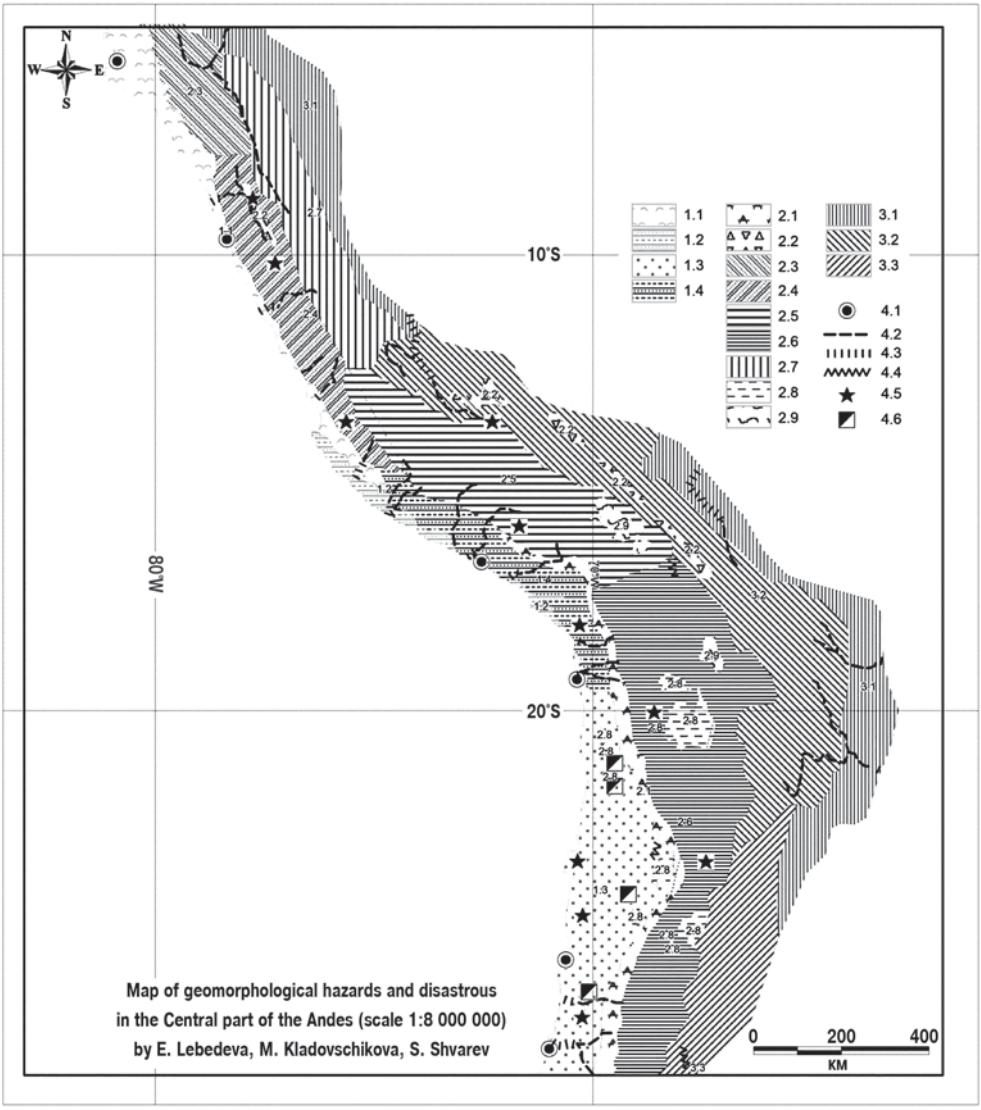

Fig. 9. Map of geomorphologic hazards and disasters in the central Andes sector (from 5° till 28° s.l.). Map symbols see Table 3

of lahars but also for vegetation destruction within the adjacent slopes. This fact allows us to forecast the extent of potential damage from mass movement, the most probable consequences of earthquakes. However, abundance of precipitation conductive for restoration of vegetation cover should mitigate the risks within 5–7 years in the region.

CONCLUSION

Geological-and-tectonic and physiographical features of the South American Pacific coast are associated with high *intensity of morpholitogenesis* including disastrous paths of some geomorphologic processes. Their combination and interaction and intensity of conductive factors increase the risk of disasters. The Andean natural disasters,

such as volcanic eruptions threatening ash-bound cities and fields, earthquakes causing avalanches and mudflows destroying human settlements, large flooding in mountains breaking highways and destroying villages and farm lands, are responsible for significant economic damage now and in the past.

Human economic activity makes considerable contribution to environmental transformation in the way of additional activation of many natural processes. Human impact enhances development of natural disasters. For example, cutting of slopes, deforestation, and desert advancement as a result of overgrazing bring negative consequences. Slope processes, erosion, and deflation (in dry areas) intensify. Mining causes soil erosion and surface and ground water pollution.

Thus, terrain-forming processes are influenced by many natural and human drivers that provoke high intensity of geomorphologic processes. Thereby terrain morphology and rock lithology, precipitation type, and vegetation conditions influence the character and intensity the terrain-forming processes. Large hydrometeorological events, frequent seismic shocks, volcanic eruptions, and human impact intensify disasters development.

The South American Andes extension allows drawing out principles of geomorphologic disasters of these continental marginal mountains in various natural zones – from temporal to subequatorial latitudes that are characterized by the unique individual features, e.g., heat-moisture ratio, that governs both typical and extreme geomorphologic processes. An important feature of the study area is the asymmetric distribution of geomorphologic processes within the coastal and inland slopes of the mountain system, as well as latitudinal zoning of this distribution. Mapping with quantitative assessment of intensity of potential natural and human impact is necessary for understanding of principles of areal distribution of geomorphologic stress in the region and defining the zones of potential risk of disasters development.

ACKNOWLEDGMENTS

Authors are grateful to G.S. Ananiev (Faculty of Geography, Lomonosov Moscow State University), S.S. Zavgorodniaya (Pontifical Catholic University of Ecuador) and V.P. Chichagov (Institute of Geography, Russian Academy of Sciences) for data and valued opinion about the issues discussed in the paper. Special thanks to S. Shvarev for assistance with map material. ■

REFERENCES

1. Aleksandrov S.M. (1996). Nonlinear nature of the relief-forming processes and extreme situations // Moscow: RFBR, 112 p. (in Russian with English summary).

2. Alvarado P., Beck S. (2006). Source characterization of the San Juan (Argentina) crustal earthquakes of 15 January 1944 (Mw 7,0) and 11 June 1952 (Mw 6,8) // Earth and Planetary Science Letters. N 243 (3–4). P. 615–631.

3. Ananiev G.S. (1998). Catastrophic relief-forming processes // Moscow: MSU Publishing House, 101 p. (in Russian).

4. Ananiev G.S. (1999). Exogenous processes at the north-west of South America during El-Nino 1997–1998 // Proceedings of the Russian Geographic Society. Vol. 131, Issue 4, pp. 18–25. (in Russian).

5. Angillieri M.Y. (2008) Morphometri analysis of Colangьil river basin and flash flood hazard, San Juan, Argentina // Environ Geol. N 55. P. 107–111.

6. Budarina O.I., Perov V.F., Sidorova T.L., Belaya N.L. (2000). Genesis and regime of mudflows in South America // Records of Glaciological Studies, Iss. 88, pp. 50–55. (in Russian with English summary).

7. Cembrano J., Lara L. (2009). The link between volcanism and tectonics in the southern volcanic zone of the Chilean Andes: a review // Tectonophysics, N 471, pp. 96–113.

8. Charrier R., Hйrail G., Pinto L., Garcна M. et al. (2013). Cenozoic tectonic evolution in the Central Andes in northern Chile and west central Bolivia: implications for paleogeographic, magmatic and mountain building evolution // Intern. Journ. of Earth Sciences (Geol Rundsch). N 102. P. 235–264.

9. Codron J.C., Cervera F.S. (2000) Riesgos naturals en Los Andes: cambio ambiental, percepciУn y sosteniilidad // Boletin de la A.G.E.N. N 30. P. 69–84.

10. Enman V.B. (1973). Modern Earth crust movements and earthquakes // Modern Earth crust movements. Tartu: Estonian SSR Academy of Science, pp. 633–642. (in Russian)

11. Garreaud R. (1992). Impacto de la variabilidad de la lнnea de nieve en crecidas invernales en cuencas pluvio-nivales de Chile Central // XI Congreso Chileno de la Sociedad Chilena de Ingenierна Hidrбulica, Santiago. 15 p.

12. Garreaud R. (2009). The Andes climate and weather // Advances in Geosciences. N 22, pp. 3–11.

13. Garreaud R., Vuille M., Clement A.C. (2003). The climate of the Altiplano: observed current conditions and mechanisms of past changes // Palaeogeography, Palaeoclimatology, Palaeoecology. N 194, pp. 5–22.

14. Geomorphologic hazards and disaster prevention (2010). Ed. Alcбntara-Ayala I., Goudie A. Cambridge: University Press. 291 p.

15. Golubev G.N. (1969). Chile rivers nourishment // MSU Bulletin. Series 5 – Geography, N 2, pp. 36–41. (in Russian with English summary).

16. Gotvanskiy V.I., Lebedeva E.V. (2010). Natural and anthropogenic factors influence on geomorphologic processes intensity in the Far East // Geomorphology, N 2, pp. 26–36. (in Russian with English summary).

17. http://inosmi.ru/infographic/20111226/181319543

18. http://finam.info/need/news2478800001

19. http://www.ncedc.org/anss/catalog-search.html

20. http://www.volcano.si.edu/world

21. Kazakov N.A. (2000) Possible mechanism of formation of seismogenic avalanches // Records of Glaciological Studies, Iss. 88, pp. 102–106 (in Russian with English summary).

22. Kladovschikova M.E. (2008). Relief development and relief-forming processes of marginal continental mountains (the Andes case) // Author's abstract of a thesis, Moscow: MSU Geographic department, p. 24. (in Russian with English summary).

23. Korotkiy A.M., Korobov V.V., Skrylnik G.P. (2011). Anomalous natural processes and its influence on geosystems stability in the south of Russian Far East // Vladivostok: Dalnauka, 265 p. (in Russian with English summary).

24. Lebedeva E.V. (2013). Natural and anthropogenic basis of geomorphologic processes intensity in the Andes // Geomorpology, N 4, pp. 58–71 (in Russian with English summary).

25. Levin B.W., Sasorova E.V. (2009). Latitudinal distribution of earthquakes in the Andes and its peculiarity // Advances in Geosciences. N 22, pp. 139–145.

26. Lukashova E.N. (1958). South America // Moscow: Uchpedgiz, 467 p. (in Russian).

27. Marcato G. , Pasuto A., Rivelli F.R. (2009). Mass movements in the Rio Grande Valley (Quebrada de Humahuaca, Northwestern Argentina): a methodological approach to reduce the risk // Advances in Geosciences. N 22, pp. 59–65.

28. Montgomery D.; Balco G., Willett S. (2001). Climate, tectonics, and the morphology of the Andes // Geology. N 29 (7), pp. 579–582.

29. Nicholson Sh.E. (2011). Dryland climatology. Cambridge Univ. Press. 516 p.

30. Novoa J. E. (1993). Eficacia geomorfolygica sistema de playas y dunas Bahна de Coquimbo (IV Regiyn, Chile sem6rido): discusion metodolygica y resultados // Anales Sociedad Chilena de Ciencias Geogr6ficas. N 1, pp. 26–33.

31. Novoa J.E (2013). Mass land movements on slopes and its influence on the Western Andes morphogenesis (Chile) // Geomorpology, N 2, pp. 81–96. (in Russian with English summary).

32. Novoa J.E., Araya A.A., Fern6ndez R.M., Araya M.C. (1995). Potential tsunami effects in La Serena area North-Central Chile / Late Quaternary coastal records of rapid change: Application to present and future conditions. Chile, Antofagasta. 12 p.

33. Novoa J. E., Meza M., Moreno I. et al (1988). An6lisis morfodin6mico aplicado al diagnystico de riegos naturales en los sistemas de La Gasca y San Carlos (Quito, Ecuador) // Geografна y Desarrollo. N 2, pp. 303–330.

34. Pararas-Carayannis G. (1974). An investigation of tsunami source mechanism off the coast of Central Peru // Marine Geology. V. 17. Amsterdam: Elsevier. P. 235–247.

35. Perov V.F. (2012). Mudflow studies // Moscow: MSU Geographic department, 272 p. (in Russian).

36. Phillips J. (2011). Emergence and pseudo-equilibrium in geomorphology // Geomorphology. N 132 (3–4), pp. 319–326.

37. Porter M., Savigny K.W. (2002). Natural hazard and risk management for South American pipelines // Proceedings of IPC 2002: 4th International Pipeline Conference. Calgary, Canada. IPC02-27235. 8 p.

38. Rantsman E.Y., Glasko M.P (2004). Morphostructural centres – places of extreme natural phenomena // Moscow: Media-PRESS, 223 p. (in Russian).

39. Sergio A. Sepъlveda, Alejandra Serey, Marisol Lara . et al. (2010). Landslides induced by the April 2007 Aysйn Fjord earthquake, Chilean Patagonia. Landslides N 7, pp. 483–492. DOI 10.1007/s10346-010-0203-2.

40. Stillwell D. (1992). Natural hazards and disasters in Latin America // Natural Hazards. N 6, pp. 131–159.

41. Tectonic Evolution of South America (2000) // 31° Intern. Geol. Congress, Rio de Janeiro. 650 p.

42. The Andes: Active Subduction Orogeny. (2006). Springer-Verlag Berlin Heidelberg. 440 p.

43. Tilling R. I. (2009). Volcanism and associated hazards: the Andean perspective // Advances in Geosciences. N 22, pp. 125–137.

44. Troshkina E.S., Kondakova N.L. (2000). New data on the avalanche mode mountainous areas of the Southern Hemisphere // Records of Glaciological Studies, Iss. 88, pp. 92–101 (in Russian with English summary).

45. Ufimtsev G.F. (2011). Andes diary (relief and morphotectonics of the Peruvian Andes) // Moscow: Scientific World, 164 p. (in Russian).

46. Zhidkov M.P. (1985). Morphostructure of continental-oceanic suture zones of Pacific Rim concerning powerful earthquakes places forecast (Kamchatka, west of South America) // Author's abstract of a thesis. Moscow: IG RAS, 27 p. (in Russian).

47. Zavgorodnaya S.S. (1996). Modern geomorphologic processes and its inventory for ecologic and commercial purposes in Ecuador // Author's abstract of a thesis. Moscow-Quito: MSU, 43 p. (in Russian).

Ekaterina V. Lebedeva is Senior Researcher of the Laboratory of Geomorphology of the Institute of Geography RAS. She graduated from the Lomonosov Moscow State University and received PhD in 1992. Her scientific interest: relief evolution in changing natural conditions and under the influence of anthropogenic factors, intensity of geomorphological processes, ecologic-geomorphological problems. Regions of Research: Far East and European Russia, South and East Africa, South and Central America, Australia. She is the author of approximately 100 scientific papers.

Dmitry V. Mikhalev is Senior Researcher of the Laboratory of Geoecology of the North of the Lomonosov Moscow State University. He received his PhD in 1990. The area of his scientific interest: isotope geocryology, paleogeography, paleoclimatology, cryogenic processes, and geoecology. The regions of research: Russian Arctic, South Africa, South and Central America, Australia. He is the author of approximately 70 scientific papers.

José E. Novoa Jerez, PhD, is Professor in Physical Geography, University of La Serena, Research Member of the Center for Advances Studies in Arid Zones (CEAZA-Chile), Chair of Applied Physical Geography Program, and Steering Member of the Risk and Natural Disaster Chapter of the International Geography Union (IGU). His research interests are in applied physical geography (from local to regional scale) related to natural hazards, climatic change, applied climatology, and natural resources planning in arid environments. Dr. Novoa has had a long career in research and teaching in physical geography in South America. During last two decades, he was responsible for the research development and operational implementation of theoretical models and studies in arid environments related to physical geography oriented to urban and rural planning strategies in mountain, coastal, and fluvial ecosystems of Chile, Argentina, Peru and Bolivia.

Mariya E. Kladovschikova is Researcher of the Department of Geomorphology of the Institute of Geography of Russian Academy of Sciences. She obtained her PhD from the Lomonosov Moscow State University in 2008 under supervision of Professor G. Anan'ev on terrain processes development in marginal continental mountains of the Andes. She joined the staff of the Institute of Geography in 2009. Her academic interest encompasses geomorphologic hazard in dynamic mountainous ranges, anthropogenic geomorphology, and cultural landscapes and is supported by her professional experience in Khibiny, Greater Caucasus, South Urals, Crimean Mountains, Andes, and Sino-Tibetan Mountains.

Irina N. Rotanova[1], Vladimir S. Tikunov[2*], Guldzhan M. Dzhanaleeva[3], Anar B. Myrzagaliyeva[4], Chen Xi[5], Nyamdavaa Gendenjav[6], Merged Lkhagvasuren Choijinjav[7]

[1] Altai State University, Faculty of Geography, 61, Lenina av., Barnaul, 656049, Russia; e-mail: rotanova07@inbox.ru

[2] Lomonosov Moscow State University, Faculty of Geography, Leninskie Gory, Moscow, 119991, Russia; e-mail: tikunov@geogr.msu.su

[*] **Corresponding author**

[3] Gumilev Eurasian National University, Faculty of Natural Sciences, Munajtpasov st., 13, Astana, 010000, Republic of Kazakhstan; e-mail: lu_lala@bk.ru

[4] Amanzholov East Kazakhstan State University, Research Affairs and International Relations Department, 55, Kazakhstan st., Ust-Kamenogorsk, 070020, Republic of Kazakhstan; e-mail: anara_vkgu@mail.ru

[5] Xinjiang Institute of Ecology and Geography, Chinese Academy of Sciences, 818 South Beijing Road, 830011, Urumqi, Xinjiang, China; e-mail: chenxi@ms.xjb.ac.cn

[6] The National Ulaanbaatar University of Mongolia, School Geography and Geology, 14/3, Peace av., Ulaanbaatar, 210646, Mongolia; e-mail: nyamdavaa_geog@yahoo.com

[7] Hovd State University, Hovd, 213500, Mongolia; e-mail: hovd_lha157@yahoo.com

INTERNATIONAL MAPPING PROJECT "THE ATLAS OF GREATER ALTAI: NATURE, HISTORY, CULTURE" AS THE FOUNDATION FOR MODELS OF SUSTAINABLE DEVELOPMENT

ABSTRACT. The paper presents the concept and approaches to the creation of a special interdisciplinary Atlas of Greater Altai. The main objective of the Atlas is to ensure the maximal possible access of the international community to reliable, current, and accurate spatial information on the transboundary Greater Altai region. The paper discusses the preconditions that facilitate the development of this unique cartographic product, the main sections of its structure (nature, history, and culture), and the main themes of its maps. The paper demonstrates the need for geoinformation support and a web-based version of the GIS-based Atlas. The Atlas can be used indecision-making in the scope of the international cross-border cooperation in the Altai region.

KEY WORDS: Altai, GreaterAltai, the Altai region, Atlas of Greater Altai, GIS, web-atlas.

INTRODUCTION

"The Atlas of Greater Altai: Nature, History, Culture" is an interdisciplinary unique cartographic modelthat is being developed by an international team of scientists. The main objective of the Atlas is to ensure the maximal possible access of the international community to reliable, current, and accurate spatial information on the transboundary Greater Altai region for its effective development.

Altai is a mountain system located in the heart of Eurasia. Four countries, namely Russia, Kazakhstan, Mongolia, and

Fig. 1

China, share the Altai region (Fig. 1). The international cross-border cooperation in the Altai region has historical roots. For centuries, thisvastmountain region (about 30 thousand sq. km.) has been unified by cultural, ethnic, trade-economic, political, and migration ties. Currently, there are six administrative-territorial divisions: Altai Krai and Altai Republic (Russia), East Kazakhstan Oblast (Kazakhstan), Xinjiang Uyghur Autonomous Region (China), and Bayan-Ulgii and Hovd Aimags (Mongolia). The name "Greater Altai" symbolizes community, unity, and cooperation of the numerous peoples inhabiting this wide geographical area. In 1993, the near-border districts created the International Coordinating Council "Our Common Home Altai", which plays an important role in strengthening international relations in the region [Rotanova, Ivanov, 2013].

The Altai natural mountain formation located in the heart of a vast continent has the significant geographical uniqueness considered by many researchers who have studied it as a characteristic phenomenon in the region. Climatic, hydrological, and atmospheric processes are formed in this region; these processes then spread over vast areas of Central and North Asia. The Altai glaciers are the source of the largest rivers, i.e., Irtysh, Ob, and Hovd; these rivers are used by many millions of people in Russia, Kazakhstan, China, and Mongolia. In the depths of Altai, the rich mineral resources have been explored. The region contains almost the entire periodic table, including a full range of non-ferrous metals and rare earth elements.

Diversity of climatic conditions, created by mountain and basin landforms, altitude, and exposition, defines a rich set of features of the species and communities of flora and fauna. High levels of biodiversity and preservation of much of the landscape in a state little affected by human activities were the crucial factors for the inclusion of Altai, at the end of the XXth century, in the list of two hundred virgin or little altered regions of the Earth ("Global – 200"), which received the international status of ecoregions.

One of the priority areas of cooperation, implemented by all countries of Greater Altai, is environmental activities, including preservation of biodiversity and other environmental issues. In all the countries in the Greater Altai border areas, there is a functional network of specially protected natural areas (SPNA). The network includes the state natural reserves, national and natural parks, and wildlife and refuge complexes. Greater Altai represents the region of the priority implementation of the ecoregional approach to environmental protection. The agreement between the Governments of the Russian Federation and the Republic of Kazakhstan to establish a transboundary reserve "Altai" based on the Katun Biosphere Reserve and the Katon-Karagaisky National Park has been signed and is being implemented. The importance of natural and cultural values of Altai has been confirmed by the inclusion of the area "Golden Mountains of Altai" (Russia) in the List of the World Cultural and Natural Heritage; this area consists of five clusters: the Altai and the Katun State Biosphere Nature Reserves, the Natural Park "Belukha", the Natural Park "The Quite Area Ukok", and Teletskoe Lake. It is noteworthy that the area "Golden Mountains of Altai" may soon become the international, four-lateral, World Natural and Cultural Heritage object,

extended to the neighboring countries: China, Mongolia, and Kazakhstan [Badenkov, Rotanova, 2011; Badenkov, Andreeva, Rotanova 2012].

Greater Altai is rich in archaeological, historical, and cultural values, ethnic and cultural diversity, and the extant traditional way of life of its peoples. Within this region, Slavic, Turkic, Mongolian, and Chinese ethnic groups come into intercultural interaction. The religious situation in Greater Altai is also unique: Christians, Buddhists, followers of Islam, and traditional shamanic cults coexist peacefully. Altai today represents the center of Eurasian ethno-cultural consolidation.

The above-mentioned facts and factors explain the increased interest to Greater Altai from the positions of many spheres of activity and, primarily, as a very promising region for tourism and recreational activities, including international/cross-border tourism. The tourism industry within Greater Altai, currently, has some level of development in all countries located in the region. It is mainly based on the ecological and natural potential and utilizes natural attractiveness of each country and the situation of the environmental well-being of the region.

The idea of developing the Atlas arose from the results of years of work of different groups of researchers who accumulated a large volume of information indifferent databases, thematic maps, and geographic information systems (GIS) for environmental and target programs running in the countries of Greater Altai.

THE CONCEPTUAL FRAMEWORK OF THE ATLAS

The Atlas will be based on the studies and analysis of modern scientific-methodological and technological advances of different areas of science (geography, biology, ecology, history, cultural studies, geoinformatics, etc.) and computer mapping, while maintaining continuity of the best examples of Russian and foreign fundamental cartographic works. Novelty and uniqueness of "The Atlas of Greater Altai" are predetermined by the conceptual provisions of the original thematic structure. The internal unity of the Atlas is ensured by comparability, complementarity, and linkage of the sections and individual maps, appropriate choice of projections and scales, a single approach to cartographic generalization, a coherent system of symbols, and a common design.

The year of 2013 was the phase of conceptualization. At this stage, a coordination system for work under the compilation of the Atlas in the participating countries was established. The year of 2014 is the phase of development of conceptual solutions and the Atlas programs.

The Atlas concept is based on the idea of the balanced development of the transboundary area of Greater Altai. The concept, in the same way as all phases of its implementation, utilizes the advances in theoretical and practical cartography, which have been accumulated and developed in the last decades. This information will be substantially improved in the course of the geographic information implementation of the concept.

The compilation of the thematic maps of the Atlas will be based on the modern scientific approaches: comprehensive, historical, cultural, dynamic, etc. The Atlas will use three approaches for the information representation. The main one is the analytical (comparative) representation at the macro-regional level with the network model elements (summary maps of Greater Altai).The second approach incorporates the transition from the national (state, macro-regional) level to the regional and local levels. Finally, the third approach is a matrix, whereby the blocks of maps at the administrative-territorial divisions are defined (local).

Several methodological approaches developed in the practice of atlas mapping will be used to represent the thematic maps

most completely and expressively. Thus, the Atlas will utilize multi-level mapping of phenomena and objects at the national (state), regional, and local (respectively, at different scales) levels. In some cases, they are very well rendered as anamorphic images. The comparative method is widely applicable for the representation of features of Greater Altai in relation to other administrative units of the Russian Federation, Kazakhstan, China, and Mongolia.

Mapping will be performed at three levels of aggregation of information: analytical, integrated, and synthetic. The analytical maps will enable the isolation and rendering of individual and the most important properties and/or characteristics of objects and phenomena of the mapped territory from an array of numerous features. The integrated maps will render not only multifaceted (polythematic) characteristics of the region, but will also help analyzing and exploring relationships, interactions, and dynamics of covered objects and phenomena. The synthetic maps will rely mainly on the integration of a number of individual parameters and will facilitate derivation of integral characteristics of the mapped objects, reflect typological zoning, isolate clusters, and present the results of mathematical-cartographic modeling.

The tasks of the Atlas require addressing a number of issues at different levels of research: methodological (concept development, conceptual apparatus, selection of priorities); scientific-procedural (design of the informational structure, GIS-based format, etc.), informational (uniformity, availability, reliability of the mapped data), structural (map compilation), etc. The greatest difficulty is associated with differences in the data collected in the Russian Federation, Kazakhstan, China, and Mongolia.

THE STRUCTURE OF THE ATLAS

The structure, content, and thematic division of the Atlas are currently at the stage of development and coordination. The title of the main sections of the Atlas corresponds to the names of the Atlas title: Nature, History, and Culture. These sections will be preceded by the introductory section that will contain geographic information on the borders of the countries and the near-border administrative-territorial divisions of Greater Altai and space images of the region.

Section "Nature" will contain spatial-temporal information on the natural conditions, economic impact on the natural environment, and environmental quality in Greater Altai in the beginning of the XXIth century. The quality of the environment is perceived as the consequence of the economic, social, and cultural development of the near-border administrative-territorial entities of the four countries located within the Altai mountain system.

Section "Nature" will have three major subsections:

- Natural conditions
- The impact of economic activity on the environment.
- Sustainable development of the territories. Protection and optimization of the natural environment.

Subsection "Natural conditions" will cover the following areas: landscapes, sustainability of the environment, climatic zoning, climatic comfort, hydrological areas, glaciers and mudflows, permafrost (distribution, temperature, thickness, seasonal freezing and thawing), soil zoning, bioclimatic mapping of the vegetation types, biodiversity, and biodiversity uniqueness coefficient.

Subsection "Impact of economic activity on the environment" will have the following thematic maps: population distribution, population density, urban population, functional types of settlements, age-structure of the population, main types of the culture of natural resource use, agricultural level of development of the landscapes, agricultural

land, anthropogenic load on the landscapes, impact of economic activities on the environment, anthropogenic changes of the soil-forming processes, pollution of the snow cover, atmospheric emissions of pollutants from stationary sources, emissions structure, wastewater, wastewater composition, extreme pollution of surface water, impact of the mining industry on the environment, toxic waste, hazards from oil and natural gas transport, forest cover, forest logging, forest fires, secondary forests, volume of solid municipal waste of large settlements, conflicts in natural resource use at different territorial levels, and environmental-economic map.

Subsection "Sustainable development of territories. Protection and optimization of the natural environment" will include the following maps: natural, technological, biological and social risks, hazards and risks of natural emergencies, hazards and risks of endogenous processes (earthquakes, avalanches, glacial activity, landslides, mudslides, karst, subsidence, erosion, flooding, permafrost processes), hazards and risks of meteorological processes (desertification, drought, climate extremes, extreme air temperatures, snow, blizzards, fog, black ice and icing, thunderstorms, hail, hurricanes), hazards and risks of hydrological processes (floods, flash floods),hazards and risks of wildfires, monitoring, methods and means of mitigation of hazardous natural processes and phenomena, hazard and risk of technogenic situations, synergetic manifestation of hazardous natural and man-made processes, biological and social hazards (natural focal infectious, parasitic, and other diseases of humans and farm animals, spread of insects – pests of forests and crops, distribution of midges),and organization of prevention and mitigation of emergency situations.

Subsection "Sustainable development of the territories. Protection and optimization of the natural environment" will cover the following areas: distribution ranges of the Red-Book rare and disappearing species of plants and communities, distribution ranges of the Red-Book rare and disappearing species of animals, the Red-Books of the Russian Federation and of its administrative entities (on soils, plants, and animals), SPNAs, development of the environmental network, sustainable development of territories, optimization of the natural environment, environmental monitoring, environmental public organizations, youth and children public organizations, international environmental organizations operating in Greater Altai (Greenpeace, WWF, etc.), and international cooperation in environmental protections.

The main purpose of section "History" is to consistently reveal the course of historical development of Greater Altai from antiquity to the present and to provide spatial and temporal information about the historical heritage of the region. This section will include a series of interrelated maps describing stages of settlement and development of the territory: settlement sites of primitive people, habitats of the peoples, emergence of statehoods, changes in the state borders, changes in the structure of settlements and population, objects of heritage, archaeological sites, military conflicts, trails of discoverers and expeditions of travelers and scientists, etc. The section will present known extant cartographic works of past centuries [Barnaul, 2006; Borodayev, Kontev, 2006; Special ..., 1998].The section will conclude with a glossary of terms and a chronological table of important dates and events related to Greater Altai.

Section "Culture" will be composed of two subsections, one of which is dedicated to the rich cultural heritage of Greater Altai and the other – to the modern culture. Culture is seen as a social phenomenon and as a branch of the social sphere. Cultural heritage is one of the most modern resources that determine the socio-economic and socio-cultural development of Greater Altai globally. The maps of the section will be created using modern information and knowledge about the laws and practice of information sharing and the development of

regional and national cultures, ethnography and folklore, and their existing relationships and prospects for cooperation in the conservation and restoration of the cultural environment of Greater Altai. The main themes of the maps of contemporary culture are: public education, literature, theater, music, museum, library, cultural heritage, and famous people (natives of Altai and those who worked in Altai).

The maps will also show monuments and other various forms of monumental art, locations of folk arts and crafts (wood, metal, stone, bone, glass, weaving, and knitting crafts, etc.). The maps will also show the network and the activities of various cultural institutions: theaters, museums, libraries, archives, clubs, and institutions of higher education in the field of culture.

The Atlas will have a separate block of maps dedicated to cognitive tourism and excursions showing the use of cultural facilities in the tourism sector. Thus, the theme of one of the maps will be the systematized data on the potential international tourist route "Golden Ring of Altai", as well as the information on the roadside infrastructure and services.

These themes of the maps, sections, and subsections selected through mutual effort and coordination will be the foundation of the Atlas and map layouts and will provide for the logical interconnection of the map content.

The Atlas will be presented in the traditional printed format; however, it will be created with the use of GIS-technology, which will ensure the systemic integrity of its content and coherence of the maps. Thus, there will be an electronic version of the Atlas.

GEOINFORMATION SUPPORT OF THE ATLAS

The GIS-component of the Atlas will allow assessing the natural, economic, social, and demographic situation in the Altai transboundary region and could become the framework for the subsequent creation of a permanent geoinformation monitoring system available for use over the Internet. In addition, the mapping, aerial-space, and text data consolidated into a single GIS database and designed as a hypermedia system capable of rendering graphics, hypertext, slides, and, possibly, a small film with a soundtrack, will provide for the full integral characterization of the region in comparison with other parts of the four countries. This will also help tracking the nature of changes and creating a strategy for the environmentally sound sustainable development of Greater Altai.

The electronic mapping of Greater Altai will be done at different scales that correspond to the size of the territories: local – 1:10 000, 1:25 000, 1:50 000 (cities); sub-regional – 1:100 000, 1:200 000 (administrative regions, Somons); regional – 1:1 000 000, 1:1 500 000, 1:2 000 000, 1:2 500 000, 1:3 000 000 (Altai Republic, Altai Krai, Hovd Aimag, etc.), the inter-regional or macro – 1:1 000 000, 1:2000 000, 1:3000 000, 1:5 000 000, 1:8 000 000 (Greater Altai within the territories of the bordering countries, etc.).

In general, the thematic database (TDB) of the electronic version of the Atlas will be based on the following requirements: it must be uniform in terms of time-scale, i.e., the quantitative data stored must have the same point in time for all its parameters; must have a sufficient degree of detail; must be spatially accurate; must be compatible with other data; must adequately reflect the nature of phenomena; and must be accessible to users.

Special activities will be undertaken to establish the necessary framework for the digital mapping. They should be brought to a common geodetic coordinate system and created as the digital topographic bases for the region. Landscape and land use maps will represent the framework for mapping of different geographical phenomena.

Table 1. The maps of the introductory section of "The Atlas of Greater Altai: Nature, History, Culture"

Map themes	Scale
Structure and boundaries of Greater Altai	1: 3 000 000
Russian part of Greater Altai	1: 1 000 000
Mongolian, Kazakhstan, and Chinese parts of Greater Altai	1: 1 000 000
The Greater Altai region on the world map	1: 30 000 000
Greater Altai as part of the Central Asian region	1: 20 000 000
Greater Altai on the maps of Russia, China, Kazakhstan, and Mongolia	
The Russian part of Greater Altai on the map of Russia	1: 10 000 000
The Mongolian part of Greater Altai on the map of Mongolia, China, and Kazakhstan	1: 5 000 000
The Russian part of Greater Altai as part of the Siberian Federal District	1: 5 000 000
The administrative-territorial division of Greater Altai, the Russian part	1: 2 500 000
The administrative-territorial division of Greater Altai, the Mongolian, Kazakhstan, and Chinese parts	1: 2 500 000
Barnaul – the capital of Altai Krai	1:50 000
Gorno-Altaisk – the capital of Altai	1: 50 000
Hovd – the capital of Hovd Aimag, Mongolia	1: 50 000
Bayan-Ulgii – the capital of Bayan-Ulgii Aimag	1:50 000
Altai – the capital of the Altai District of China	1: 50 000
Ust-Kamenogorsk – the capital of the East Kazakhstan Oblast	1: 50 000
Space imagery of Greater Altai	1: 20000 000

The structure of the GIS-based TBD will provide for the characteristics of the maximal possible number of the geo-system elements of Greater Altai in the digital version of the Atlas.

The TDB and its thematic coverage will reflect the physical-geographic and socio-economic conditions of the mapped territory, character of the covered phenomena and processes, and the assessment of the current conditions.

The list of the themes and working scales of the introductory section of the Atlas presented below is an example of the information contained in the Atlas. The digital maps of this section will relate the geographical locations and boundaries of the administrative-territorial division of Greater Altai (Table 1).

CONCLUSION

The Atlas of Greater Altai can be considered as part of the digital atlas of sustainable development of the Russian Federation, whose main purpose is to present a unified geoinformation space for development and improvement of the management system. The Atlas is important not only for the electronic-cartographic representation of one of the largest territorial formations of North Asia, but also contributes significantly to the development of the national information resources in Russia.

The potential range of its users is extremely wide. The maps of the Atlas may help raising the investment attractiveness of the region and enhance innovation activities for the entire region and its parts. The Atlas will be useful for resource mobilization, including business structures for the integrated development of environmentally oriented sectors. The Atlas will help its users to stay current and, thus, make informed decisions on a wide range of issues determining the development of Greater Altai. ■

REFERENCES

1. Badenkov, Yu.P., Andreeva, I.V., Rotanova, I.N. (2012) Nature protection projects in the Altai-Sayan region in the context of adaptation to climate change based on the concept of management of sustainable bio- and landscape diversity // Geography and Natural Resource Use of Siberia: Proceedings / Prof. G.Ya. Baryshnikov (Ch. Ed.). – Issue 14. – Barnaul: Altai University Press, pp. 12–23.

2. Badenkov, Yu.P., Rotanova, I.N. (2011) New nature protections initiatives and approaches in the Altai-Sayanecoregion. // Polzunov Herald, №. 4–2, pp. 34–38.

3. Barnaul. Scientific-Reference Atlas (2006) / I.N. Rotanova, B.V. Borodaev, V.I. Bulatov, V.G. Vedukhina, etc. -Novosibirsk: FSUE "PE Engeodesia" Roskartografia.

4. Borodaev, V.B., Kontev, A.V. (2006) Historical Atlas of the Altai Krai: Cartographic materials on the history of the Upper Ob Region and the Irtysh Region (from the antiquity to the beginning of the 21st century). – Barnaul: Azbuka, 119 p.

5. Rotanova, I.N., Ivanov, A.V. (2013) International cooperation in the Altai region – 10 years of activities of the Multinational Coordination Council "Our Common Home Altai" // Protection of Environment and Natural Resources of the Countries of Great Altai; Proceedings of the International Scientific-Practical Conference (Barnaul – Gorno-Altaisk, 23–26 September 2013) / G.Ya. Baryshnikov (Ch. Ed.) – Barnaul: Altai University Press, 298 p. – pp. 211–214.

6. Specially Protected Areas and Sites of the Altai Krai (1998) / P.I. Dianov, I.N. Rotanova, L.V. Pestova, L.N. Purdik – 1:1 000 000. – Map. – Moscow.

Irina N. Rotanova, Ph.D in geography, is Associate Professor, Department of Physical Geography and Geoinformation Systems (Faculty of Geography) and Scientific Researcher of the Scientific-Research Sector of the Altai State University; Leading Scientist of the Laboratory of Hydrology and Geoinformatics of the Institute for Water and Environmental Problems, SB RAS. She was in charge and participated in several federal programs and contracts, programs of RAS and SB of RAS, including the Program of SB RAS "Environmental Mapping of Siberia". She directly participated and led research efforts under large projects: assessment of impacts on the environment of the Katun Hydroelectric Station, development of the system of Specially Protected Environmental Reserves in Siberia, Systems of Territorial Planning of the Municipalities of the Altai Krai, System of Integrated Use and Protections of Waters of the Ob-Irtysh Basin, etc. She is one of the principal co-authors and scientific editor of several environmental thematic maps including the map of Specially Protected Areas and Sites of the Altai Krai, which received the Diploma of the All-Russian Competition for the Natural Heritage Protection. She is Scientific Secretary of the Altai Krai Branch of the Russian Geographical Society. She is a member of the International Cartographic Association. She is a scientific expert for the International Coordination Council "Our Common Home Altai". She is a laureate of the Environmental Award "Ecomir–2006" (as a member of a group of authors), the National Environmental Award of the Vernadsky Foundation in 2006 (as a member of a group of authors), and the Diploma recipient of the Competition "National Environmental Award 2007" for a series of water-environmental maps. She has over 600 published works, including 10 monographs (with co-authors).

Vladimir S. Tikunov is Professor, Head of the Integrated Mapping Laboratory, Faculty of Geography, Lomonosov Moscow State University, and Director of the Center of the World Data System for Geography. His research has been used in many thematic maps and atlases: National Atlas of Russia (editor-in-chief of Vol. 3), Environmental Atlas of Russia, Atlas of Socio-Economic Development of Russia, Atlas of the Khanty-Mansi Autonomous District – Yugra, etc. He was Vice-President and, currently, is Chairman of the Commission of the International Cartographic Association and a member of the Commission on Geographic Information Science of the International Geographical Union. He has been a member of the editorial boards of 9 Russian and international journals. He lectured at a number of national and international universities. He has been organizing, since 1994, annual international conferences InterCarto-InterGIS "Sustainable Development of Territories: GIS Theory and Practical Experience" that take place both in Russia and abroad. He is a recipient of the Anuchin Award for his work in mathematical cartographic modeling. He is also a recipient of the Award in Science and Technology of the Russian Federation Government for the development of environmental and natural-resources atlases of Russia. He published over 500 scientific works, including 14 monographs, texbooks, and manuals in 28 countries of the world and in 14 languages.

Guldzhan M. Dzhanaleeva is D.Sc. in Geography, Professor of the Department of Physical and Economic Geography of the Gumilev Eurasian National University, Director of the Scientific-Research Institute of Geography and Geoecology. She has led a number of scientific projects of the Ministry of Education and Science of the Republic of Kazakhstan (MES RK) and the Ministry of Environmental Protection of the Republic of Kazakhstan. Under her academic advising, 16 candidates of sciences and 2 doctors of sciences defended their dissertations. She is the author of several papers published in foreign magazines (in English). She has administered several international scientific conferences on theoretical and applied problems of geography. She is a member of the Expert Council of the MES RK and a founding member of the National Geographical Society of the Republic of Kazakhstan. She has published over 250 works (including 6 monographs and tutorials) in the Republic of Kazakhstan.

Anar B. Myrzagaliyeva is Professor, Director of the Department of Research Affairs and International Relations of the Amanzholov East Kazakhstan State University. She is involved in research work on environmental issues and study of medicinal plants resources. She studied vegetation and plant resources of the ridges of Kazakhstan Altay. The results of this work were used in the compilation of the map on the distribution ranges of medicinal plants forming large commercial stocks. A. Myrzagaliyeva received the state research grant of the Ministry of Education and Science of the Republic of Kazakhstan for Talented Young Scientists for her active involvement in research and contribution to the development of science. She is Corresponding Member of the Russian Academy of Natural Sciences and a member of the Kazakh Geographic Society. A. Myrzagaliyeva has published more than 100 works, including 8 monographs, textbooks, and tutorials.

Chen Xi is Professor, Director General of the Xinjiang Institute of Ecology and Geography of the Chinese Academy of Sciences and Director of the Center of Environment and Ecosystems in Central Asia. He has led 40 UNDP and UNEP projects in China and EU. He is a recipient of the Award in Science and Technology of the China Government for Sustainable Development of Environmental and Natural Resources in China. He was Vice-President of the Association for Natural Resources of China and President of the Xinjiang Association for Remote Sensing. He has been a member of editorial boards of several international journals and Chief Editor of the *Journal of Arid Lands*. He published over 200 scientific works, including 18 monographs and textbooks in three languages.

Nyamdavaa Gendenjav, Ph.D. (geography), is Professor of the School of Geography and Geology, National University of Mongolia. Under his scientific supervision 23 undergraduate and graduate students successfully received their degrees. He participated in 4 research projects and was a leader and consultant on 5 research projects. He was engaged in teaching activities during 6 years and for 8 years he was President of Hovd University. He was a member of the Mongolian State Great Khural. For 8 years, he was Governor of the Hovd Aimag. He published 85 scientific works, including 12 books and scientific proceedings. He is the author of 70 scientific presentations.

Merged Lkhagvasuren Choijinjav is Professor of Hovd University and the University President's Advisor in charge of scientific research and innovation. He has been a leader, administrator, and researcher of joint research projects, a leading member of the Mongolian Geographical Association, and a member of the organizing committee of the State Geographical Olympiad. He published over 100 research papers in national and foreign professional journals, including 6 monographs and 12 books and textbooks.

FORUM "ARCTIC – THE TERRITORY OF DIALOGUE"

On September 24–25, 2013, Salekhard (the Yamal-Nenets Autonomous District, Russia) hosted the III International Arctic Forum "Arctic – the Territory of Dialogue" held with the support of the Russian Geographical Society (RGS). The Forum is the largest political and expert platform for exchange of views on the issues relating to the Arctic region

The I International Forum "Arctic – the Territory of Dialogue" was held in September 2010, in Moscow, and marked the beginning of the Russian initiative to discuss issues of peaceful and sustainable development in the Arctic. The I Forum, dedicated to the problems of preservation of the Arctic environment, secure implementation of economic and infrastructure projects, as well as to the sustainable development of the region, was attended by more than 300 participants. The II International Arctic Forum took place in September 2011, in Arkhangelsk, and was jointly organized by the RGS and the Northern (Arctic) Federal University. The Forum brought together more than 400 delegates from Russia, the Arctic and the Arctic-region states, and more than 100 journalists. The Forum was dedicated to the formation of the Arctic transport system as the foundation for the development of the Arctic region. The Forum addressed the development of navigation, polar aviation, ports, airports, and the transport corridor of the Northern Sea Route.

The theme of the III Forum was "Environmental Security in the Arctic". Its purpose was to unite the efforts of all stakeholders to seek consensus between governments, academia, business, and the population, inhabiting high latitudes, on the preservation of the Arctic environment and mitigation of impacts of increasing economic activity and global climate change. The III Forum was conducted in the Cultural and Business Center of Salekhard. There were more than 700 participants, including more than 250 participants from Finland, USA, Serbia, Poland, China, Denmark, Georgia, Germany, Azerbaijan, Norway, Italy, Bulgaria, the Netherlands, Spain, and the United Kingdom. More than 100 journalists from dozens of different media sources were accredited to the Forum. The selection of Yamal was not accidental, since it is at the forefront of the implementation of the national policy of the Russian Federation on the development of the Arctic region. Also, the Yamal-Nenets Autonomous District has been implementing many large-scale projects in the economic, environmental, scientific, and other sectors.

Artur Chilingarov, Hero of the Soviet Union and Russia, First Vice President of the RGS, Corresponding Member of the Russian Academy of Sciences, opened the Forum. He stated that the main objective of the Forum is to provide a free and open dialogue on the most pressing issues in the Arctic. The Yamal Peninsula is the gateway to the Arctic. The Yamal-Nenets Autonomous District is one of the examples of the responsible and balanced environmental policy in the Arctic.

The second presenter was *Dmitry Kobylkin*, Governor of the Yamal-Nenets Autonomous District. In his address to the Forum participants, he stated that all activities in the region are based on three fundamental principles: the preservation of culture, customs, and traditional economic activities of indigenous peoples (the number of

indigenous northern people has increased in the last 10 years by 11%); insurance of environmental safety of the region (every tenth km of the Yamal Peninsula is a reserve); and preservation of harmony and balance between the interests of energy companies and indigenous peoples (each project of oil and gas companies must pass public hearings, where representatives of tundra communities act as experts).

At the opening session of the Forum, *Aqqaluk Linge*, Head of the Inuit Circumpolar Council, and *Alexander Aseyev*, RAS Vice-President, Chairman of the Siberian Branch of the RAS, made welcoming speeches. *Sergei Kharyuchi*, Chair of the Council of Elders Indigenous People of the North, Siberia, and the Far East, suggested making the issue of indigenous peoples the main theme of the next Forum.

The first thematic section "Environmental Safety and Health of the Arctic Population" (moderators: *Vladimir Kotlyakov*, Academician, Honorary President of the RGS, and *Susan Chatwood*, Executive and Research Director of the Institute for Circumpolar Health Research, Yellowknife, Canada) included a presentation by *Boris Revich*, Doctor of Sciences, Professor, Head of the Laboratory of the Environmental Quality and Human Population Health Forecasting, Institute of Economic Forecasting, RAS, on "Environment and Climate Change Effects on the Human Health in the Arctic". Several participants took part in the discussion, e.g., *Susan Chatwood*, *Anne Husebekk* (Rector, University of TromsШ, Norway), and *Valery Chashchin* (Professor, Director of R. Koch and I.I. Mechnikov International Center of the Public Health). *Vladimir Shepovalnikov*, Head of Polar Medicine Center, "Arctic and Antarctic Research Institute", Roshydromet, Russia, made a presentation on the impact of space and heliophysical factors on health in the Arctic region.

The second thematic session "Legal Regime for the Arctic Environmental Protection" was moderated by *Anton Vasiliev*, MFA Ambassador-at-Large, Representative of Russia in the Arctic Council, and *Lars Kullerud*, President of UArctic, Norway. This session included presentations by *Timo Koivurova*, Research Professor of the Northern Institute for Environmental and Minority Law, Arctic Center, University of Lapland, Finland, on "The Effectiveness of Multilateral Environmental Agreements in Protection of the Arctic Environment" and by *Natalia Lukasheva*, Professor, University of Akureyri, Iceland, on "Environmental Governance and Legal Issues in the Arctic (Security, Cooperation, New Issues, the Role of Indigenous Peoples)". The presentations were followed by a lively debate on the issues. *Mikhail Slipenchouk*, Professor, Deputy Chairman of the Russian State Duma Environmental Committee, raised a question on the feasibility of entering into new agreements between the Arctic countries. In his response to the question, Ambassador *Anton Vasiliev* stated that there already exist many agreements and accords on the Arctic. In 2008, the Arctic countries have agreed not to take any actions unilaterally and to address the issues by mutual agreements between the Arctic states. *Tamara Zlotnikova*, Professor, former Chairman of the Russian State Duma Environmental Committee, suggested that the Arctic states should enter into a convention on pollution in the Arctic, by analogy with the Convention for the Protection of the Marine Environment of the Baltic Sea Area (Helsinki, 1992).

At the end of the first day of the Forum, *Nikolay Kasimov*, Academician, Dean of the Faculty of Geography, M.V. Lomonosov Moscow State University, First Vice President of the RGS, Chairman of the Public Council under the Ministry of Natural Resources of Russia, and *Lars Kullerud* , President of UArctic, signed a cooperation agreement.

On the second day of the Forum, the third thematic section "Environmental Safety for the Arctic Development" took place (moderators: *Mikhail Slepenchuk*, Professor, Deputy Chairman of the Russian State Duma Environmental Committee, and *Lawson Brigham*, Professor of Geography

and Arctic Policy of the University of Alaska, Fairbanks, Senior Fellow of the Institute of the North, Anchorage, USA). The first speaker was *Jan Helge Skogen*, President of Statoil Russia, Norway, on the issue of "Modern Challenges of the Arctic Shelf Development". He spoke about the latest technologies and technical means used by Statoil to produce hydrocarbons on the Arctic shelf. *Pettery Taalas*, Director General of the Finnish Meteorological Institute, talked about "The Optimal Use of Energy and Environmental Security in Northern and Arctic Areas". He also presented a film about the activities of the Hydrometeorological Service of Finland in the Arctic. *Alexander Chuprian*, Deputy Minister of Emergency Control Ministry of Russia / Ministry of the Russian Federation for Civil Defense, Emergencies, and Elimination of Consequences of Natural Disasters, made a presentation on "Prevention and Management of Emergency Situations in the Arctic". *Alexander Frolov*, Head of Federal Service for Hydrometeorology and Environmental Monitoring (Roshydromet), spoke on the "Federal Monitoring of the Russian Arctic Environmental State and Pollution". The fourth speaker was *Sergey Donskoy*, Minister of Natural Resources and Environmental Protection of the Russian Federation, with a presentation "Development of Resource Potential and Ensuring Ecological Safety of the Arctic".

In the afternoon, President of Russian Federation and Chairman of the Board of Trustees of the RGS *Vladimir Putin* opened the Plenary Session of the III International Arctic Forum. President of the Republic of Finland *Sauli Niinistų* and President of Iceland *Ylafur Ragnar Grimsson* (who participated in all three Forums "Arctic – the Territory of Dialogue") also addressed the Forum. *Patrick Borbey*, Chair of the Arctic Council's Senior Arctic Officials, President of the Canadian Northern Economic Development Agency, spoke about the state and the existing problems in the international cooperation of the countries of the Arctic region and the activities of the Arctic Council.

The Plenary session of the second day was moderated by *Sergei Shoigu*, Minister of Defense of the Russian Federation, President of the RGS. In his opening remarks, he welcomed the participants on behalf of the RGS, the driving force of the Forum, and noted that the number of the participants of the Forum has been increasing and its geography has been expanding. He stressed that the environment and biodiversity protection and climate change constitute the most sensitive topics in the region today. He also pointed out that all these issues have been historically in the focus of the RGS. To summarize the results of the Plenary Session of the III International Arctic Forum,

Sergei Shoigu gave the floor to the Chairman of the Board of Trustees of the RGS *Vladimir Putin*.

First Vice President of the RGS, Academician *Nikolai Kasimov* opened the fourth session on "Climate, Pollution, and Biodiversity". The first presentation was made by *Vladimir Kotlyakov*, Academician, Honorary President of the RGS. He delivered an informative and well-illustrated report on "Climate Change Scenarios in the Arctic and Environmental Effects Forecast". The report by *Lars-Otto Reiersen*, Executive Secretary, AMAP Secretariat, Norway, on "Environmental Pollution in the Arctic: Current Level, Trends, Risk Assessments" elaborated on the activities of Arctic Monitoring and Assessment Programme (AMAP), presented the latest publications on the state of the environment of the Arctic by the AMAP working groups, and talked about promising areas of activity within the AMAP. *Alexander Shestakov*, Director of the Global Arctic Program of the World Wildlife Fund (WWF, Canada), spoke on the priorities in the area of preservation of nature in the Arctic. *Vladimir Melnikov*, Academician, Director of the Institute of the Earth Cryosphere of the SB RAS, Tyumen, Russia, focused on the prospects for obtaining highly profitable eco-friendly products from the diatom raw material – an analog of cellular glass. *Yevgeny Syroechkovsky*, Chairman of the Working Group on the Conservation of Arctic Flora and Fauna of the Arctic Council, talked about a project on the conservation of migratory species of birds. *Boris Morgunov*, Assistant to the Minister of Economic Development of the Russian Federation, spoke about the status of work on six projects in the Arctic under the Global Environment Facility (GEF) "Arctic Agenda 2022". *Vasily Bogoyavlensky*, Corresponding Member RAS, Deputy Director of the Institute of Oil and Gas Problems, SB RAS, focused on the status of development of hydrocarbon deposits on the continental shelf in the Arctic region.

Under the framework of the Forum, Academician *Viktor Sadovnichy*, Rector of the Lomonosov Moscow State University, and *Anne Husebekk*, Rector of University of Tromsø, Norway, signed an agreement. Academician *V. Sadovnychy* presented A. *Husebekk* a just recently printed atlas "The Arctic of the XXI Century: Natural Conditions and Development Risks" prepared by the scientists of the Faculty of Geography, Lomonosov Moscow State University, together with other scientists under the RGS grant policy.

Nikolay G. Rybalsky
Vladimir S. Tikunov

INSTRUCTIONS FOR AUTHORS CONTRIBUTING TO "GEOGRAPHY, ENVIRONMENT, SUSTAINABILITY"

AIMS AND SCOPE OF THE JOURNAL

The scientific English language journal "GEOGRAPHY, ENVIRONMENT, SUSTAINABILITY" aims at informing and covering the results of research and global achievements in the sphere of geography, environmental conservation and sustainable development in the changing world. Publications of the journal are aimed at foreign and Russian scientists – geographers, ecologists, specialists in environmental conservation, natural resource use, education for sustainable development, GIS technology, cartography, social and political geography etc. Publications that are interdisciplinary, theoretical and methodological are particularly welcome, as well as those dealing with field studies in the sphere of environmental science.

Among the main thematic sections of the journal there are basics of geography and environmental science; fundamentals of sustainable development; environmental management; environment and natural resources; human (economic and social) geography; global and regional environmental and climate change; environmental regional planning; sustainable regional development; applied geographical and environmental studies; geo-informatics and environmental mapping; oil and gas exploration and environmental problems; nature conservation and biodiversity; environment and health; education for sustainable development.

GENERAL GUIDELINES

1. Authors are encouraged to submit high-quality, original work: scientific papers according to the scope of the Journal, reviews (only solicited) and brief articles. Earlier published materials are accepted under the decision of the Editorial Board.

2. Papers are accepted in English. Either British or American English spelling and punctuation may be used. Papers in French are accepted under the decision of the Editorial Board.

3. All authors of an article are asked to indicate their **names** (with one forename in full for each author, other forenames being given as initials followed by the surname) and the name and full postal address (including postal code) of the **establishment(s)** where the work was done. If there is more than one institution involved in the work, authors' names should be linked to the appropriate institutions by the use of 1, 2, 3 etc superscript. **Telephone and fax numbers and e-mail addresses** of the authors could be published as well. One author should be identified as a **Corresponding Author**. The e-mail address of the corresponding author will be published, unless requested otherwise.

4. The GES Journal style is to include information about the author(s) of an article. Therefore we encourage the authors to submit their photos and short CVs.

5. The optimum size of a manuscript is about 3 000–5 000 words. Under the decision (or request) of the Editorial Board methodological and problem articles or reviews up to 8 000–10 000 words long can be accepted.

6. To facilitate the editorial assessment and reviewing process authors should submit "full" electronic version of their manuscript with embedded figures of "screen" quality as a **.pdf file.**

7. We encourage authors to list three potential expert reviewers in their field. The Editorial Board will view these names as suggestions only. All papers are reviewed by at least two reviewers selected from names suggested by authors, a list of reviewers maintained by GES, and other experts identified by the associate editors. Names of the selected reviewers are not disclosed to authors. The reviewers' comments are sent to authors for consideration.

MANUSCRIPT PREPARATION

Before preparing papers, authors should consult a current issue of the journal at http://www.geogr.msu.ru/GESJournal/index.php to make themselves familiar with the general format, layout of tables, citation of references etc.

1. Manuscript should be compiled in the following **order**: authors names; authors affiliations and contacts; title; abstract; key words; main text; acknowledgments; appendices (as appropriate); references; authors (brief CV and photo)

2. The **title** should be concise but informative to the general reader. The **abstract** should briefly summarize, in one paragraph (up to 1,500 characters), the general problem and objectives, the results obtained, and the implications. Up to six **keywords**, of which at least three do not appear in the title, should be provided.

3. The **main body** of the paper should be divided into: (a) **introduction**; (b) **materials and methods**; (c) **results**; (d) **discussion**; (e) **conclusion**; (f) **acknowledgements**; (g) **numbered references**. It is often an advantage to combine (c) and (d) with gains of conciseness and clarity. The next-level subdivisions are possible for (c) and (d) sections or their combination.

4. All **figures** (including photos of the authors) are required to be submitted as separate files in original formats (CorelDraw, Adobe Photoshop, Adobe Illustrator). Resolution of raster images should be not less than 300 dpi. Please number all figures (graphs, charts, photographs, and illustrations) in the order of their citation in the text. **Composite figures** should be labeled A, B, C, etc. Figure captions should be submitted as a separate file.

5. Tables should be numbered consecutively and include a brief title followed by up to several lines of explanation (if necessary). Parameters being measured, with units if appropriate, should be clearly indicated in the column headings. Each table should be submitted as a separate file in original format (MS Word, Excel, etc.).

6. Whenever possible, total number of **references** should not exceed 25–30. Each entry must have at least one corresponding reference in the text. In the text the surname of the author and the year of publication of the reference should be given in square brackets, i.e. [Author1, Author2, 2008]. Two or more references by the same author(s) published in the same year should be differentiated by letters a, b, c etc. For references with more than two authors, text citations should be shortened to the first name followed by et al.

7. **References** must be listed in alphabetical order at the end of the paper and numbered with Arabic numbers. References to the same author(s) should be in chronological order. Original languages other than English should be indicated in the end of the reference, e.g. (in Russian) etc.

Journal references should include: author(s) surname(s) and initials; year of publication (in brackets); article title; journal title; volume number and page numbers.

References to books should include: author(s) surname(s) and initials; year of publication (in brackets); book title; name of the publisher and place of publication.

References to multi-author works should include after the year of publication: chapter title; "In:" followed by book title; initials and name(s) of editor(s) in brackets; volume number and pages; name of the publisher and place of publication.

8. Authors must adhere to SI units. Units are not italicised.

9. When using a word which is or is asserted to be a proprietary term or trade mark, authors must use the symbol ® or TM.

10. As Instructions for Authors are subjected to changes, please see the latest "Example of manuscript style" at http://www.geogr.msu.ru/GESJournal/author.php

MANUSCRIPT SUBMISSION

Authors are encouraged to submit their manuscripts electronically. Electronic submissions should be sent as e-mail attachments to GESJournal@yandex.ru

ISSN 2071-9388

SOCIALLY SCIENTIFIC MAGAZINE "GEOGRAPHY, ENVIRONMENT, SUSTAINABILITY"

No. 01(v. 07) 2014

FOUNDERS OF THE MAGAZINE: Faculty of Geography, Lomonosov Moscow State University and Institute of Geography of the Russian Academy of Sciences

The magazine is published with financial support of the Russian Geographical Society.

The magazine is registered in Federal service on supervision of observance of the legislation in sphere of mass communications and protection of a cultural heritage. The certificate of registration: ПИ МФС77-29285, 2007, August 30.

EDITORIAL OFFICE
Lomonosov Moscow State University
Moscow 119991 Russia
Leninskie Gory,
Faculty of Geography, 2108a
Phone 7-495-9392923
Fax 7-495-9328836
E-mail: GESJournal@yandex.ru

DESIGN & PRINTING

Advertising and Publishing Agency "Advanced Solutions"
Moscow, 119071 Russia,
Leninskiy prospekt, 19, 1
Phone 7-495-7703659
Fax 7-495-7703660
E-mail: om@aov.ru

DISTRIBUTION

East View Information Services
10601 Wayzata Blvd, Minneapolis, MN 55305-1526 USA
Phone +1.952.252.1201 Fax +1.952.252.1202
E-mail: periodicals@eastview.com
www.eastview.com

Sent into print 07.02.2014
Order N gi114

Format 70 × 100 cm/16
9.43 p. sh.
Digital print
Circulation 600 ex.